OSCCAR:
FUTURE OCCUPANT SAFETY FOR CRASHES IN CARS

Homologation scenario demonstration using advanced harmonized HBMs

Document Type	Deliverable
Document Number	D4.3
Primary Author(s)	Christoph Klein	VIF
Document Version / Status	1.1	Final
Distribution Level	PU (public)

Project Acronym	OSCCAR
Project Title	FUTURE OCCUPANT SAFETY FOR CRASHES IN CARS
Project Website	www.osccarproject.eu
Project Coordinator	Werner Leitgeb	VIF	werner.leitgeb@v2c2.at
Grant Agreement Number	768947
Date of latest version of Annex I against which the assessment will be made	2019-01-25
Upload by coordinator:	First submitted: 2021-12-16 Re-submitted: 2022-04-11

CONTRIBUTORS

Name	Organization	Name	Organization
Christoph Klein	VIF	Martin Schachner	TU Graz
Jens Weber	Volkswagen AG	Dominik Breitfuss	VIF
María González García	Volkswagen AG	Pronoy Ghosh	MBRDI
Richard Lancashire	SISS	Christian Kleinbach	Mercedes Benz AG
Sabine Compigne	TME		
Krystoffer Mroz	Autoliv		
Maja Wolkenstein	Robert Bosch GmbH		

FORMAL REVIEWERS

Name	Organization	Date
Daniel Schmidt	Robert Bosch GmbH	2021-12-03
Johan Davidson	Chalmers	2021-12-10

DOCUMENT HISTORY

Revision	Date	Author / Organization	Description
0.1	2021-11-17	Christoph Klein	Chapter 1 – 3.5
0.2	2021-11-28	Christoph Klein	Chapter 3.5 - 6
1.0	2021-11-30	Christoph Klein	Included reviewers comments
1.1	2022-04-07	Manuela Klocker	Updates after EU review

TABLE OF CONTENTS

LIST OF FIGURES

LIST OF TABLES

1 EXECUTIVE SUMMARY

This report documents necessary alignment for conducting comparable pre- and in-crash occupant simulations with Human Body Models (HBMs) in Finite Element (FE) and Multi Body (MB) codes in a validated environment. In particular, the HBMs involved versions of 50% male Total Human Model for Safety (THUMS) in LS-Dyna (v3, SAFER HBM v9, v6.1, THUMS TUC), the Madymo AHM and a THUMS TUC in VPS. The results for THUMS Thums User Community (TUC) Virtual Performance Solutions (VPS) and LS-Dyna are compared additionally in detail in this report.

A validated environment (OSCCAR Workpackage 2) was used and two in-crash pulses were applied. A pre-crash pulse (OSCCAR Workpackage 2) was applied in combination with one of the in-crash pulses to demonstrate a combined assessment of pre- and in-crash phase.

In this report the actions required for obtaining aligned HBM simulations are listed first. To ensure equal boundaries for the simulations, acceleration pulse and activation times for the belt system are verified first. It is further assessed, if the contact forces between the HBM and the environment (seat, belt) indicates any issues. Next, the kinematics of selected anatomical landmarks are compared. Finally, injury indicators and injury risk parameters are assessed. This report documents the mentioned checks for two in-crash simulations and for a combined pre- and in-crash simulation. Prior to the simulation results, the testcase (pulses, environment) is described.

It is demonstrated, that the simulations are conducted with the same pulses and that the components of the belt system are activated at the same time. Differences are observed for the pull in of the buckle. Belt and seat contact forces do not indicate further issues. The same applies to the trajectories of the selected anatomical landmarks. Differences in contact forces and trajectories can be observed, but the six different HBMs (three solvers, MB and FE) cannot be expected to show identical results. Although all HBMs represent the 50% male, different anthropometrical details between the models exist. Besides that, all of them also have a different validation basis. The overall target is to simulate the six HBMs under the same boundary conditions and to ensure that the same assessment and post processing procedure is applied to all of them. That goal could be achieved, except for one model which shows differences in the buckle pretensioning (pull in) and deviations between the used tools for rib strain assessment.

Keywords:

Harmonized Human Body Model simulation, Harmonized assessment, Continuous assessment, Pre- to in-crash, active Human Body Models

2 OBJECTIVES

Virtual assessment and virtual testing (VT) of vehicle performance in simulated crashes will play a rising role in the consumer information programs and regulated approval tests. For example, the homologation of some components can be performed with VT as specified for type approval of door latches and hinges or towing hooks [2]. One possibility of assessing the injury risk in crashes for occupants or Vulnerable Road Users (VRUs) using VT are the use of Human Body Models (HBMs). HBMs are, for instance, already used in the Euro NCAP TB024 [3] for vehicle safety ratings.

Corresponding to real world crash tests with Anthropometric Test Devices (ATD), which require, e.g., certain corridors for initial sitting position and calibrated sensors, the boundary conditions under which these virtual tests are to be conducted need to be harmonized to make the results comparable and reproduceable.

For that virtual process, it is neither expected nor even reasonably practicable, that it requires a specific pre- or post-processing software, a particular HBM or a certain simulation solver. Therefore, procedures and methodologies need to be specified, independent from a certain software or HBM. For instance, a certification process will need to be defined for the HBMs. Once certified they can be used in a virtual homologation process.

This report documents the OSCCAR homologation testcase. The aim is to develop a methodology that is able to run comparable pre- and in-crash occupant simulations with different HBMs in a generic environment with different solver codes (LS-Dyna, Madymo, VPS). That requires a harmonized objective assessment in terms of occupant kinematics, boundary conditions and injury related responses (e.g., accelerations, forces, moments, strains, etc.). However, this work package is a demonstration of the homologation methodology and not a comparative investigation of the validity of different HBMs.

3 DESCRIPTION OF WORK

This chapter documents the steps for a harmonized continuous pre- and in-crash VT procedure.

First, subchapter 3.1 gives an overview of tools, which enable the positioning of HBMs, the kinematic transition from pre- to in-crash phase, the assessment of HBMs and a numerical quality check. These tools were developed or enhanced in OSCCAR. A more detailed description for them can be found in Deliverable D4.2 [4].

The following subchapters demonstrate the method which was applied:

- **Definitions for in-crash simulation alignment**

  Subchapters 3.2 and 3.3 define the necessary alignment as well as the assessment for ensuring comparable simulations. It is defined, what needs to be aligned prior to a simulation (e.g., HBM sitting position, acceleration pulses, etc.) and which simulation results need to be assessed to ensure that the simulation are carried out under the same boundary conditions.

- **Application on an in-crash simulation**

  Application on an in-crash simulation with an OSCCAR developed pulse (Left turn across path – opposite direction / LTAP-OD) is demonstrated in chapter 3.4. The pulse was selected and developed in Deliverable D 1.3, in particular pulse for LTAP-OD2 [32]. Links to the public available data and models are given in chapter 4 in this report. This in-crash simulation is conducted with six HBMs (50% male) in three different solver codes (Ls-Dyna, Madymo, VPS).

  A selective comparison among all simulations, including HBM kinematics, belt routing and injury risk parameters, for THUMS TUC models in LS-Dyna and VPS is given in chapter 3.5.

- **Definitions for combined pre- and in-crash simulation alignment**

  Following, necessary alignment and assessment is defined for a continuous transition from pre- to in-crash simulations are shown in subchapter 3.6.1.

- **Application on a combined pre- and in-cash simulation**

  The used pre-crash pulse is defined in Deliverable D2.5 [27]. The before mentioned LTAP-OD2 pulse was used again in the in-crash phase. In addition to the definitions for the pre-cash phase, the definitions for the in-crash phase are applied.
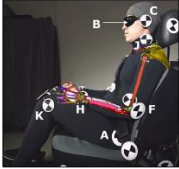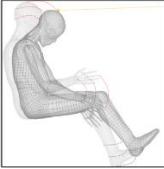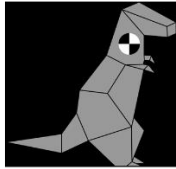
  This simulation is again conducted with six HBMs. For considering the pre-crash phase, active models were used. The simulation testcase is described in subchapter 3.6.2 and the results are reported in subchapter 3.6.3

- **Influence of the pre-crash phase**

  Finally, the influence of the considered pre-crash phase to the results of the in-crash is demonstrated in chapter 3.7. It is done by comparing maximum values of forward excursion, pelvis rotation, section forces and injury risk indicators and parameters.

3.1 Tools for continuous assessment of pre- and in-crash simulations

To enable a continuous assessment approach, several methods and tools were developed in OSCCAR (see Figure 1 and Deliverable D4.2 [4]). These tools allow the execution without the need of commercial products. These tools are not mandatory to be used in the OSCCAR Homologation testcase, but certain boundary conditions have to be met as described in the following chapter (3.2).

	Quality check	Positioning	Transition	Assessment
OSSCAR activity	Check list / tool **Task 4.1**	Positioning tool & method **Task 4.2.1**	Transition tool **Task 4.2.2**	Harmonized assessment based on DynaSaur tool **Task 4.2.3**

Figure 1: Steps and OSCCAR activities for comparable HBM simulations

Quality check:

Quality criteria were split in pre- and post-simulation criteria. For the pre-simulations it needs to be verified, that the necessary output definitions are set to get comparable simulation outputs. The criteria and the developed script are described in Deliverable D4.1 [5]. The defined criteria for the pre-simulation were developed and summarized from literature from a global perspective. During the working process of the homologation test-cases several model details of the simulation model had to be aligned and checked which does not meet the requirements of defining general quality criteria, as the alignment was on model details. Moreover, the model for the simulations were provided in a way, that no adaption of the output parameters was necessary for the participating partners. Therefore, the developed tool to verify the pre-simulation settings was not used by all partners in the homologation test-case.

The post-simulation criteria, which are described in detail in Deliverable D4.2 [4], are done with the used assessment tools and are listed later in this report.

Positioning

A positioning tool was developed to enable the positioning without any commercial products. It was decided that partners can also use their own positioning methods and tools. The tool and the underlying method are described in detail in Deliverable D4. [4] and in reference [6]. An additional script was written to automatically check the positions of all involved HBMs defined by the coordinates of anatomical landmarks. These anatomical landmarks and their coordinates are taken from literature [1].

Belting

A method to fit a belt model onto the different HBMs was suggested in Deliverable D4.2 [4], chapter 3.2.3.2. It was decided, that participating partners can also make use of their own methods and tools for the homologation testcase.

Transition

A transition method, which enables the handover of kinematic HBM data from the pre-crash to the in-crash simulation was developed.. The developed method in Task 4.2 is capable of handing over kinematic information between two models, even if their anthropometry does not match exactly. Hence the transition from Multi Body (MB) to Finite Element (FE) models is possible, too. The transition tool, method, and application are documented in Deliverable D4.2 [4].

Assessment

Assessment of environment and HBM kinematics as well as the post processing for injury risk indicators and the data preparation for injury risk parameter calculation. was done with DYNASAUR (Dynamic simulation analysis of numerical results). It is an open-source software launched by the Vehicle Safety Institute of TU Graz for FE and MB simulations. It was enhanced during OSCCAR (see Deliverable D4.2 [4] chapter 3.4) and is available on gitlab.com (https://gitlab.com/VSI-TUGraz/Dynasaur).

It was used to post-process the simulation results for all codes and determine nodal data (for trajectories), forces/moments, stresses/strains as well as simulation quality criteria.

3.2 Alignment and definitions for comparable occupant simulations with HBMs

The aim of this chapter is to demonstrate the necessary definitions and alignments for comparable simulations using Human Body Models under the same boundary conditions in two FE codes (VPS and LS-Dyna) and in a Multibody code (Madymo).

That requires following definitions

- Predefined boundary conditions (crash pulse and environment)
  - Pulse
  - Belt anchor points
- Predefined anthropometric percentile
- Predefined initial HBM position (harmonized landmark definitions)
- Seamless occupant model transition from pre- to in-crash and a comparable kinematic and
- Injury assessment of the occupant and a corresponding method/tool for each step (from D4.2)

Claiming that simulations are comparable means that "it is possible to compare them sensibly" in this report. That means, that (1) the simulations are executed under harmonized boundary conditions like environment, pulse, and sitting position, (2) the same output is used for assessment and (3) the assessment method is harmonized. It is not expected, that the results match exactly, since different versions of HBMs (of the same anthropometric percentile and gender) with a different level of validation in different solver codes are used. As mentioned in the objectives, this report is not a comparative investigation of the validity of HBMs, so no ranges for validity are defined beforehand.

General information about used HBMs is provided below as background information:

- THUMS v3: The original Total Human Model for Safety (THUMS) version 3.0.3 is used in this investigation, which was published in references [7] and [8]. The height of the model is 175 cm and the weight 77 kg. 107000 nodes and 145000 elements are used for the model.
- THUMS TUC 2020.01 (LS-Dyna- / VPS-version), in the following referred to as THUMS TUC, is originally developed from the Total Human Model for Safety (THUMS) version 3.0. Within

the scope of the TUC project [9] the model was further improved in terms of mesh quality, contact definitions and translatability (from LS-Dyna to VPS). In detail, modifications affect the modelling of legs, elbow, shoulder and rib cage. Mesh refinements led to an increase in model size up to approximately of 237.000 nodes and 311.000 elements. Between both software versions, there is only a small difference in total mass: 75.73 kg (LS-Dyna) vs. 75.61 kg (VPS). The only modification of the THUMS TUC model which is applied in OSCCAR affects the material of the lumbar vertebra. They are modelled rigidly in the original model, but were switched to deformable material in order to enable section output of forces and moments. Further details are provided in chapter 3.5.

- A-THUMS-D is an AHBM developed for internal applications at Mercedes-Benz AG in LS-DYNA. The model represents a 50th percentile male with 175 cm height and 75.7 kg weight. The modifications related to the implementation of the muscle modelling and controller is provided in detail in Deliverable D3.2 [10].

- THUMS TUC-VW AHBM is based on the above mentioned THUMS TUC (VPS). The enhancements performed at Volkswagen AG for the generation of an active model, namely the muscle modelling and activation control, are described in detail in Deliverable 3.2.

- THUMS v6.1 [11] geometry and anatomical details are mainly based on THUMS v4 [12] However, the model geometry and meshes have been refined at the rib cage to improve its rib fracture prediction and at the pelvis, lumbar spine and abdominal flesh to ensure a more biofidelic engagement of its lower torso with the lap belt. THUMS v6.1 includes muscle activation for various muscle conditions as already implemented in THUMS v5 [13] in which the muscles are modelled by 1D bar elements using Hill-type model. THUMS v6.1 50th percentile male height is 179 cm and its weight is 79 kg. Its number of elements is approximately 1.9 million.

- The SAFER HBM, originally developed from the THUMS v3 [8], has been updated with new head, neck, and rib cage models [14]. To improve the biofidelity, the lumbar spine was also modified, with updated geometric modelling of the vertebras and the material properties of the intervertebral ligaments and discs, as well as new contact definitions [15][16]. The capability of the HBM model to predict kinematics and rib fractures in the upright posture has been evaluated [16], as has its capability to predict whole-body kinematics in the reclined posture [17]. Active muscle postural control was also implemented as reported in [18][19].

- The Simcenter Madymo AHM is a multibody model of a human with active control powered by actuators and Hill-type muscle models. The geometry is based on the RAMSIS database for a 50th percentile male: the model has a height of 1.76 m and a weight of 75.3 kg. The surface is modelled using the Madymo facet approach, with a rigid surface mesh that captures contact interactions with an advanced penalty function. Details of the model structure and validation can be found in reference [21].

3.3 Assessment and evaluation parameters to ensure objectively comparable environment performance in occupant simulations

This chapter demonstrate which parameters are evaluated to ensure that the environment models (belt and seat, detailed description see chapter 3.4.1) perform comparable. That includes pulses, seat and seatbelt interaction, which are evaluated in a first step. If this evaluation confirms, that the simulations are done with the same boundary conditions, the next steps can be taken which are HBM kinematic and injury risk assessment.

Numerical quality checks

The numerical quality checks ensure, that the numerical quality of the results meets certain requirements. That is necessary to identify simulations which are sensibly not comparable due to numerical issues. Details can be found in Deliverable D4.2 [4]. The checks are applied to the complete system (environment and HBM).

- Hourglass energy < 10% of total energy
- Artificial mass increase < 3%

Environment

Following tables show the assessed parameters in the post-processing step. Following tables contain the part or the measurement location and the type of information which is evaluated.

Seat

Following output is assessed from the seat (see Figure 2).

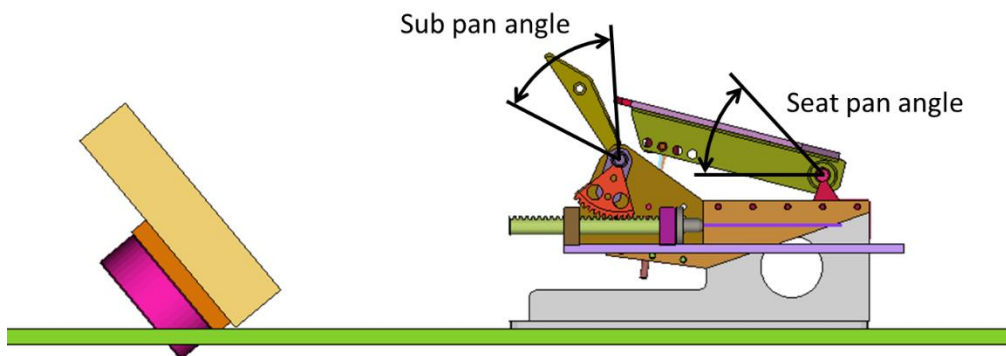| Assessed seat output	Information
Seat pan	Angle (t)
Sub pan	Angle (t)
Contact force HBM – seat force x/z	Force (t)
Contact force HBM – sub pan force x/z	Force (t)

Figure 2: Seat pan and sub pan angle on the LAB CEESAR seat

Seatbelt system

Assessed belt output	Assessed data
Belt forces (B2, B3, B4, B5, B6)	Force (t)
Belt pay in/out shoulder belt retractor	Displacement (t)
Belt pay in/out lap belt retractor	Displacement (t)
Buckle pull in	Displacement (t)
Webbing transport through tongue	Displacement (t)
Shoulder belt force (B2, B3)	Force (t)
Lap belt force (B4, B5, B6)	Force (t)
Buckle force (B4, B5)	Force (t)

Floor / Vehicle

Assessed floor output	Assessed data
Toe pan resultant force	Force (t)

Proposed landmarks for HBM kinematic assessment

The selected kinematic responses were based to capture overall global response of the head, thorax, spine and pelvis due to its importance when investigating risks of injuries to the head, thorax, lumbar spine and pelvis. More specifically, the head kinematics were selected to assess the risk of impact to potential surrounding structures and the T1, T8, L1 and pelvis kinematics for their close correlation to shoulder belt force and payout, chest loading, lumbar spine injuries and submarining, respectively. The T11 and L3 signals were selected to increase the details on how the lumbar spine is deforming in its potential stiffness discontinuity relative to the thoracic spine. Since y-direction displacements are expected to be small for the lower spine and pelvis, those are not included.

Landmark	Assessed data
Porion (left/right)	x(t), y(t), z(t)
T1 (Left/right midpoint)	x(t), y(t) z(t)
T8 (Left/right midpoint)	x(t), y(t) z(t)
T11 (Left/right midpoint)	x(t), z(t)
L1 (Left/right midpoint)	x(t), z(t)
L3 (Left/right midpoint)	x(t), z(t)
Acetabular centre (left/right)	x(t), z(t), rotation y-axis(t)

ASIS / PSIS	Pelvis angle (t)

To allow tracking of the belt routing at the initial position and also during the crash phase, four anatomical landmarks were defined. They can be used to document the belt position relatively to these defined points on the HBM. Two of them are located on the sternum and two of them on the clavicle. The intention was to compare the belt routing when different models and belt routing tools are used. Since in OSCCAR the three belt anchor points have the same position, it was assumed that the belt routing is comparable and no further check is needed. In future projects a goal could be to analyse whether a comparison of the belt routing is useful to ensure better comparability.

Landmarks for belting check	Assessed data
Ventral point of sternoclavicular joint	z(y)
Dorsal point of acromioclavicular joint	z(y)
Suprasternal notch	z(y)
Xiphoid process or a lower sternum point	z(y)

Injury indicators and injury risk parameters

The assessment and comparison of injury related parameters are divided in two groups. The first one, injury indicators, contains parameters, which might be relevant for injury assessment in the future especially in new sitting positions. Currently, to determine a certain AIS level, no risk curves exist for these parameters. The second group of parameters, injury risk parameters, contain parameters which allow the determination of the risk for a certain AIS level based on HBM kinematics or on tissue stress/strain.

Injury indicators

The definitions for lumbar spine and pelvis section forces can be found in Deliverable D3.3 [22], chapter 3.7. Depending on the modelling strategy of the HBMs they are capable of determining section force, which does not apply to Madymo AHM and the THUMS v.

Injury indicator	Assessed data
Lumbar spine forces	z-Force (t)
Lumbar spine moments	y-Moment (t)
ASIS forces	Resultant Force

Injury risk parameters

Additionally, injury risk criteria are assessed for head and thorax. In contrast to the injury indicators, following parameters allow the determination of the injury risk on a certain AIS level. As a comparison on tissue level is not possible between FE and MB models, the comparison of injury risk closes this gap.

Body region	Criteria	AIS level
Head	HIC 15	AIS 2+
	BrIC	AIS 2+
	SUFEHM	AIS 2+
Thorax	Forman criteria	AIS 1 - 3
	Maximum rib strain	

The SUFEHM Box, which is used for Head injury assessment uses local accelerations and rotational velocities of the head to run a FE head model simulation and identify the injury risk on tissue level by means of axion strains [23]. Further, HIC 15 and BrIC are generated by the SUFEHM Box.

Within OSCCAR, recommendations for the application of the probabilistic rib fracture risk according to Forman [24], were defined in Deliverable 3.3. Besides an updated risk curve, suggestions were formulated, how the rib strains should be determined. The LS-Dyna partners use DYNASAUR, whereas the VPS users extract their rib strains with the TUC Tool. For both tools a detailed description is given in chapter 3.4.2.6 how the maximum strain per rib is determined. For the detailed comparison between THUMS TUC VPS and TUMS TUC LS-Dyna, the rib fracture risk according to the Forman criteria is calculated.

3.4 Demonstration for left turn across path – opposite direction (LTAP-OD)

This chapter demonstrates the application of the parameters defined in Chapter 3.3.

3.4.1 Description of the testcase

Following models were used for the Homologation testcase

Solver	Model	Partner
LS-Dyna	THUMS v3	VIF
	SAFER HBM v9	Autoliv
	THUMS TUC v2020.01	Mercedes
	THUMS v6.1/TME	TME
Madymo	Simcenter AHM v3.1	Bosch, Siemens

| VPS | THUMS TUC V2020.01 | Volkswagen AG |

Figure 3 shows the used HBMs in its initial position (48 deg. reclined).

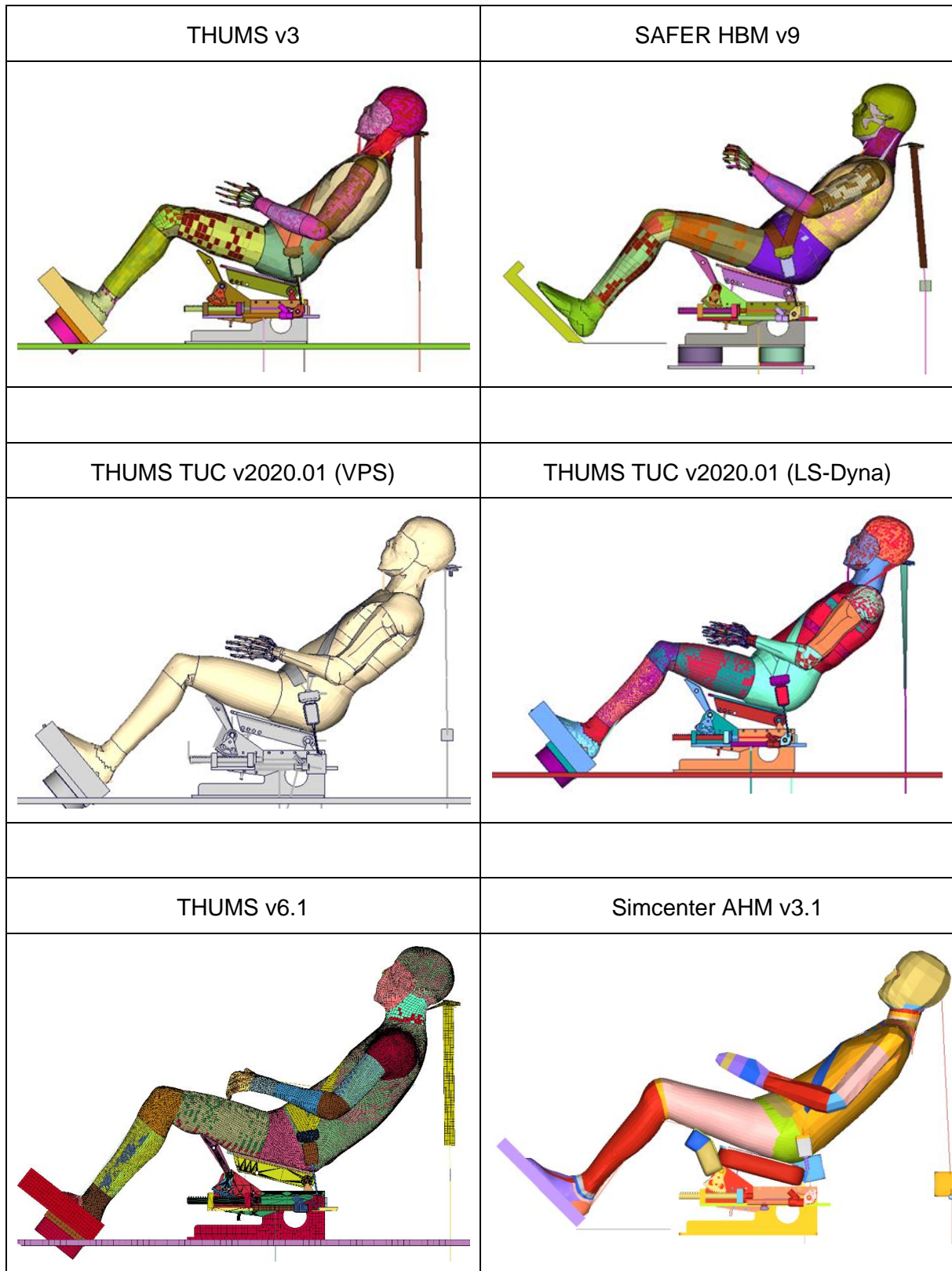| THUMS v3	SAFER HBM v9
THUMS TUC v2020.01 (VPS)	THUMS TUC v2020.01 (LS-Dyna)
THUMS v6.1	Simcenter AHM v3.1

Figure 3: Used HBMs in initial position

The following list shows the **harmonized boundary conditions** for the simulations:

- Environment (Deliverable D 2.2 [25])

  - Seat

    Numerical models in all three codes of a semi-rigid seat (Figure 4, LAB CEESAR) were used. The seat models were validated in OSCCAR (Deliverable D2.5 [27]) with a THOR Dummy in an upright and reclined sitting position with a 50 kph full frontal pulse [1]. The seat model will be available on TUC (THUMS User Community) repository [28]. More information can be found in Deliverable D5.2 [29].
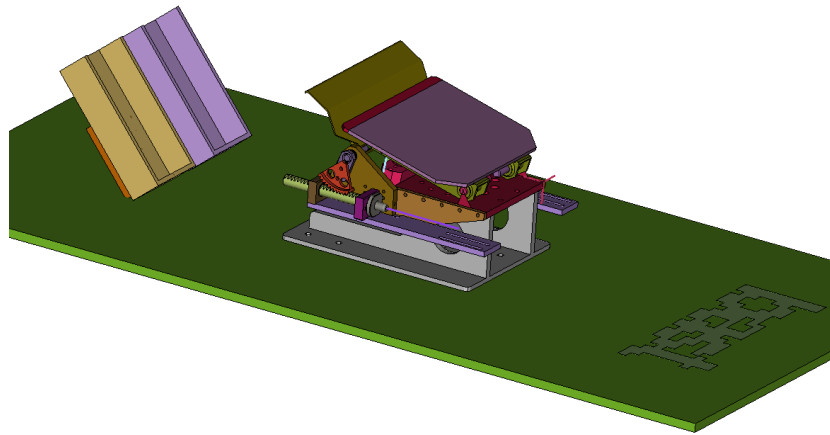
**Figure 4: FE Model of the semi rigid seat (LAB CEESAR)**

Figure 5 shows the seat model in a top view in relation to the vehicle's centre of gravity (CoG) to which the pulse was applied to. The distance of vehicle CoG to the seat coordinate system is in accordance with Deliverable D 1.3 [32].
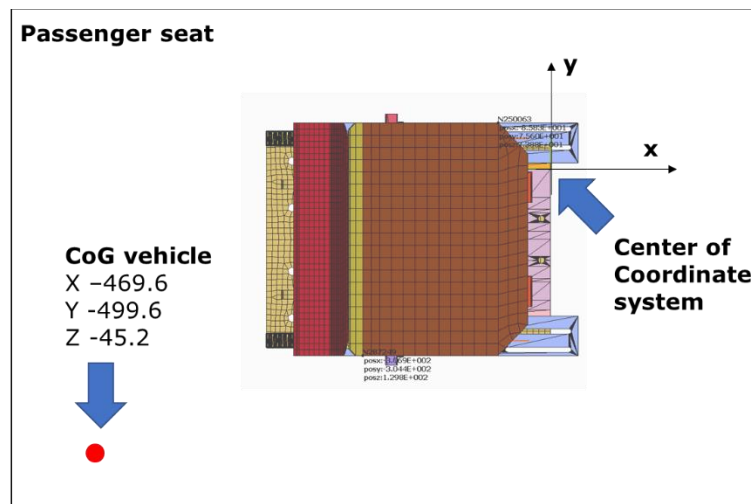
Figure 5: Seat model and position of vehicle CoG

  - Belt system
    A seat back mounted seat belt system in a passenger side configuration was used in the study, Figure 6 [30][31]. The seat belt system was triple-pretensioned and 3.5 kN load-limited, with a crash locking tongue, that mitigates webbing transfer

from the shoulder belt to the lap belt. The buckle pretensioner was activated at 3 ms and the shoulder and outboard lap pretensioners at 9 ms. This conceptual belt system was designed to improve pelvis restraint in order to avoid submarining for reclined occupants.
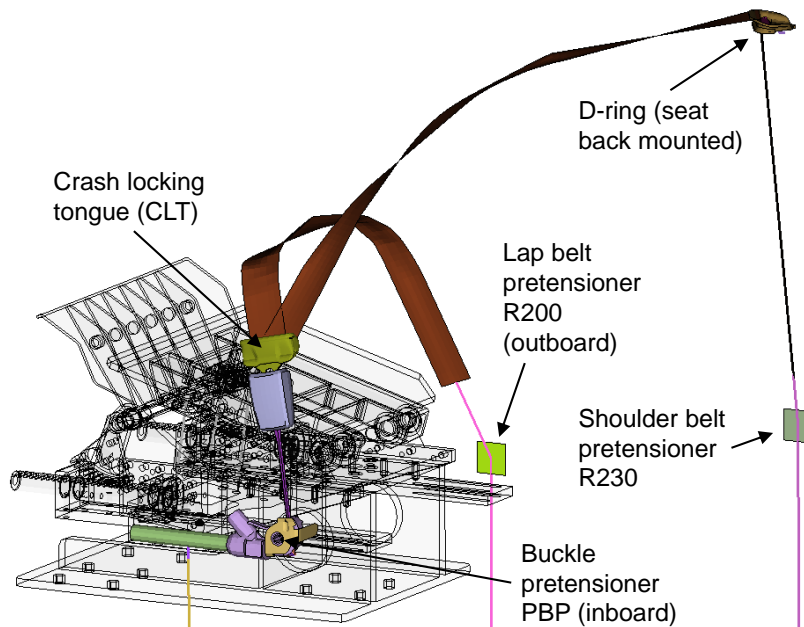

Figure 6: Generic seat belt model (FE)

- Pulse

  In the homologation testcase, two in-crash pulses are used. First one is full frontal (FF) 50 kph which was also used for seat model validation [33]. The analysis of the homologation testcase simulations with this pulse are reported in A.

  The second pulse is of a "left turn across path – opposite direction" (LTAP-OD) scenario. This pulse was elaborated in OSCCAR WP1 and is documented in Deliverable D 1.3 [32]. The detailed naming of the used pulse for the simulations in this report is 14_LTAPOD2_66_19_1717_1717_AD_ID01_v (in short LTAP-OD2). The pulse consists of accelerations in x- and y-direction and a rotation about the z-axis (compare Figure 7).
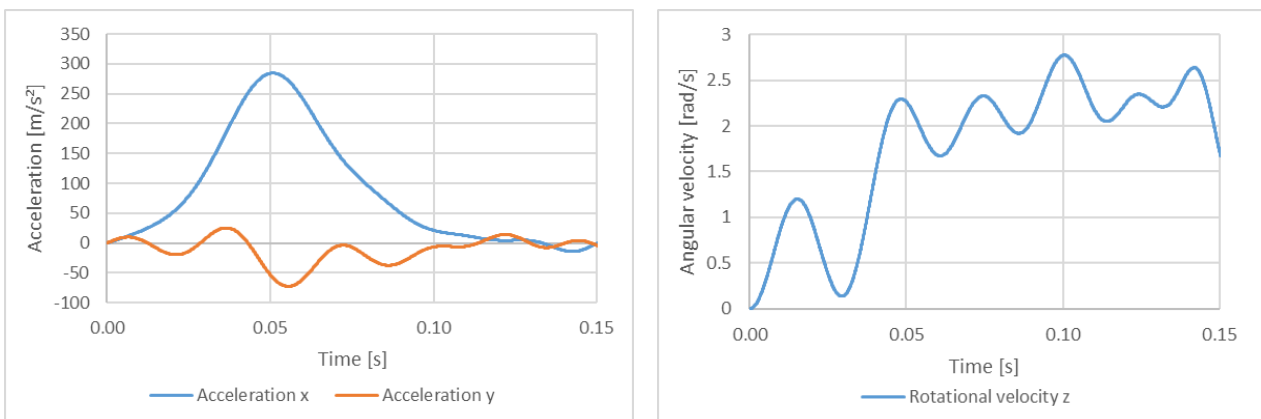
Figure 7: Acceleration in x- and y-direction and rotational velocity (z axis) (LTAP-OD2 pulse)

Sitting position

The sitting position was defined by the coordinates for anatomical landmark in the local seat coordinate system. A 48° reclined position from a Post Mortal Human Subject (PMHS) test series [1] was used. The coordinates for the acetabular centre should match in x-position. Due to different buttock geometries and materials of the used HBMs, an equivalent z-position in combination with realistic contact forces to the seat are not possible. It was decided to prefer realistic contact force, which roughly match with the HBMs weight.

- Anatomical landmark definition

Definitions for anatomical landmarks follow the recommendations in literature (see references [34][3]) and are documented in Deliverable D4.2 [4].

3.4.2 Simulation results for all models

In chapter 3.3 parameters have been identified to ensure that the environment models have a similar performance. In this chapter the parameters like pulses, seat contact forces, seat kinematics and restraint system responses will be compared based on the simulation results with the LTAP-OD2 crash pulse.

If the assessment shows that the different models have similar characteristics and performance it is reasonable to compare HBM kinematics, injury indicators and carry out an injury risk assessment.

3.4.2.1   Finite element quality criteria

Table 1 shows, that the simulations are within the required range which is defined for the numerical quality criteria.

Model	Added Mass [%] <= 3% of Initial Mass	Hourglass Energy [%] <= 10% of Total Energy
THUMS v3	0.72	1.23
THUMS v6.1	0	0.3
SAFER HBM v9	0.027	1.73
THUMS TUC Ls-Dyna	0.32	0.63
THUMS TUC VPS	0.003	0.24

Table 1: Added mass and Hourglass energy of the LTAP-OD2 simulations

3.4.2.2   Acceleration pulse

Figure 8 shows the acceleration in x- and y-direction, which documents, that the partners run their simulations with the same pulses.
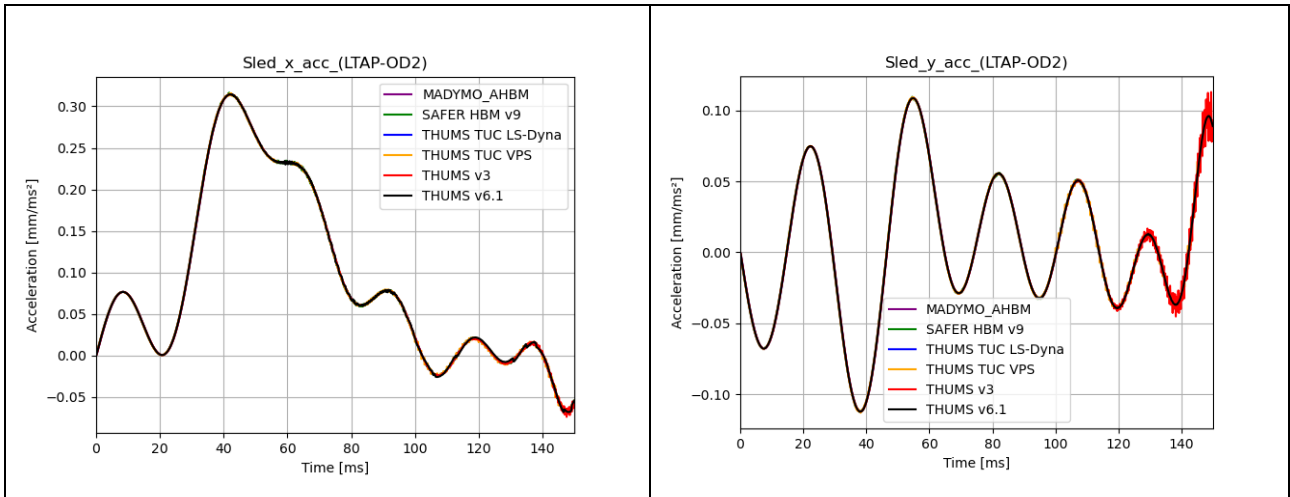
Figure 8: Acceleration pulse LTAP-OD2
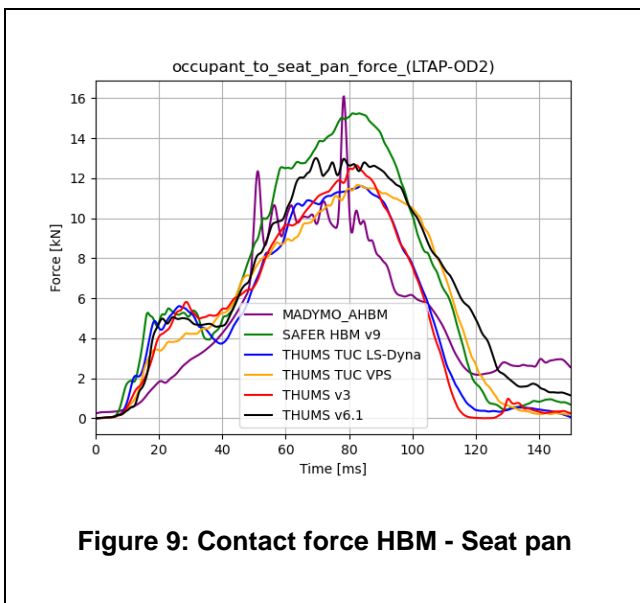
3.4.2.3   Seat

Seat Pan

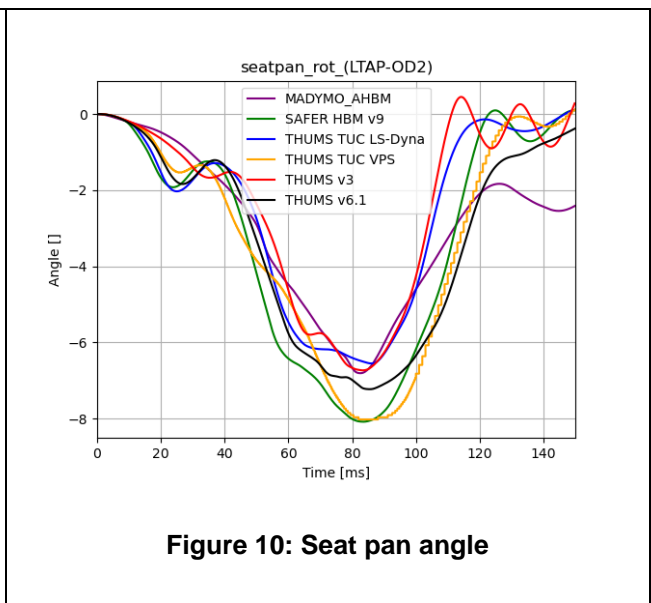**Figure 9: Contact force HBM - Seat pan**

Figure 10: Seat pan angle

The left graph in Figure 9 shows the contact force between HBM and the seat pan. The start of the force increase occurs at similar time for all models. The first maximum of the forces and the seat pan angle (Figure 10) at 20 – 30 ms is not seen in the Madymo and not that pronounced in the VPS. The first maximum of the seat pan angle for THUMS v3 is shifted in time. The maximum force level and maximum. angle differ for all models whereas the time at which the max. force and maximum angle occurs is similar in all models.

Sub Pan

Figure 11: Contact force HBM - sub pan

Figure 12: Sub pan angle
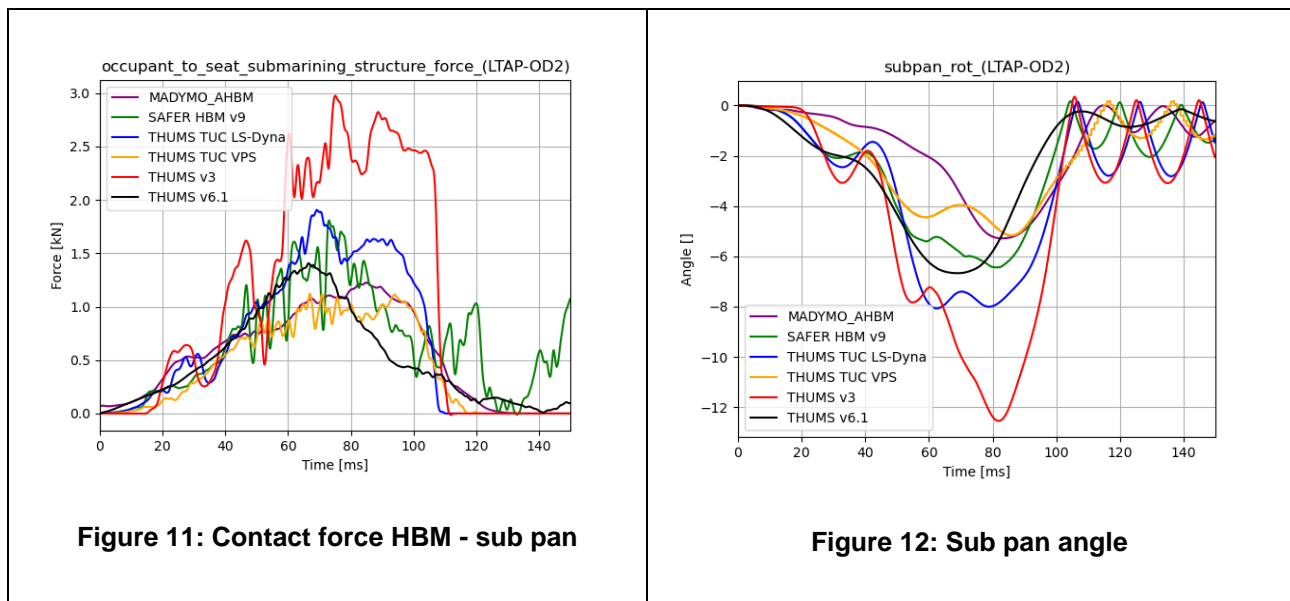
The force on the anti-submarining pan (Figure 11) is clearly influenced by the initial angle of the femur and whether the thighs are already in contact with the sub pan at the onset of the simulation. That depends on slight anthropometric differences in the buttock and thigh region as well as on the respective material properties of these soft tissues which, in addition, results in slightly different initial sitting positions in z-direction (see Figure 13).

Figure 13: Initial position of the HBMs depicted with anatomical landmarks
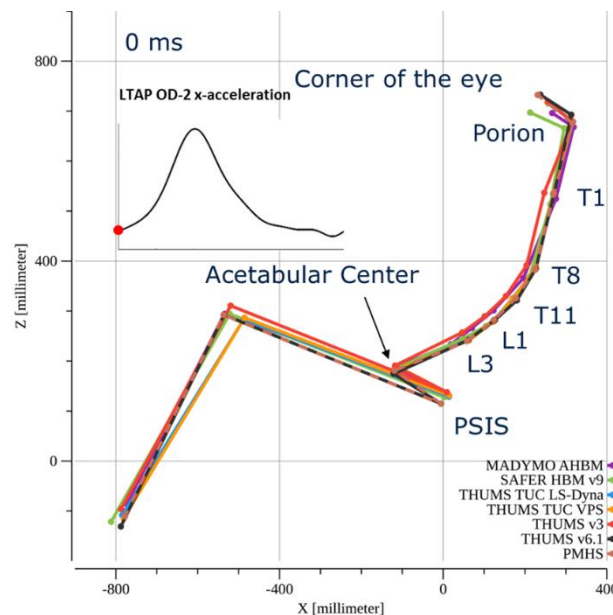
In case there is no contact between the HBM and the anti-submarining pan, the angle (Figure 12), as well as the contact force, starts to raise later but with a higher gradient and to a higher amplitude. This is the case of THUMS v3 at the beginning of the simulation.

Toe to pan resultant force

occupant_to_foot_support_force_(LTAP-OD2)
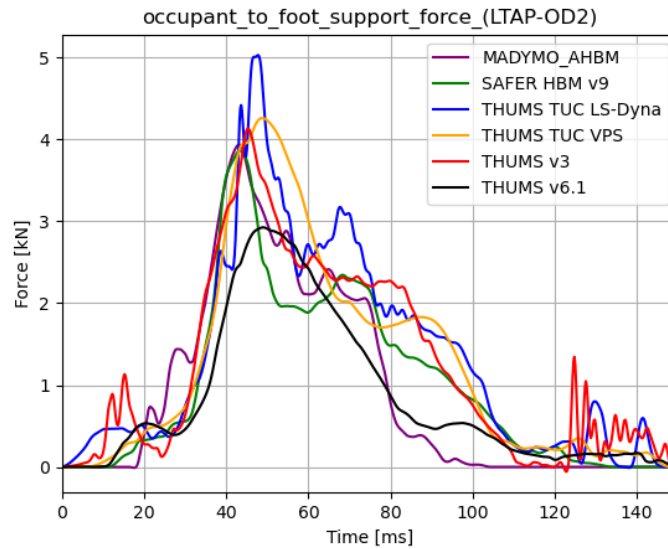
Figure 14: Contact force between HBM and foot support

The toe pan force (Figure 14) shows basically a similar characteristic for all models. The initial raise of the force (before 20 ms) differs in time due to differences in the distance between the foot and the toe pan. Although these distances are low, the time varies obviously, since the pulse, and therefore the motion of the sled is slow at the beginning.

3.4.2.4   Seatbelt system

Belt pay in/out shoulder belt retractor

Figure 15 Belt pay in/out at the shoulder belt retractor
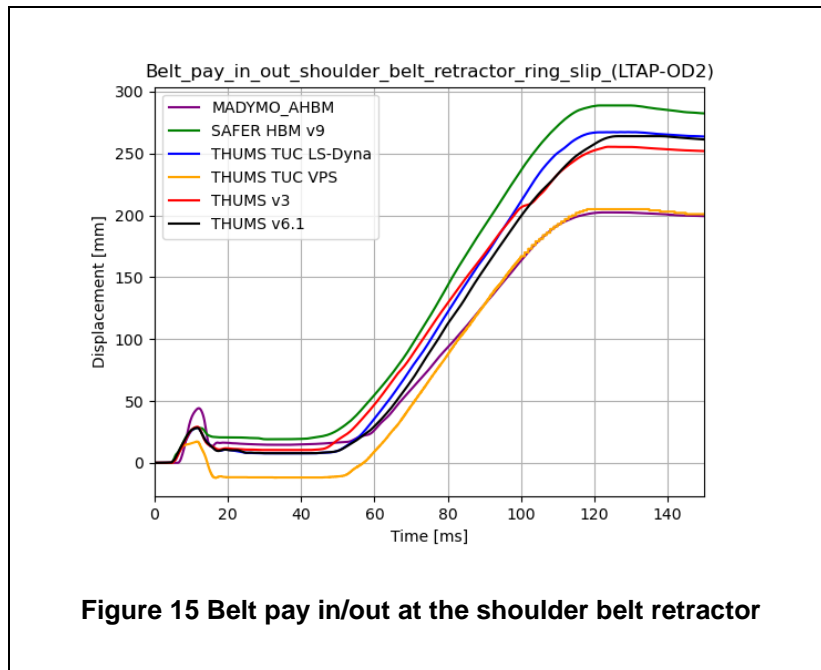
The shoulder belt retractor is fired at 9 ms. As shown in Figure 15 this activation time is applied correctly in all models. A small overshoot is observed for Madymo and in general the graphs correlate with the buckle pretensioning (Figure 18).

Belt pay in/out lap belt retractor

Figure 16: Belt pull in/out for the lap belt retract

Figure 17: x-position of the Acetabular centre
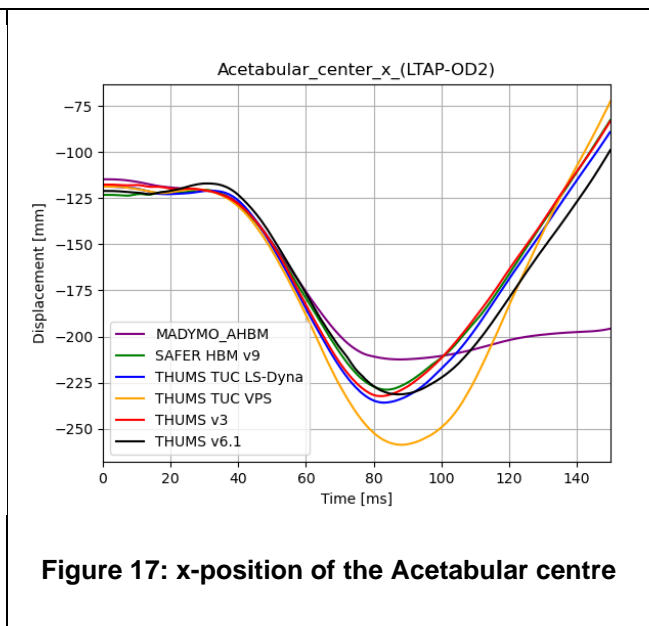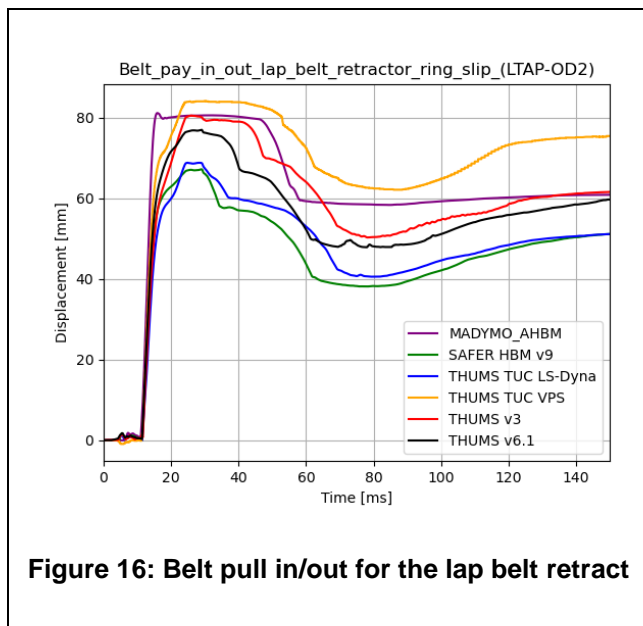
The lap belt pretensioner is fired at 9 ms, which works properly in all three codes (Figure 16). The maximum pull-in differs slightly between the models due to HBM model stiffness. As the forward motion of the HBMs differ, the belt pay out differ, too.. The pay in and out between 40 ms and the end of the simulation is correlating to the x-position of the pelvis. A significant forward motion of the pelvis starts at approximately 40 ms and the rebound starts approximately at 85 ms with a higher return for the FE models (Acetabular centre Figure 17).

Buckle pull in
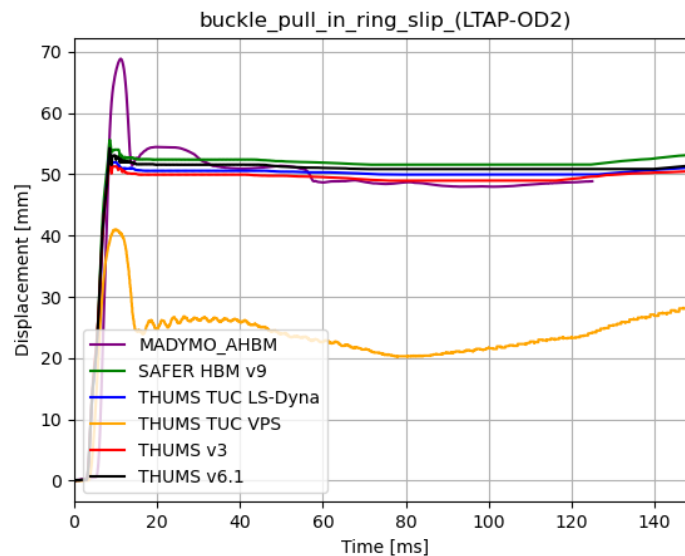
Figure 18: Buckle pull-in

The buckle is pulled in at 3 ms, which is the same for all three codes (Figure 18). The LS-dyna models reach the same level of pull-in as well as the Madymo model. The initial overshoot in the Madymo model might be caused by different modeling techniques in the MB model. In contrast, the VPS model shows a noticeable difference in the behavior of the buckle compared to the other models which results in an up to 30 mm less pull-in length. As the buckle applies a pre-defined amount of energy during pretensioning, the pull-in length is dependent on the resistance from both the occupant body parts and the two belt anchorages, but also from the initial belt slack in the models. Although this was aligned between the original model in LS-Dyna and its translation to VPS, the resulting pull-in length is different. In comparison, the belt forces in the B4, B5 and B6 locations (Figure 20. Figure 21 and Figure 22) match up well between the models during pretensioning, as does the outer lap belt pretensioner pull-in length (Figure 16). For the lap belt portion, the resistance to pull-in can depend on the stiffness difference in the soft tissue stiffnesses between the HBMs. Since the whole model was yet calibrated by the dummy simulation as reported in detail in Deliverable 2.5, the buckle pull-in in the VPS model could not be adapted for this comparison. A single change or adaption of the buckle pull-in, e..,. from 20 to 50 mm for the plateau phase after initial peak would be possible, but would also bias all other belt parameters. Hence, this difference needs to be taken into account for all other comparisons in the following. Further differences are expected for the VPS restraint model behavior due to its differences as far as the crash locking tongue or the sliprings are concerned.

Webbing transport through tongue

webbing_tansport_trough_tongue_ring_slip_(LTAP-OD2)
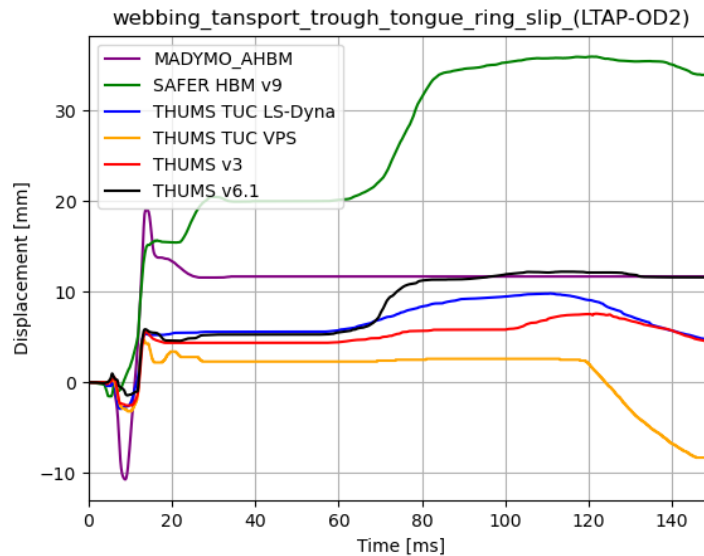
Figure 19: Webbing transport through tongue

The webbing transport through the tongue (Figure 19) depends from the differences in upper body and pelvis kinematics. At 40 ms a locking mechanism is activated, which is modelled different in all three codes. LS-Dyna changes the friction in the sliprings of the tongue, in VPS a model approach of applying two clamping plates for the 1D belt elements at the buckle was implemented (see Deliverable D2.5 [27]) and Madymo completely locks the transport through the slipring. Caused by the different modelling approaches and by different HBM kinematic and material properties, the webbing transport has a range of approximately 35 mm between the simulations. Basically, the occupant is restraint by the belt forces. For that reason, the focus when aligning the models is on reaching similar belt forces and a range for 35 mm in the webbing transport through the tongue is accepted.

Shoulder belt force (B2, B3)
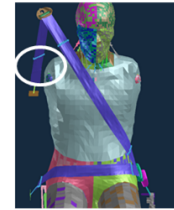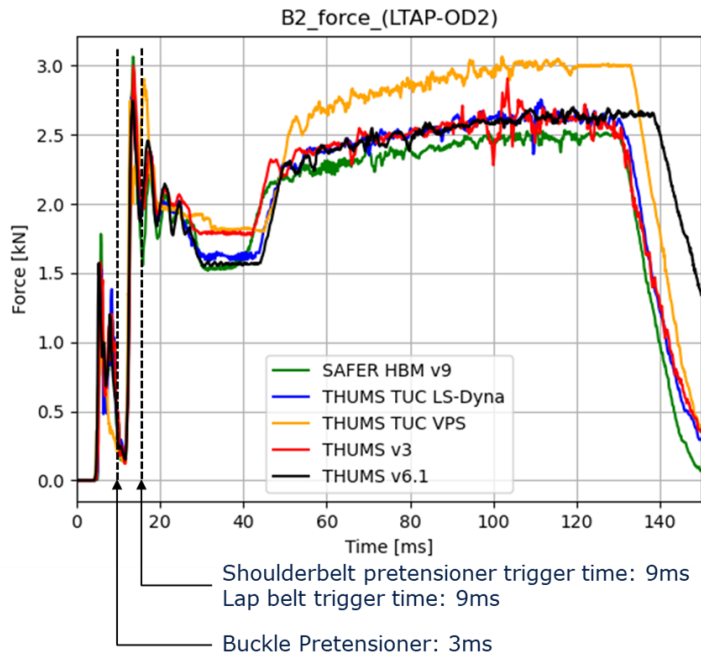
Figure 20: Beltforce at B2

Belt force at B2 shows the effect of the buckle pretensioner and the shoulder belt pretensioner for all models (Figure 20). Belt force is roughly at the same level for all the simulations. The differences, which are visible between 60 ms and 120 ms between the LS-Dyna and the VPS models also occurs in the dummy validation simulations (see Appendix B). That indicates, that the differences are environment model related and do not necessarily indicate a different behavior between the HBMs. The force at B2 is not available for the Madymo model.
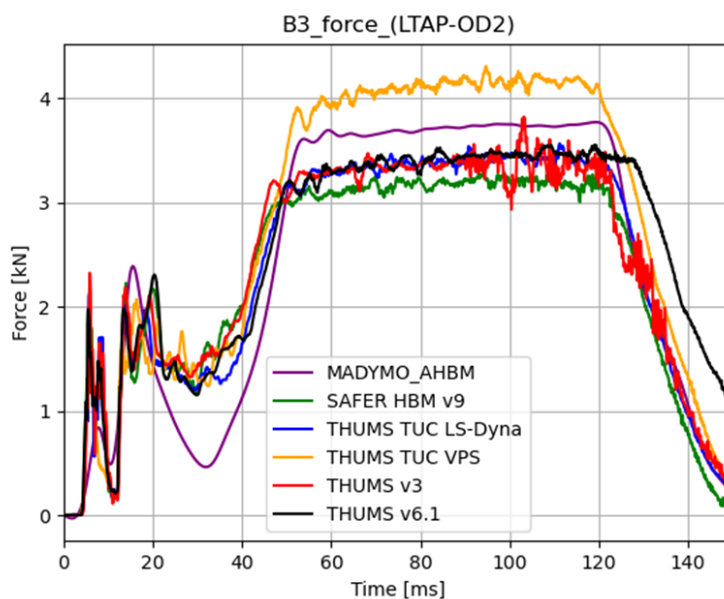
Figure 21: Beltforce B3

Maximum force levels of B3 (Figure 21) and B2 basically differ by the friction in the D-Ring. B3 is also available for the Madymo model and also shows the triggering times for the shoulder belt pretensioner and the buckle pretensioner.
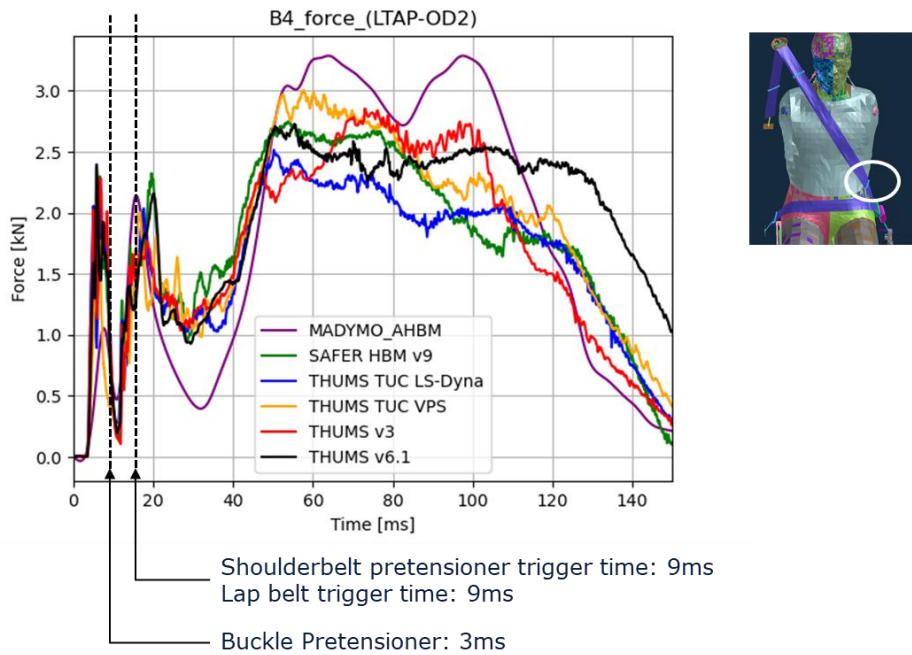
Figure 22: Belt force B4

The effect of the lap belt pretensioner and buckle pretensioner are similar for all models. Until 50 ms the forces (Figure 22) match quite well for the FE models.

Lap belt force (B5, B6)

Belt forces of B5 and B6 (Figure 23) show that lap belt and buckle pretensioner are working properly. Both forces correlate with the kinematics of the acetabular centre (Figure 24) in x-direction. The characteristic of the ASIS forces (Figure 27 and Figure 28) mostly matches with the characteristic B5 and B6 force (Figure 25 and Figure 26). It has to be considered, that several layers of soft tissues are between the ASIS section force definition and the belt.
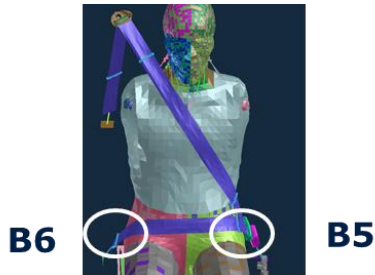
Figure **23**: Section forces at the lap belt
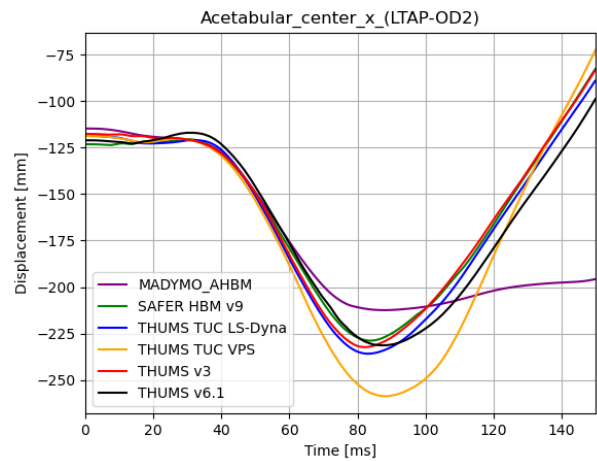
Figure 24: Coordinates (x) for acetabular centre

Figure 25: Belt force B5

Figure 26: Belt force B6

Figure 27: ASIS force (left)

Figure 28: ASIS force (right)
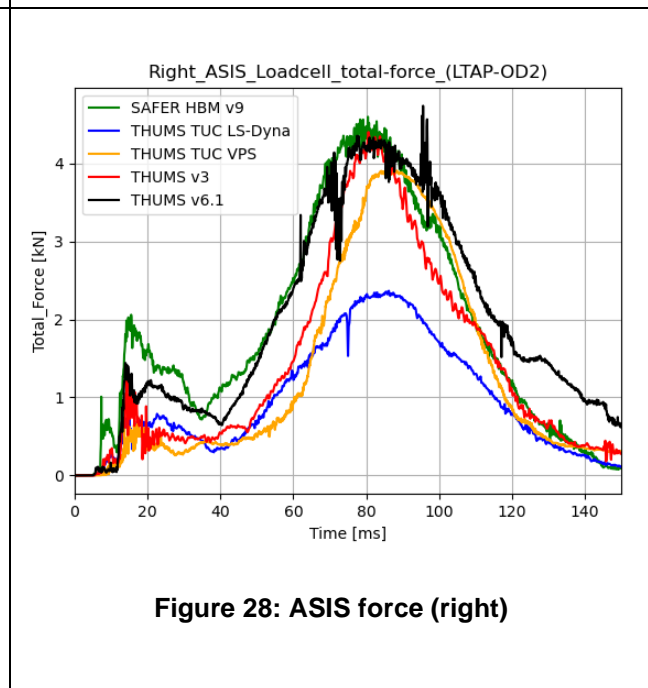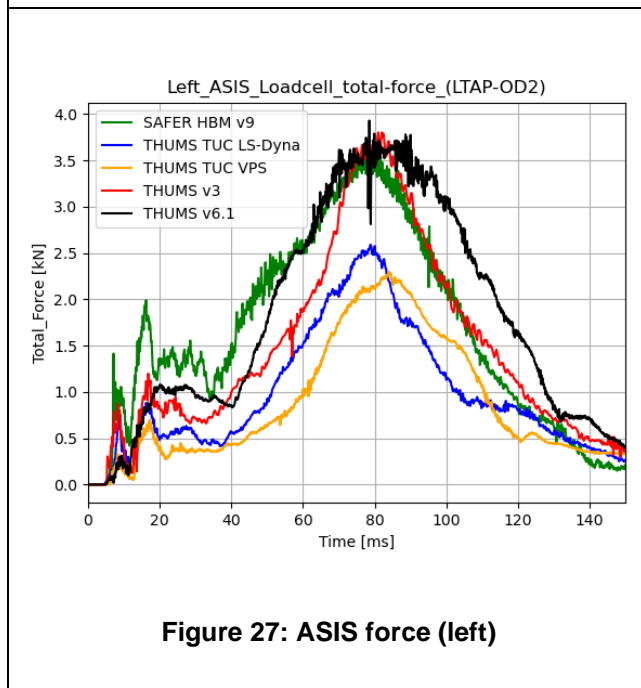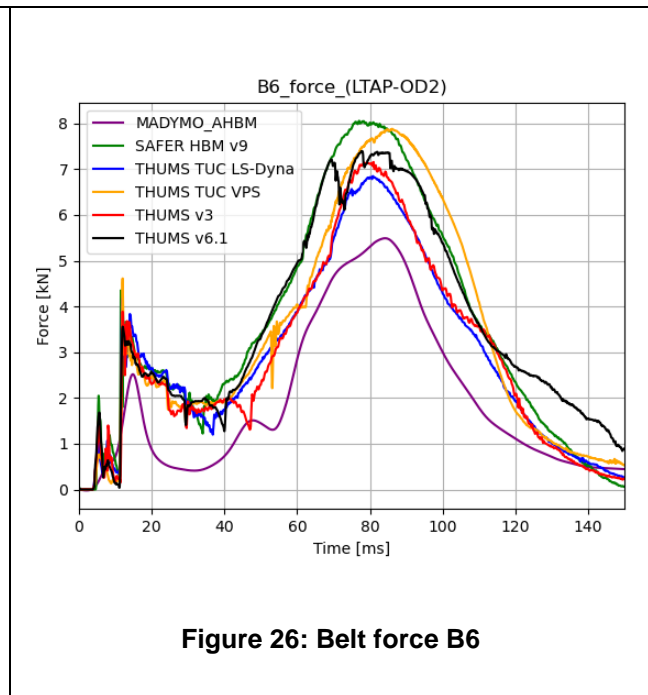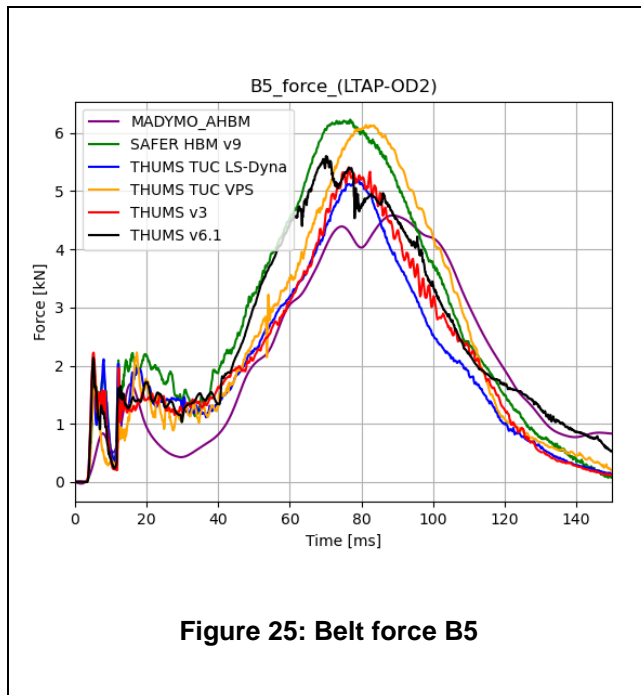
3.4.2.5   HBM kinematic assessment

The HBM kinematics are depicted using same main anatomical landmarks. For the purpose of better visualization, a time series of marionettes (defined by the landmarks) is shown in Figure 29. Diagrams with landmark coordinates as a function of time can be found in the Appendix A.

At time 0 ms, the HBM marionette is overlaid with the average marionette calculated from the PMHSs of Richardson et al. [1]. The HBM initial positioning was well aligned with the PMHS average one. HBM acetabular centres are very close to the PMHS acetabulum centre whereas more variation is observed for the Posterior Superior Iliac Spine (PSI), probably due to different pelvis geometries. Lower extremity landmarks of THUMS_v3 and both THUMS TUC show most difference with the PMHS marionette. The reason for the differences in the THUMS TUC models is a shorter upper leg length compared to the other models. For the head, variations are observed for the Porion-to-Corner

of the eye distance. The smallest distance is observed for Madymo AHM and the largest for SAFER HBM. The largest sitting height is observed for THUMS v6.1.
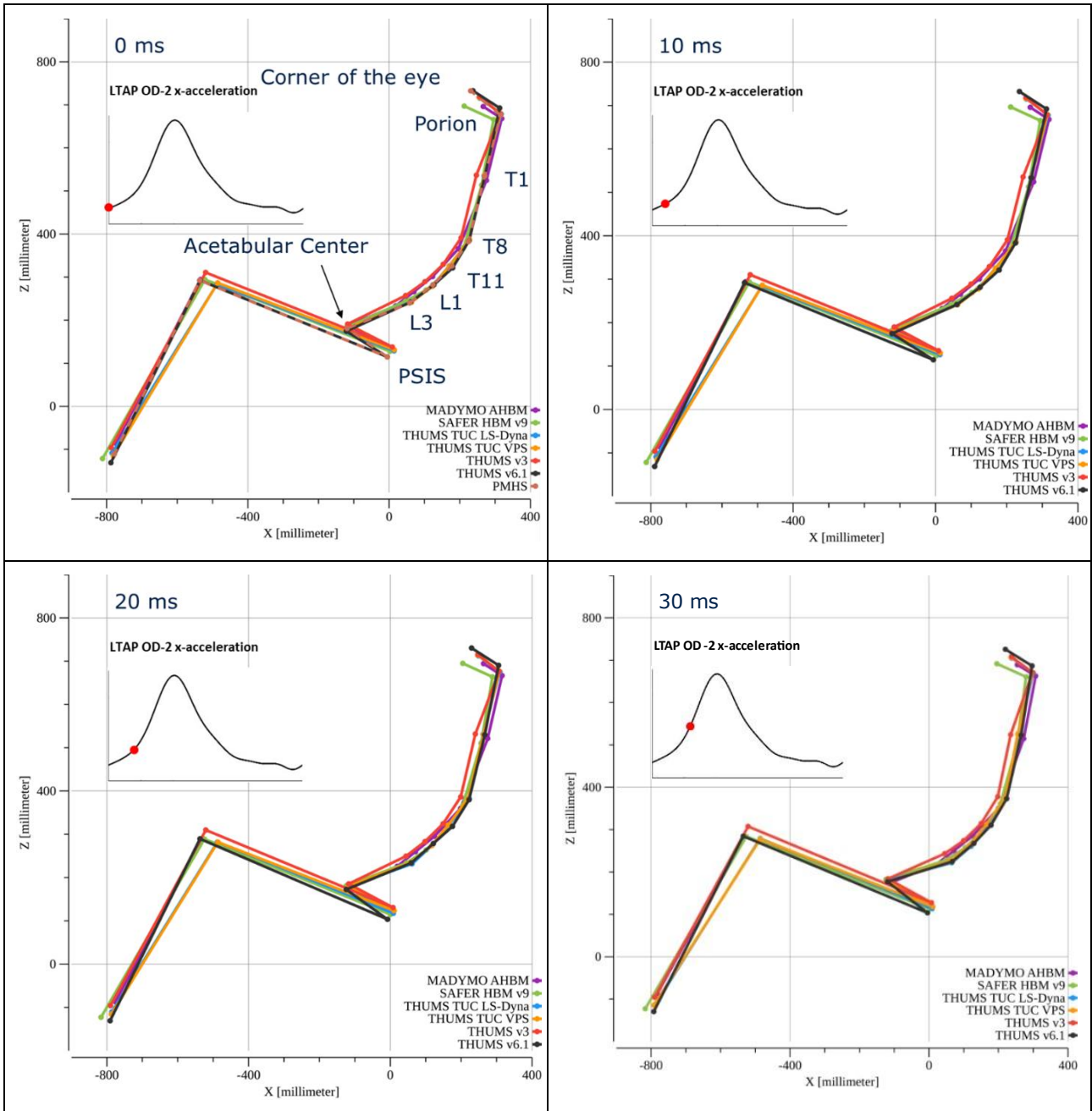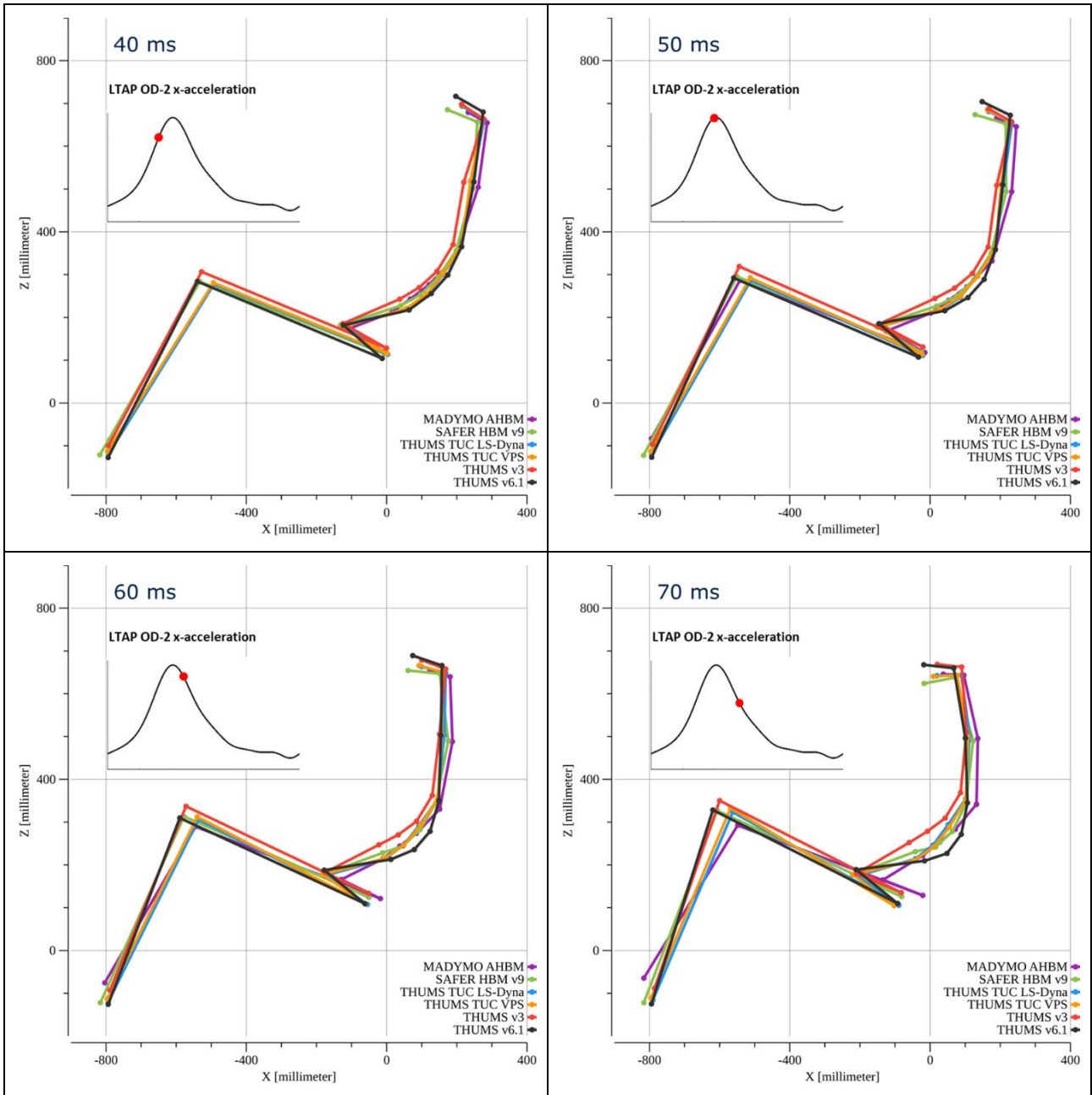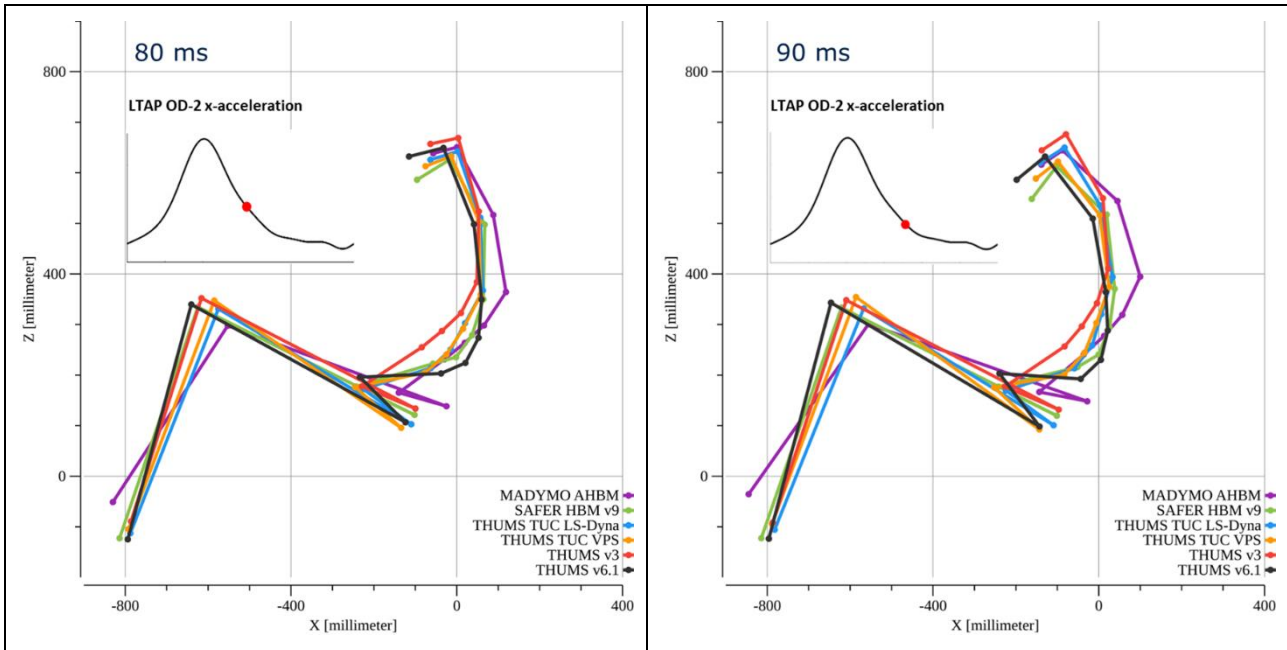
Figure 29: HBM kinematics represented by selected landmarks for LTAP-OD2 pulse

Up to 40 ms the motion and therefore the differences between the models are quite small. At 40 ms the forward excursion increases. During the forward motion different positions and different bendings are visible in the lumbar spine and in the lower thoracical spine: whereas the largest curvature is observed at L1 for SAFER HBM and THUMS v6.1, the largest curvature is seen at T8 for the other HBMs. That may result from different stiffnesses of the HBMs in these regions. Notably, the Madymo AHM has a lower acetabulum forward displacement and a different pelvis rotation compared to the other HBMs - this is most clearly seen in the rebound phase, post-80ms. Given the differences in anthropometry, belt modelling assumptions and numerical code types (including contact methods algorithms), it is impossible to draw conclusions on where the differences with the THUMS-based FE models arise.

The head excursion (Figure 30) between the models differs within a maximum range of approximately 100 mm, whereas the acetabular centre excursion differs by around 50 mm.
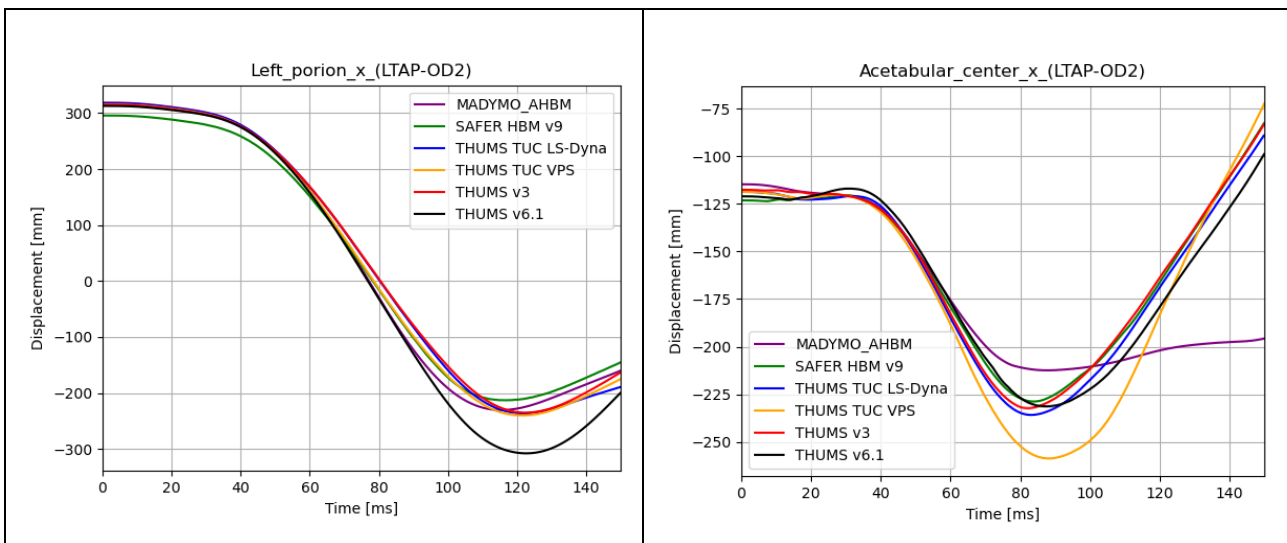

Figure 30: Forward excursion of left porion and acetabular center

As described in Chapter 3.2, THUMS v6.1 differs significantly from the other THUMS versions used for this study. Besides a more detailed description of thoracic and abdominal internal organs, THUMS v6.1 pelvis skeleton geometry and abdominal flesh thicknesses have been updated based on [35] and[38] respectively for a more human-like interaction between the pelvis and the lap belt. THUMS v6.1 has also a refined lumbar spine mesh and a more detailed modelling of the intervertebral discs and vertebras. The vertebras initially modelled as rigid bodies in THUMS v3 have been changed to deformable part and the disc material properties have been modified. Overall, THUMS v6.1 allows more bending in the lumbar spine due to a higher disc deformation which may partly explain the kinematic difference between THUMS v6.1 and other THUMS versions used here.

Similar improvements in the lumbar spine were also made for the SAFER HBM, where a more detailed modelling of the intervertebral discs, intervertebral ligaments and vertebras as well as new contact definitions [15][16] was implemented.

THUMS_TUC LS-Dyna kinematics in lumbar spine differs from THUMSv3.0. The differences could possibly have been due to the modifications made in the lumbar spine modeling to monitor the section forces in the spine. The vertebras are changed from rigid to deformable. The material properties assigned to the deformable vertebras are based on cervical properties used in the Strasbourg University Head Neck FE model [36]. A similar approach applies to THUMS TUC VPS, where lumbar vertebras were set as deformable as well, however, material parameter were taken from THUMS v4.02 VPS.

Following diagrams (Figure 31, Figure 32) demonstrate the differences between the HBMs concerning their anthropometry of the upper body. The length of the upper body from the Acetabular centre via the defined spine landmarks (L3, L1, T11, T8, T1) to the Porion shows a variation of roughly 6% (see Figure 31). That means, that the models are closer to each other in the sitting height then in specific anthropometric distances. Moreover, the documentation of the distances was useful to identify major differences in landmark definitions between the partners.
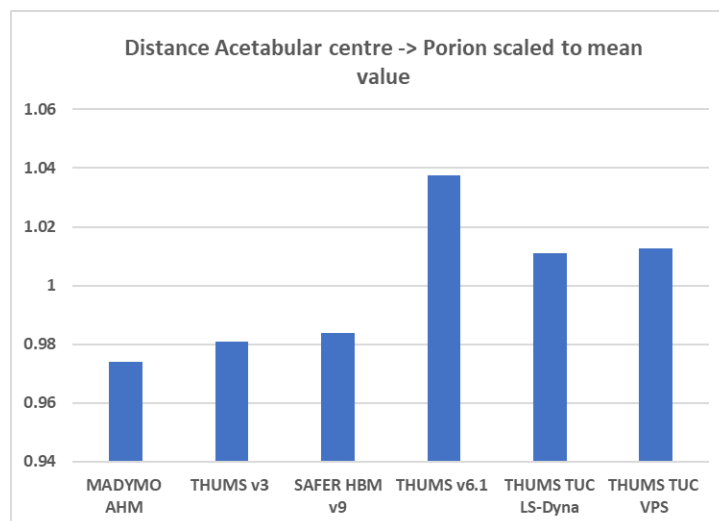
Figure 31: Distance of the acetabular centre to the porion (via spine landmarks) standardized to the mean value
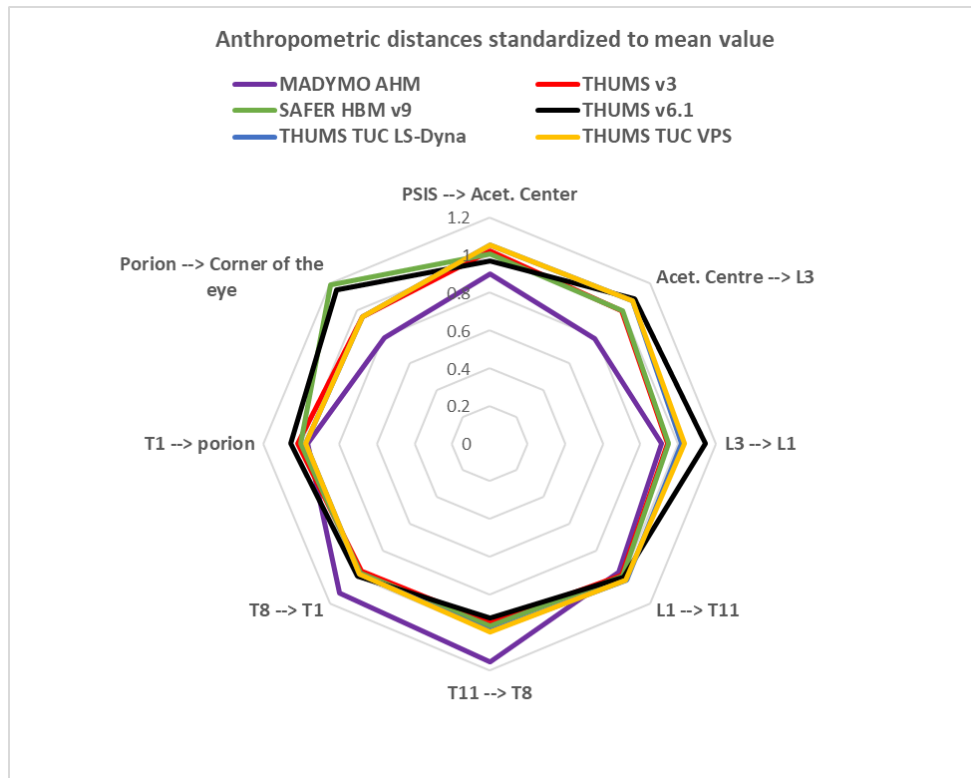
Figure 32: Distances between anthropometric landmarks of the upper body standardized to the mean value

3.4.2.6   Injury indicators and injury risk assessment

Injury indicators

Lumbar spine section forces and moments

The diagrams (Figure 33) show the maximum values for z force and y moments in the vertebras of the lumbar spine. The Madymo AHM and THUMS v3 were not included in this assessment as the involved modelling assumptions do not allow for spinal section forces to be extracted. Diagrams with force and moments as a function of time can be found in the Appendix A
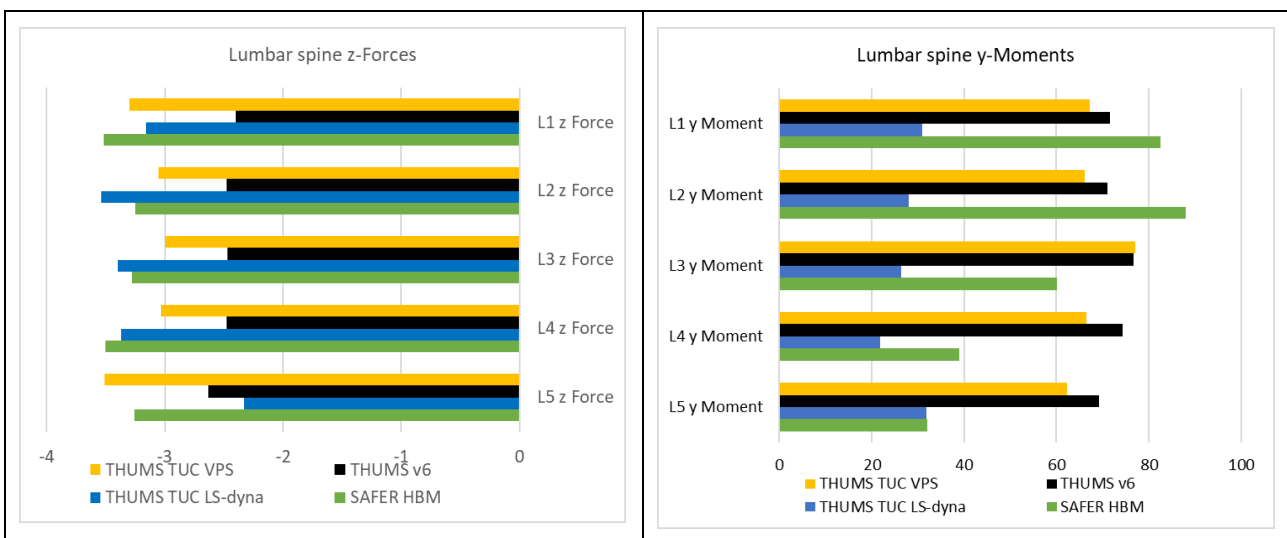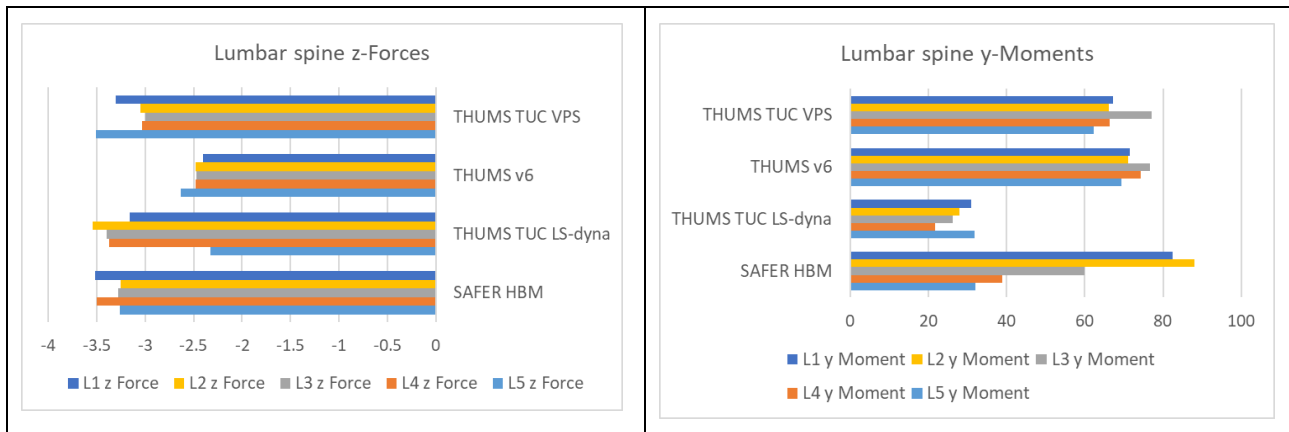
Figure 33: Lumbar spine z-forces and y-moments

The maximum moment for all models occurs directly after the maximum excursion, so at the beginning of the rebound, where the models show their maximum bending around the lap belt. A specific vertebra which shows the maximum moments or forces in all models cannot be identified. Differences between the models in the lumbar spine stiffness, as discussed above, are also affecting the forces and moments in the lumbar spine.

ASIS section forces

A relation between relative pelvis angle and the ASIS forces cannot be observed, as shown in Figure 34 and Figure 35. A positive pelvis angle represents a rearward rotation of the pelvis. Hence a high positive angel raises the risk for submarining.
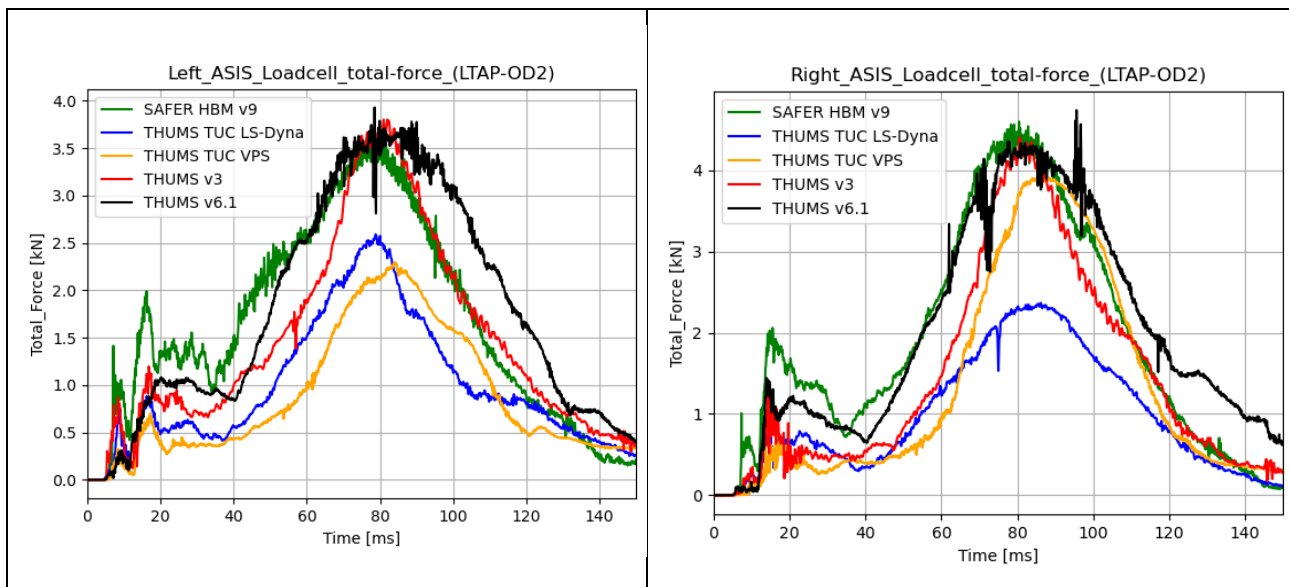
Figure 34: ASIS section force (left/right)
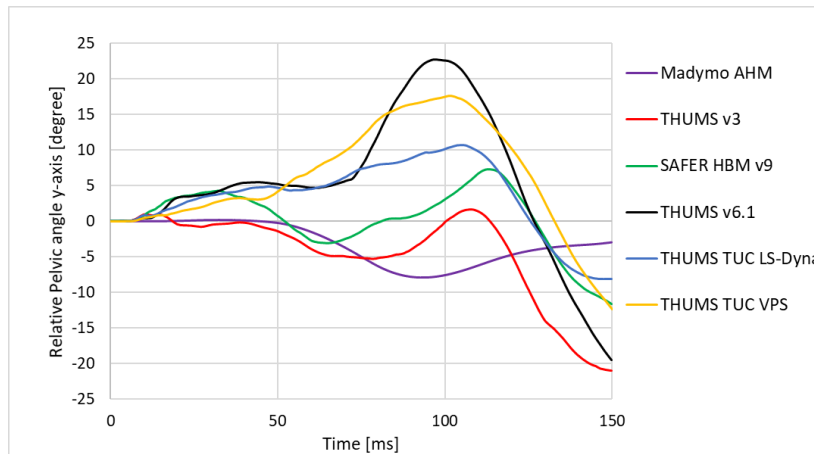
Figure 35: Pelvis rotation [degree]

Injury risk parameters

Head injury risks

Model	HIC15	HIC 15 AIS 2+	BRIC	BriC MPS AIS2+	SUFEHM [kPa]	SUFEHM_RISK [%]	A3MS
SAFER HBM v9	102	3%	0.68	75%	6.29	7%	37
Madymo AHM	136	7%	0.72	81%	5.27	6%	40
THUMS TUC LS-Dyna	117	5%	0.51	47%	5.02	6%	37
THUMS v6.1	202	19%	0.82	91%	5.01	6%	47
THUMS v3	108	4%	0.67	74%	4.96	6%	36
THUMS TUC VPS	106	4%	0.60	62%	5.87	6%	37

Table 2: Head injury criteria

In Table 2, the head AIS 2+ injury risk was determined from several parameters: head linear accelerations, head rotational velocities and using the SUFEHM tool [23][37]

The risk of sustaining an AIS2+injury by considering HIC 15 injury criterion is relatively small and ranging from 3% (SAFER HBM) to 19% (THUMS v6.1) across the HBMs. Higher risk values are generally found with HIC 15 in the case of a hard contact of the head with the vehicle interior which creates high head linear accelerations. As the homologation testcase does not include vehicle interior parts such as a steering wheel, a dashboard, A-pillar or door side structures, it was expected to have a low risk based on HIC 15 and A3MS values well below the 80 g limit.

Regarding BrIC, based on the rotational velocities only, and the SUFEHM tool, a very different risk is predicted: BrIC shows a risk going from 47% (THUMS TUC LS-Dyna) to 91% (THUMS v6.1) whereas SUFEHM tool predicts a relatively low and similar risk (6% to 7%) for all models.

Outlook to rib injury risk

The maximum rib strains per rib were assessed as suggested in Deliverable D 3.3 [22] for the LS-Dyna partners with DYNASAUR and for the VPS Users with a separate tool (TUC tool).

The strains are processed in the following way by the used tools:

- **DYNASAUR**
  - Datasource: binout (Output timestep: 0.2 ms) – shell elements are used
  - Exclusion (for output generation) of the following shell elements on each rib
    - posterior rib elements that risk unphysical (bone-to-bone) interaction with the vertebral spinous process
    - anterior rib elements located at the transition to the costal cartilage
    - elements sharing nodes with discrete elements representing ligaments or muscle insertions.
  - Determination of the maximum principal surface strain for each rib by DYNASAUR

- **TUC Tool for VPS**
  - Datasource: erfh5 file (Output timestep: 0.2 ms) – shell elements are used
  - Exclusion (for output generation) of the following shell elements on each rib (defined by the user)
    - posterior rib elements that risk unphysical (bone-to-bone) interaction with the vertebral spinous process
    - anterior rib elements located at the transition to the costal cartilage
    - elements sharing nodes with discrete elements representing ligaments or muscle insertions.
  - VPS determines the principal surface strain for each element and writes it to the erfh5 file
  - Determination of the maximum principal surface strain for each rib by TUC tool

A slight tendency can be observed, that the first and second right ribs have higher strains (Table 3), as the same ribs on the left side, caused by the belt interaction. Moreover, THUMS TUC VPS has higher rib strains in general which correlates with belt forces, which are higher for THUMS TUC VPS.
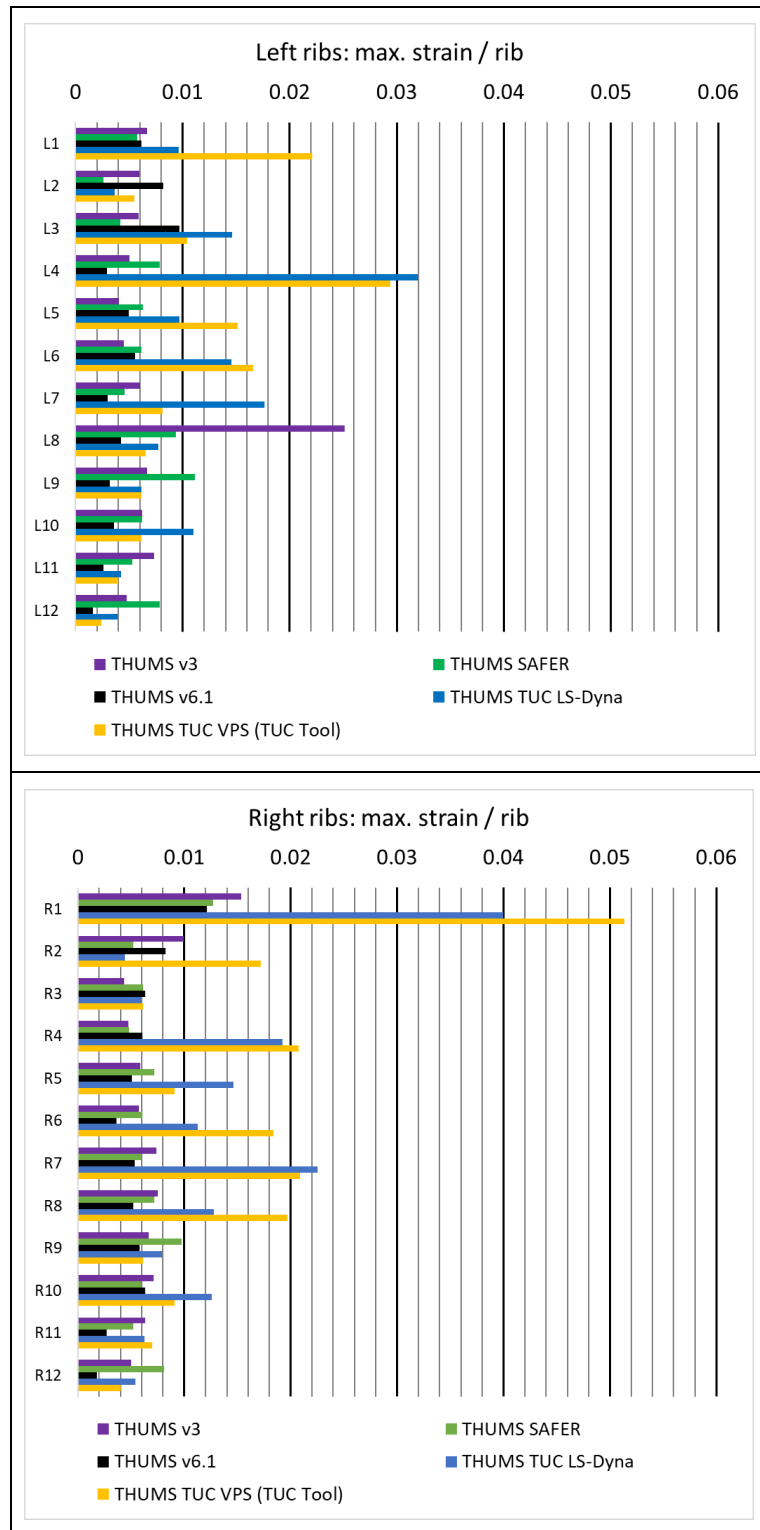
Table 3: Maximum rib strains per rib

A detailed comparison of the rib fracture risk between THUMS TUC VPS and TUC LS-Dyna is given in chapter 3.5

3.4.3 Summary for LTAP-OD2 simulations

Environment contact

Contact forces with the environment (seat pan, sub pan and toe pan) seem to be reasonable. Comparing the contact forces of the pan and sub pan with the respective rotation angles of the components also does not indicate any unexpected behavior or interaction. Buttock geometry and material properties affect the initial contact between the HBM upper legs and the sub pan.

Belt system

Firing times of pre-tensioners are similar for all models, as visible in the belt forces. Differences in the level of the belt forces are mainly visible between the different solvers, which are caused by differences in the environment. This is documented also for the comparison between the Full Frontal 50 kph pulse (FF50) simulations and the validation tests. (see Appendix B).

The belt forces of the lap belt correspond to the ASIS forces. The characteristic of the lap belt force over time also corresponds to the x-position of the acetabular centre.

HBM kinematics

Differences can be observed caused by the stiffness in the lumbar spine region. That results in different bending over the lap belt and influences also the forward excursion of the complete upper body. The range between the models in the forward excursion of the Acetabular centre is 50 mm whereas it is 100 mm in the Porion. Differences in the pelvis rotation are also observed, which can be further interpreted as different risk for submarining.

Summary for boundaries, dnvironment and HBM kinematics

Although the documented checks between the models show some differences, those checks neither indicate that the simulations are done under different boundary conditions (pulse, sitting position), nor that the environment models work different or that the HBMs kinematic is different besides explainable deviations.

For the mentioned reasons, the results are used to demonstrate parameters for injury indication and injury criteria for risk assessment.

Injury indicators and criteria

Head injury risk was determined with the SUFEHM as this allows the same assessment for both FE and MB models. It is shown, that the risks are small which is caused by the absence of vehicle interior in the sled model. As the results are consistent for all the HBMs, it is assumed that alignment in terms of injury risk prediction was done right for the head.

Rib strain assessment

The rib strains were assessed using two tools. The THUMS TUC VPS was assessed with the TUC tool, the LS-Dyna models were assessed with DYNASAUR. The steps to determine the principal surface strains are documented for both tools in chapter 3.4.2.5. Further action is required at this point to ensure the same process.

Lumbar spine z-forces and y-moments show differences in terms of maximum values between the models (see Appendix A), which are interpreted as the result of a different lumbar spines stiffness between the models. The characteristic of the lumbar spine forces is similar, which indicates an equal definition of the model output.

ASIS forces are similar concerning the characteristic of the force over time. Maximum values differ between the models. That might be caused by different soft tissue material properties and slightly different kinematics in the upper body which affects the balance between lap and shoulder belt load.

3.5 Selective comparison for THUMS TUC models in LS-Dyna and VPS

3.5.1 Motivation

In this section, the selective comparison of the THUMS-TUC models is discussed. The intention of this comparison is to analyse two HBMs which are identical in terms of anthropometry, geometry, nodes and elements in a comparable environment. The only differences between these two HBMs are due to the numerical implementation in the different software codes, namely LS-Dyna and VPS. During the development of the THUMS TUC model special focus was set on translatability between the codes as far as the material definitions are concerned. Further differences are expected for example due to differences in contact treatment. Nevertheless, these two different models can be defined as the most similar ones in this study.

Instead of the LTAP-OD2 pulse, as already shown in the previous chapter 3.4, the more challenging – in terms of maximum acceleration and hence loading to the HBM - full frontal 50 kph pulse (B Figure 65) was chosen for this analysis. Besides, this pulse excludes any rotational sled acceleration which would make the comparison even more complex. The environmental setup is the same as for the LTAP-OD2 simulations described in the previous chapter 3.4.1. Although, differences are to be expected since it was not possible to achieve a 100% comparable restraint system behaviour (cf. results obtained from dummy simulations in Deliverable D2.4 [26]), it was decided to compare kinematics, belt and contact forces as well as injury indicators between these two models.

3.5.2 Description of the model setup

THUMS-TUC v2020.01 50th percentile male model is used by Mercedes Benz and Volkswagen AG for conducting the evaluations within this section. THUMS-TUC v2020.01 model is available both in LS-Dyna and VPS codes. The models in both the codes are same in terms of weight and anthropometry, moreover, they do have comparable material properties to result in good correlation in validation setups, as exemplarily demonstrated in Figure 36.

OSCCAR positioning tool discussed in Deliverable D4.2 [4] was used for positioning both the models in LS-Dyna and VPS. It is important to mention that both, the models in LS-Dyna and VPS have the same nodes (nodal coordinates) and subsequently, have the same landmark points defined. The belt routing on the positioned model was conducted using the individual belt routing procedures discussed in Deliverable D4.2 [4] by Mercedes and Volkswagen. Figure 37 illustrates the initial position and the belt routing paths for both the TUC models in LS-Dyna and VPS. The different behaviour of the soft tissues during positioning to the reclined posture together with the individual belting process led to some differences as it is shown in Figure 37. The gap between the muscle tissue and the abdominal insert is approx. 15 mm smaller in case of THUMS TUC VPS. Furthermore, at 20 ms, a difference can be observed between the soft tissue deformations below the lap belt (Figure 38). The assessment and evaluation are conducted based on parameters defined in chapter 3.3 of this report.
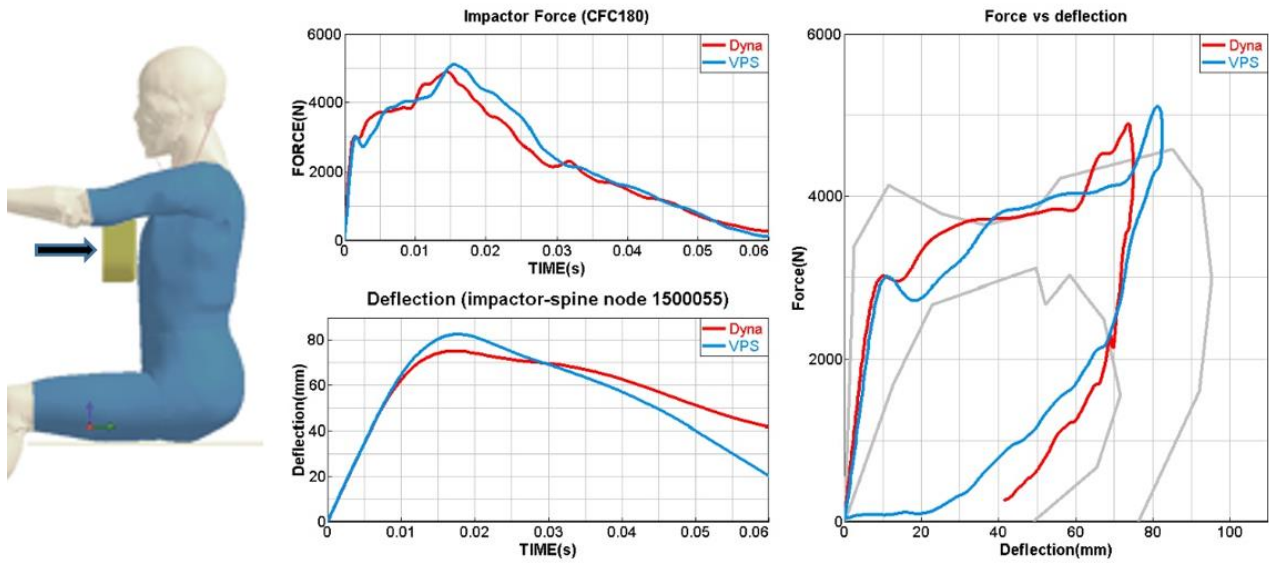
Source: THUMS User Community

Figure 36: Comparison of THUMS TUC models in VPS (blue) and LS-Dyna (red) in a chest impact setup according to [38][39][40]
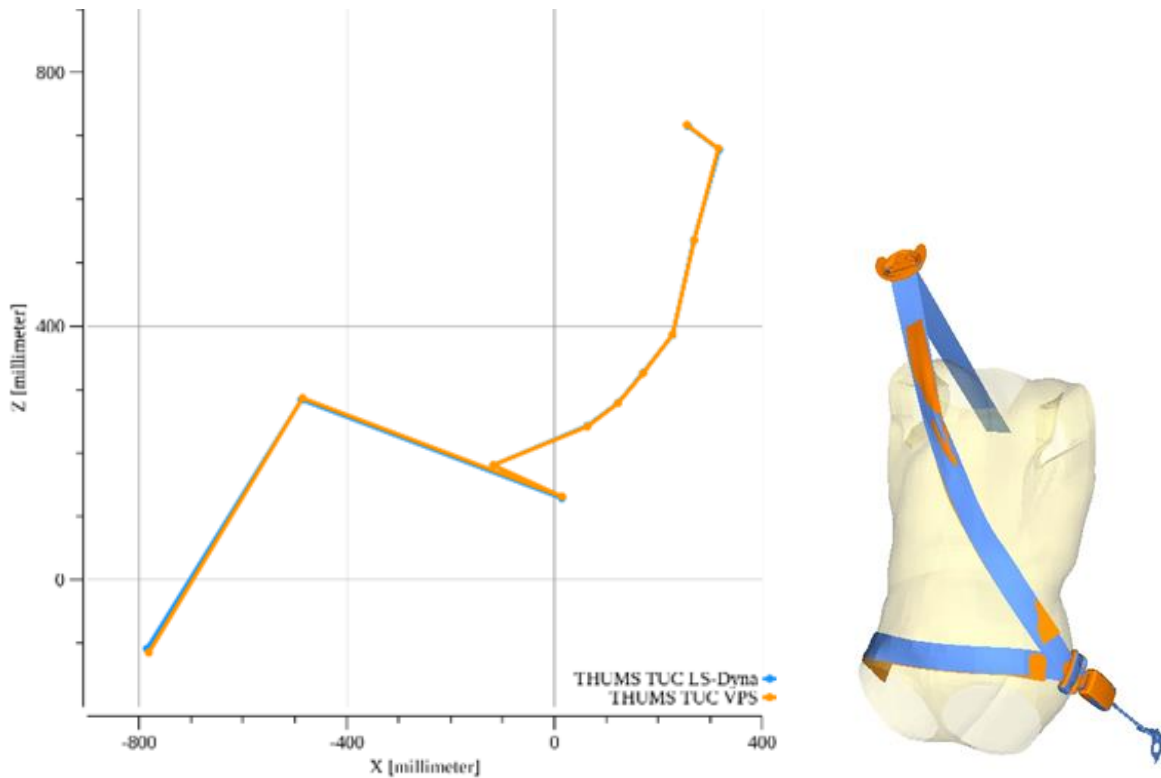
Figure 37: Initial position of the HBM based on the landmarks (left) and belt path of THUMS-TUC models in LS-Dyna (blue) and VPS (orange), (right)
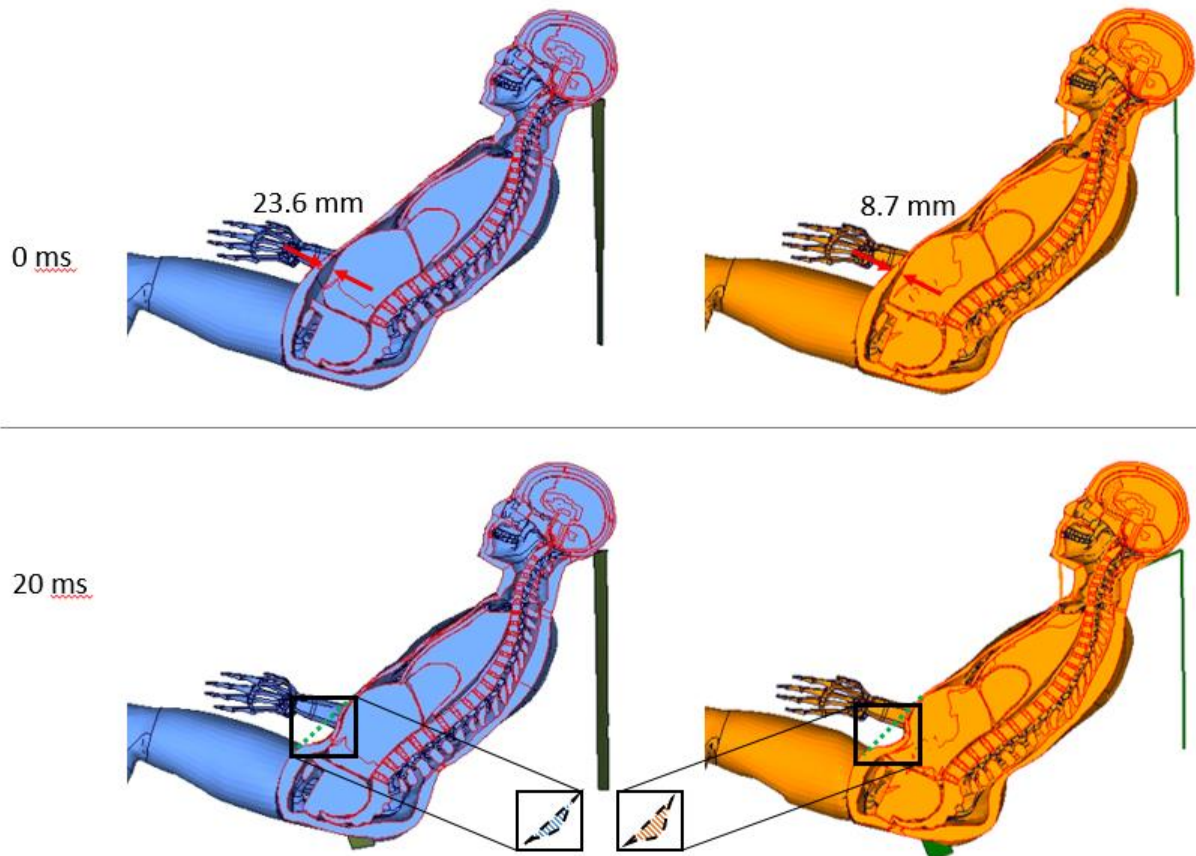
Figure 38: Section cut at the mid-sagittal plane through both HBMs, THUMS TUC LS-Dyna (blue) and THUMS TUC VPS (orange) at 0 ms and 20 ms

3.5.3 Simulation results and discussion

3.5.3.1   Positioning

The positioning of the models in LS-Dyna and VPS is conducted using the OSCCAR positioning tool. The initial position of both models is quite comparable as illustrated in Figure 37. However, a detailed comparison of the landmarks showed, that all the landmark points after positioning the model lie within 3 mm of tolerance, except in lower extremities. For the latter, the maximum deviation between the landmarks on the fibula bone is approximately 13 mm.

3.5.3.2   Basic model comparison

Table 4 shows the basic quality checks to assess the comparability of the two simulations. The total energy in both simulations differs by 1825 J and the hourglass energy is within 10% of the internal energy. The simulation models show relatively low mass addition and the drop-in time step is less or equal to 10%.

	LS-Dyna	VPS
Starting time step [µs]	0.7	0.7
Minimum time step [µs]	0.630	0.685
Total added mass [kg]	0.785	0.013
Total energy$_{max}$ [J]	28600	
Total external work$_{max}$ [J]		30425
Internal energy$_{max}$ [J]	2220	2116
Kinetic energy$_{max}$ [J]	25700	27331
Hourglass energy$_{max}$ [J]	201	154

Table 4: Overview of basic model parameter: time step, added mass and energies of both the models

3.5.3.3   Kinematic comparison

The HBM kinematics are depicted using same main anatomical landmarks. Figure 39 illustrates the overall kinematic comparison between both the models for the applied pulse. In general, the kinematics of both models are quite similar. However, some differences could be observed in the interaction with the environment. It is observed, that at 60 ms the kinematics deviate between the models. One reason is, that the soft tissues in thigh region are compressed more in case of the VPS model than in the LS-Dyna one (cf. Appendix C).
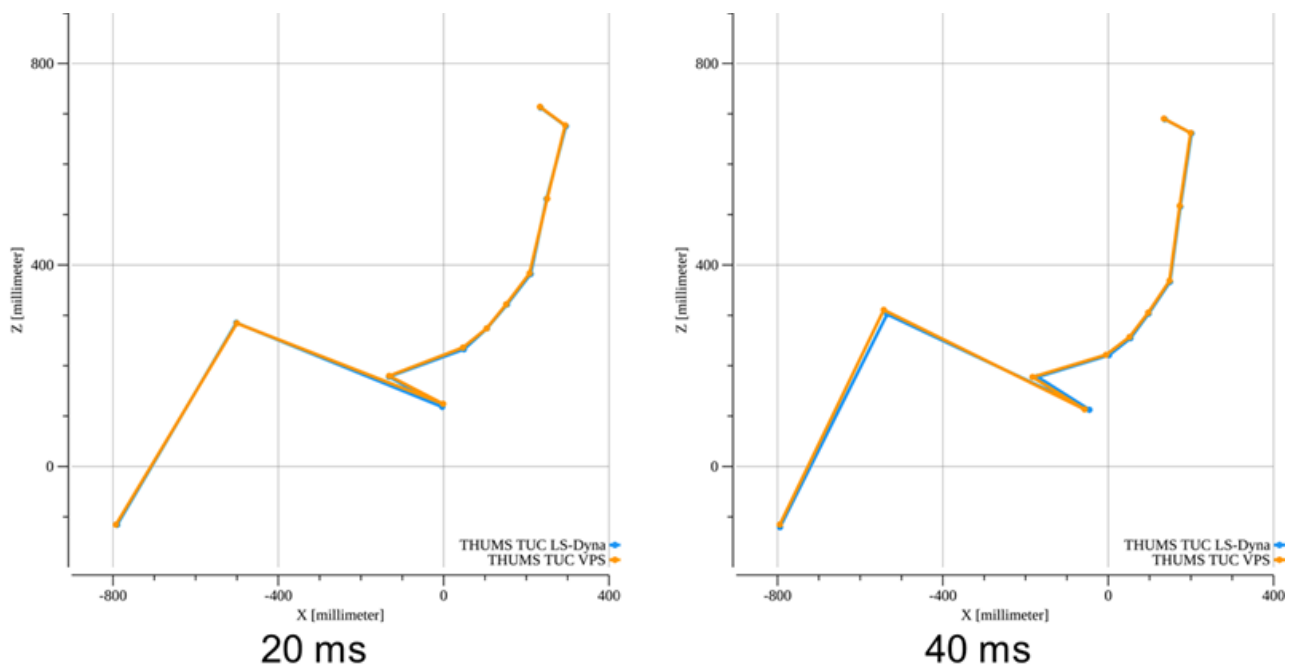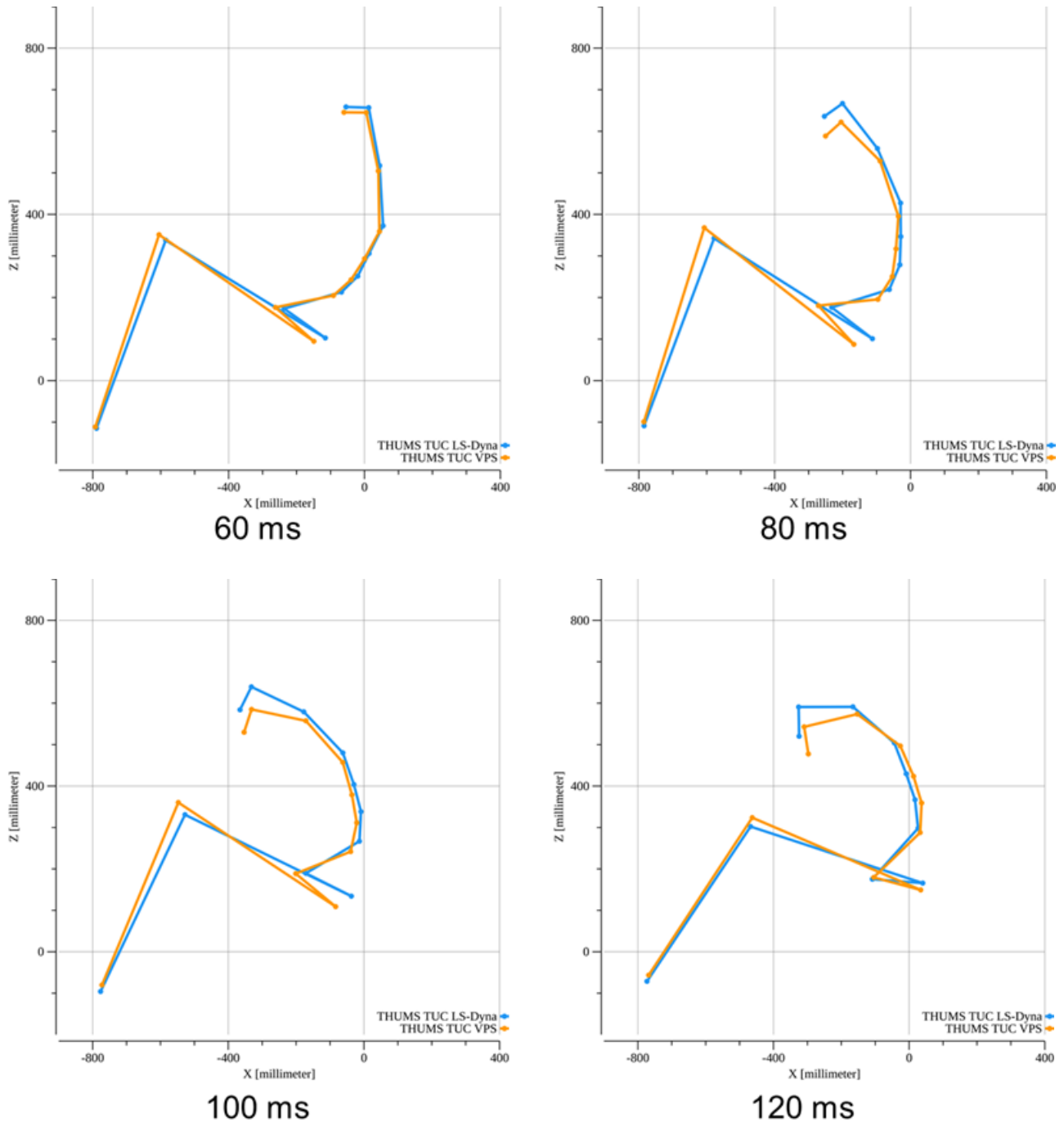
Figure 39: Kinematic comparison of THUMS-TUC models in LS-Dyna (blue) and VPS (orange)

Further detailed analysis (Figure 40) for the kinematics is performed considering only the spine, as this is one of the important focus body regions for reclined seating postures. Figure 43 illustrates, that lumbar forces in the z-direction are higher in LS-Dyna for vertebra L2 and L3, however, y-moments (Figure 42) are higher for all lumbar vertebras in the VPS. This could be attributed to higher seat pan rotation in VPS compared to the LS-Dyna supplemented by higher B3 forces in seatbelt (cf. Appendix B). This leads to larger movement of the pelvis in forward direction in the VPS model and similar greater flexion of the spine in the upper torso region. This combined phenomenon could be the potential reason for higher lumbar moments in VPS than in LS-Dyna. The lower rotation of the seat pan also leads to a more erect spine curvature in LS-Dyna and hence, higher forces in z-directions are observed in LS-Dyna evaluations. Shearing in the intervertebral discs at L2-L3 level

in LS-Dyna is observed which is not the case in the VPS model (Figure 41). This is evident from lumbar y-moment where a sudden drop in the moments is observed after 80 ms. Analysing the ligaments connecting the vertebral body, suggest that section force distribution in both the models occurred at different time and had different magnitude which leads to the curvature differences. However, the source of this could be attributed to multiple factors like the contact algorithms between HBM and foot-rest and seat pan during the positioning simulation.
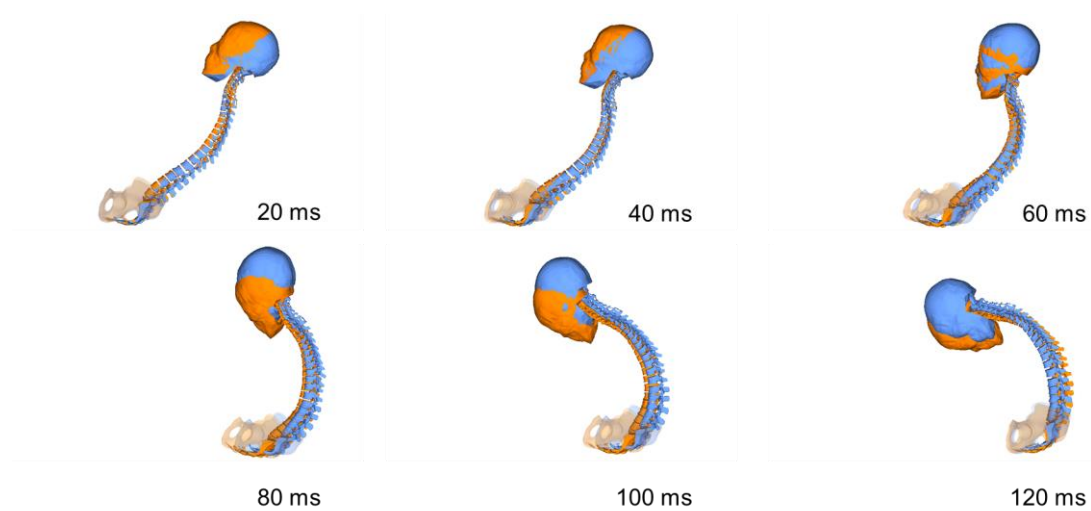
Figure 40: Kinematic comparison of THUMS-TUC spine models in LS-Dyna (blue) and VPS (orange)
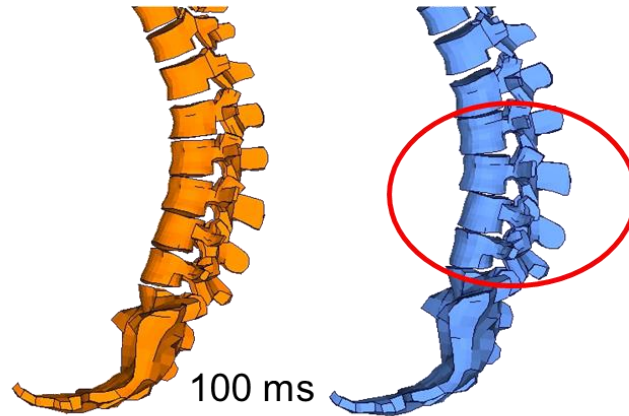
Figure 41: Shearing of lumbar vertebras in LS-Dyna (blue)
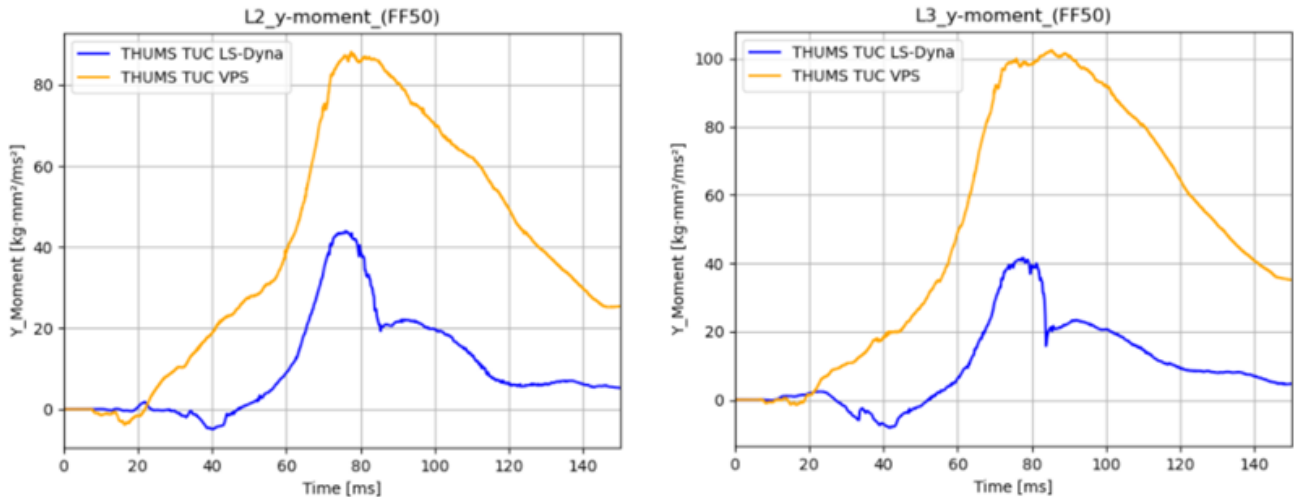
Figure 42: Lumbar y-moment comparison in LS-Dyna (blue) and VPS (orange)
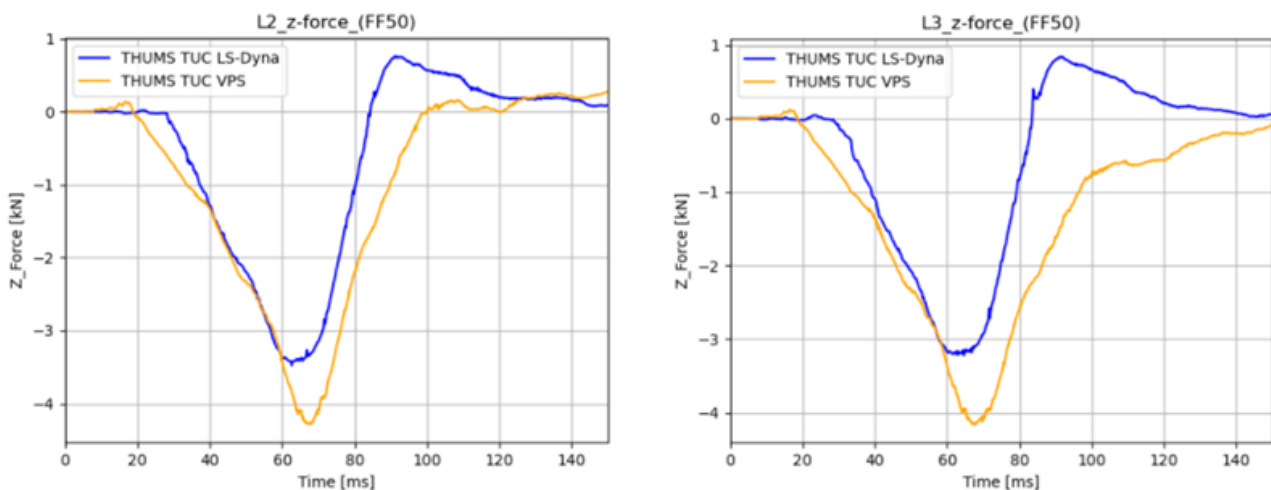
Figure 43: Lumbar z-force comparison in LS-Dyna (blue) and VPS (orange)

3.5.4 Comparison of injury indicators and injury risks

Figure 44 illustrates the rib fracture risk based on the Forman [24] criterion. In both the evaluations, the rib fractures are evaluated based on the rib injury risk implemented in the THUMS User Community rib fracture tool. In both the evaluations, rib elements are excluded based on the approach described in Deliverable D3.3.[22] The strains are extracted at the surface of every element of the rib and the maximum first principal strain for each rib is computed and forms the basis for rib fracture prediction. In the current evaluation, predicted rib fracture risks show a good fit between both LS-Dyna and VPS models. A detailed analysis of the rib strain reveals, that the loading on the first left rib is one of the strain generation regions. This strain is developed due to the stretching induced in the sterno-clavicular ligament (Figure 45), however, this element is not considered in the calculation of the rib injury risk. The other regions of high rib strains are on the posterior side of the first right rib due to loading from the seatbelt.
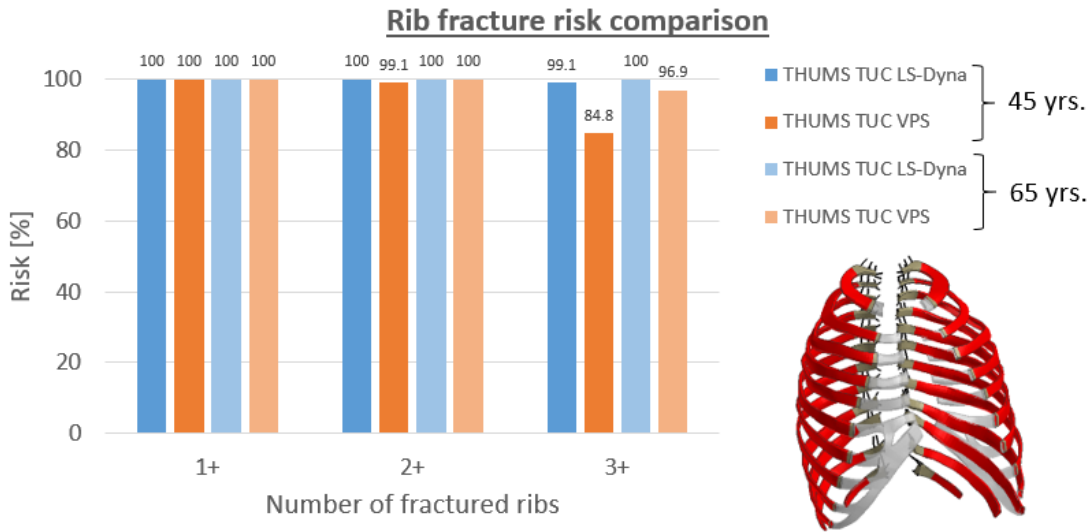
Figure 44: Rib fracture risk based on Forman [59] for age 45 and 65 based on selected elements of the ribs (red coloured rib regions)
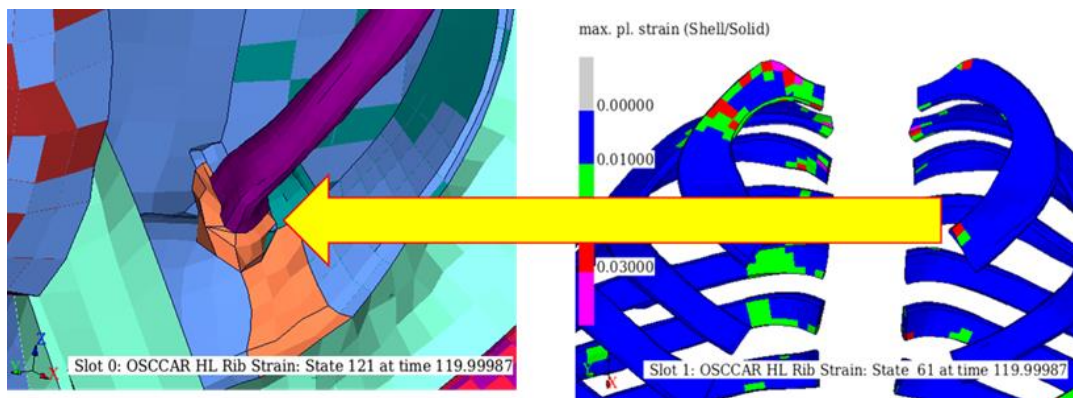
Figure 45: Max. plastic strain distribution on the upper rib cage

Table 5 illustrates the injury risks of the head for the evaluation. The risk based on BrIC and SUFEHM are comparable in both the evaluations. HIC15 and a3ms values are higher in VPS simulations than in LS-Dyna. The difference could possibly be attributed to the different belt loads experienced by the thorax in both the codes. Higher B3 belt forces in VPS translates to higher acceleration in the y- and z-direction in VPS between 80 and 100 ms (see Appendix B). The resultant acceleration in both models is quite comparable. However, higher x-acceleration is observed in LS-Dyna compared to VPS. This is compensated by the higher y- and z-accelerations in VPS (Figure 46).

	HIC_{15}	HIC_{15} AIS2+	HIC_{36}	a_{3ms}	BrIC	BrIC MPS AIS2+	SUFEHM MPS [KPa]	SUFEHM DAI risk
THUMS TUC LS-Dyna	196	18%	313	46	0.61	65%	9.7	9%
THUMS TUC VPS	229	24%	307	49	0.66	73%	7.3	7%

Table 5: Comparison of different head injury indicators and risk assessments
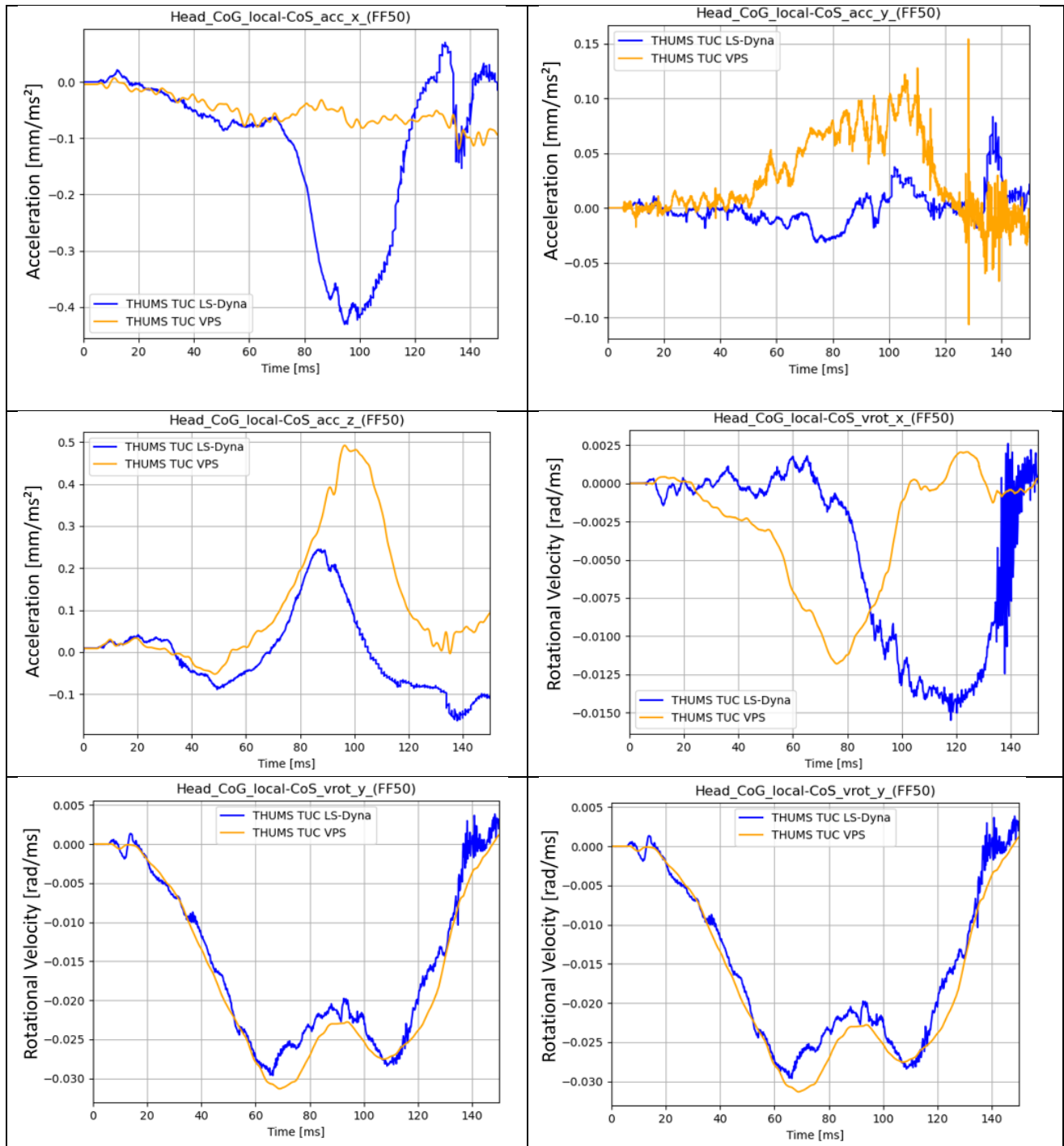
Figure 46: Comparison of the head translational accelerations and rotational velocities between LS-Dyna (blue) and VPS (orange)

3.5.5 Conclusion

Overall, both models, the LS-Dyna one as well as the VPS one, are well in agreement in terms of initial position, model responses like kinematics and finally injury prediction. The differences in the performance of the belt systems in the different codes (LS-Dyna vs. VPS) influence the overall interaction between the HBM and the environment, as previously outlined in the according subchapter (chapter 3.4.2.4). This means an important limitation in this comparative study. Ideally a generic belt system would have been used for this comparison, which would provide same

characteristics in both codes, similarly as it is the case for the semi-rigid seat model. Identical boundary conditions are required if it comes to a definition of a minimum desirable deviations between HBMs running in different software codes.

3.6 Continuous pre- and in-crash assessment

In addition to the definitions for in-crash simulations in 3.2 and 3.3, this chapter lists the necessary definitions and alignments for the pre-crash phase. In combination, that enables comparable continuous assessment.

3.6.1 Alignment for continuous pre- and in-crash assessment with HBMs

Alignments

- **Pulse transition between pre- and in-crash at t0**
  The x-acceleration at the start of the in-crash pulse, in its original definition, is zero, whereas the acceleration after the braking pre-crash pulse is 7.8 m/s^2. Thus, a gap in the acceleration at t0 would occur if the pre- and in-crash pulses are directly combined. In order to prevent numerical problems (and to keep the pulse realistic), a definition for the acceleration at t0 needs to be defined to ensure a continuous acceleration signal. See Figure 47.
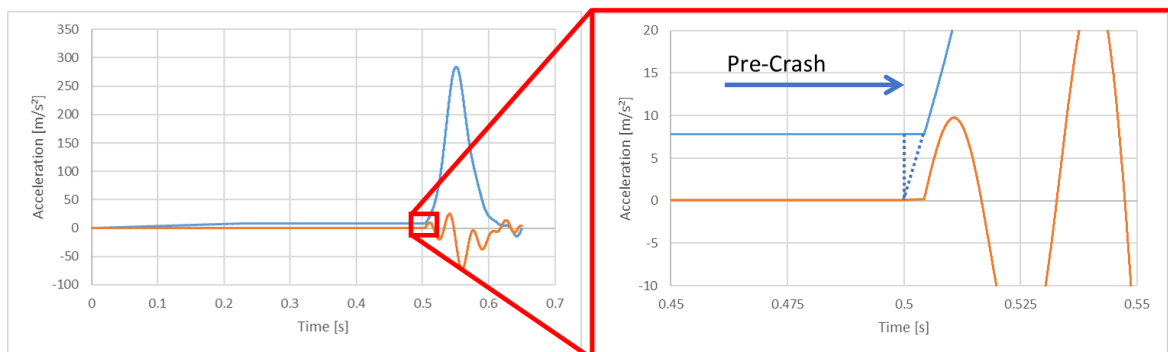
Figure 47: Combination of pre- and in-crash pulse

- **Seat preparation for pre-crash simulation**
  The same seat and belt model as described in chapter 3.4.1 is used. For the pre-crash simulations, a backrest is necessary to prevent the model from falling back, due to the lower longitudinal acceleration together with the pre-pretensioning during the pre-crash phase compared to the in-crash.

- **Initial HBM position**
  Depending on the controller concept for active models, pre-simulation time under the gravity action and without any additional acceleration pulse is necessary to initialize/stabilize the controller. During this time the position of the HBM changes, therefore, it is not possible to position different HBMs (with different controller strategies) to similar initial positions. The kinematics of the HBM during this pre-simulation phase is documented for the recommended landmarks (see chapter 3.3) to enable an interpretation.

Assessment and evaluation

- **Belt foces**
  To evaluate the proper (and harmonized) firing of pre-crash actions in the belt system and differences in the load level, the belt forces are evaluated.

- **Consider HBM pre-crash kinematics for in-crash simulation**
  To allow a comparison between continuous simulations, following parameters need to be aligned, or at least documented. That is relevant for models which use a transition between pre- and in-crash.

  - **HBM kinematics at t0**
    HBMs position and velocity

  - **Tension in the belt**
    The state of the belt concerning tension, pull out and contact with the HBM

  - **Stress/ Strains in the model**
    Stress and strain of HBM and environment (seat, belt)

  - **Activation of muscles**
    Status of active muscles during the in-crash simulation (on/off)

3.6.2 Description of the testcase

Environment

Additional to the seat (see chapter 3.4.1) a back- and a headrest were defined. Rigid shells were positioned tangential to the back and to the head of the HBMs and were attached to the sled (Figure 48).
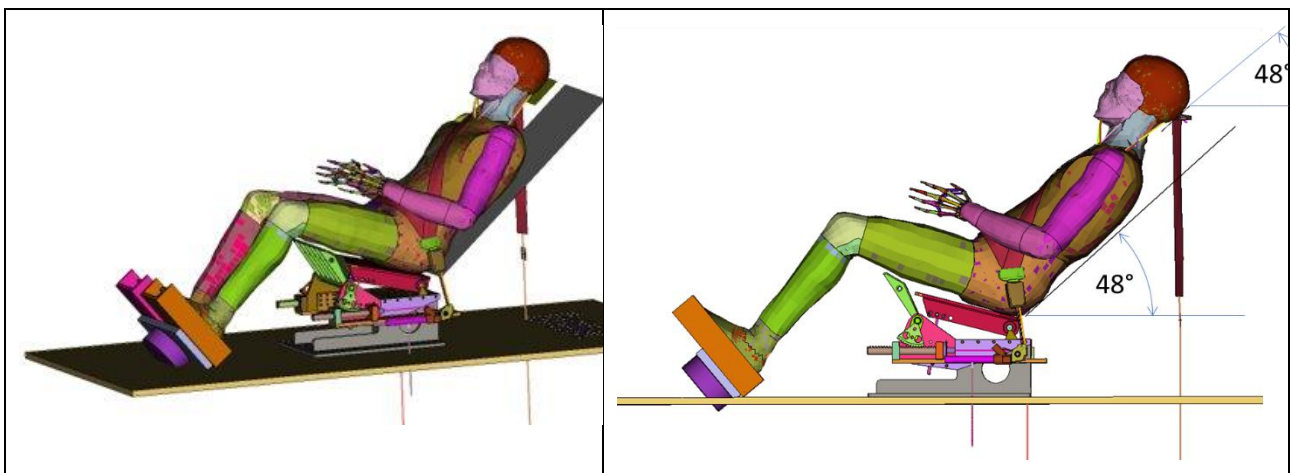
Figure 48: Environment including a head - and backrest for pre-crash simulation, shown here for THUMS v3

Environment

The LTAP-OD2 pulse is combined with a pre-crash pulse (in x-direction only), which is similar to the pre-crash pulse in Deliverable 2.4 (Figure 49).
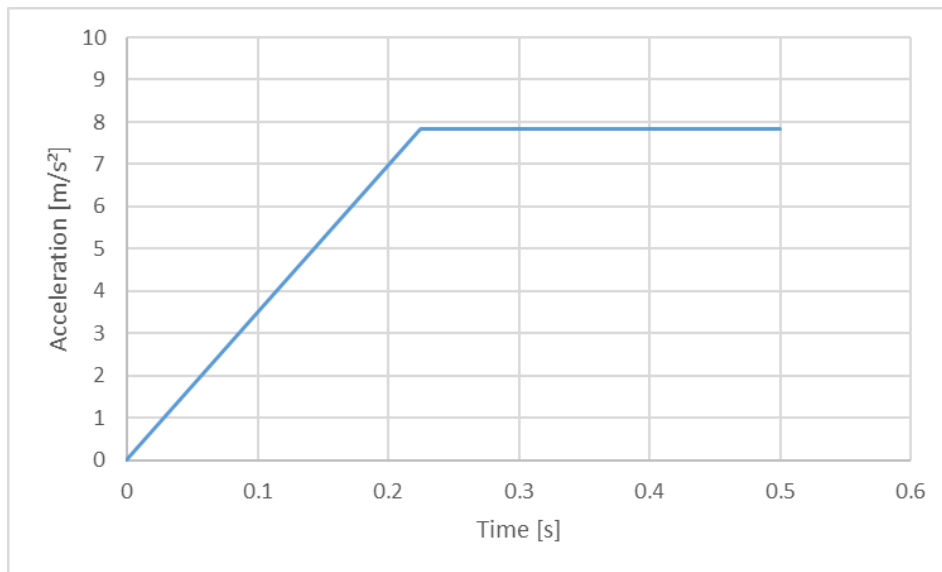
Figure 49: Pre-crash pulse

3.6.3 Demonstration for LTAP-OD2 simulations

Chapter 3.6.1 list the definitions for a combined pre- and in-crash simulation with HBMs. Following diagrams document the conducted simulations.

Pre-crash pulse (Figure 50**), In-crash pulse(**Figure 51 **and** Figure 52**) and definition of the pulse at t0**
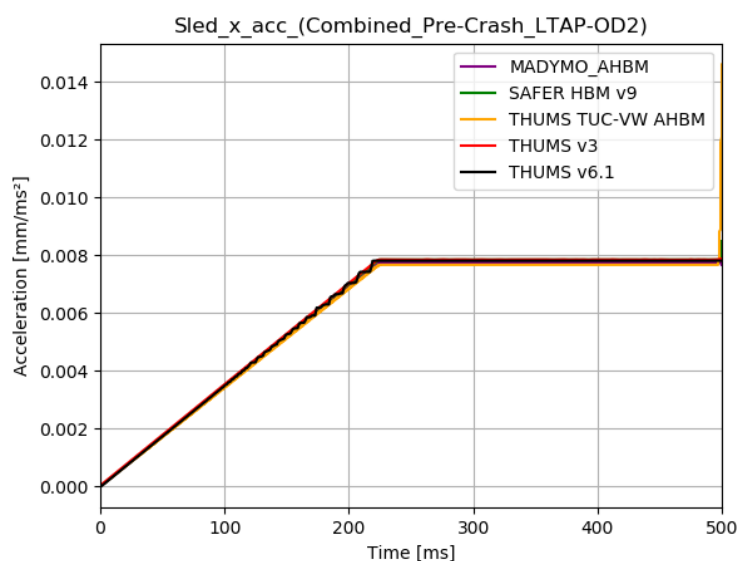
Figure 50: Pre-crash sled x-acceleration
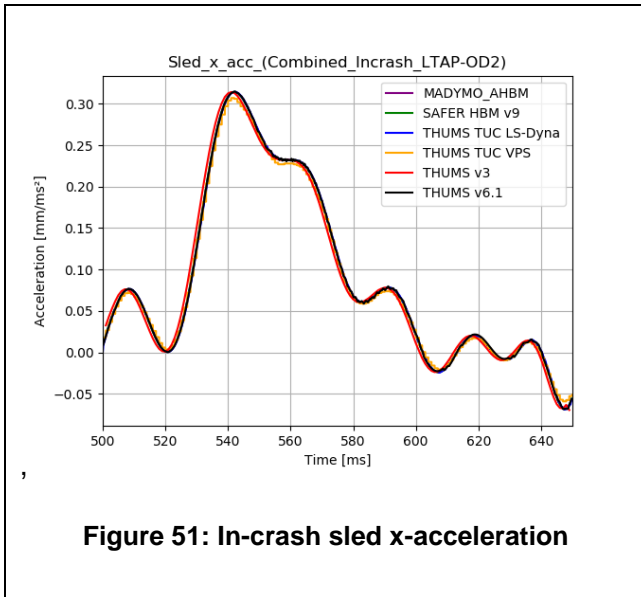
Figure 51: In-crash sled x-acceleration
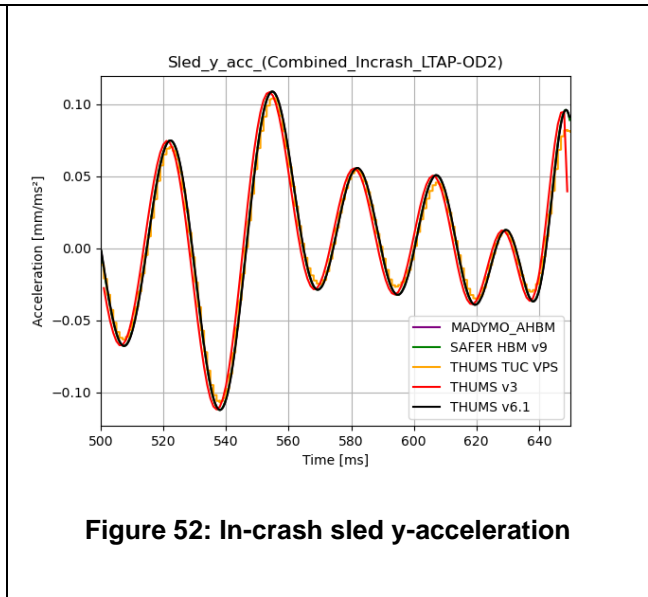
Figure 52: In-crash sled y-acceleration

Continuous HBM kinematics

Exemplary for the combined pre- and in-crash kinematics, Porion and Acetabular centre are selected to demonstrate the continuous simulations and assessment approach (Figure 53).
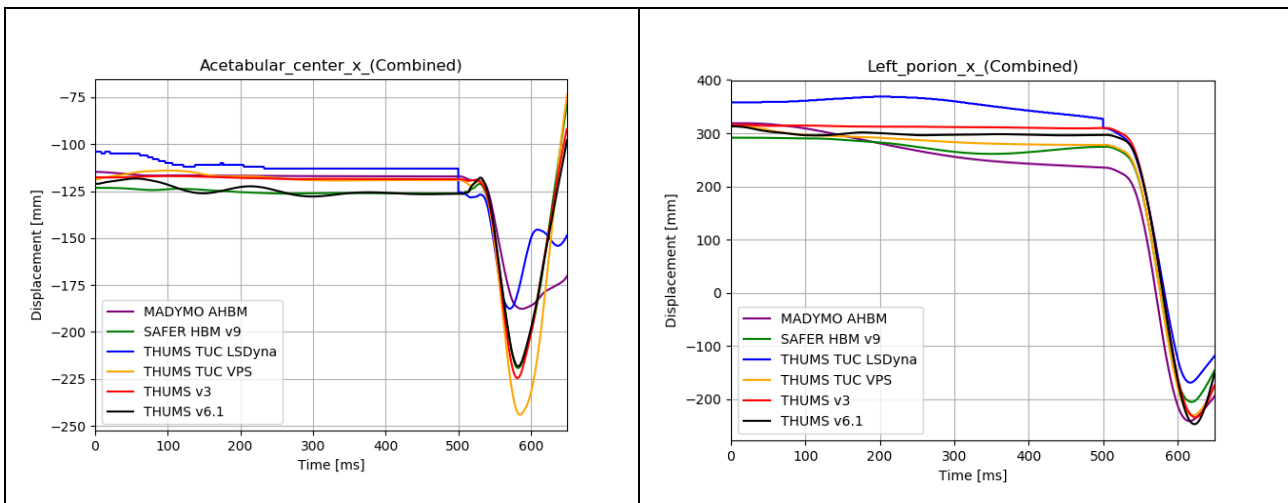
Figure 53: Combined pre- and in-crash x-position for Acetabular centre and left porion

Initial HBM position and muscle settling time for active models

Depending on the controller strategy, some models require an "settling time" to stabilize the HBM muscles prior to a prescribed acceleration pulse. Table 6 reports the respective times. During the activation time, the models change their position slightly as documented in Figure 54. The kinematics during the activation time is documented in this report, since it causes some differences in the initial position. It was not the goal of this task, to assess the used controller strategies.

Modell	Activation Time [ms]
SAFER HBM v9	300
THUMS v6.1	500

Table 6: Activation time for active HBMs
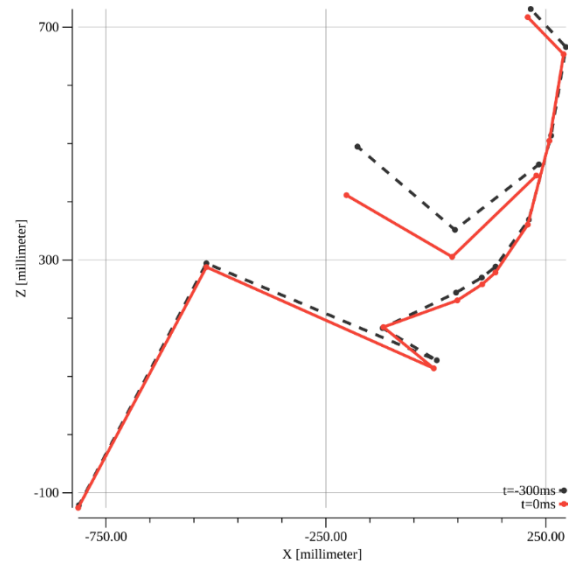
Figure 54: Influence of activation time for SAFER HBM v9

Details of HBM approaches for pre- to in-crash simulation

Table 7 summarizes the used controller strategies and HBMs concerning the definitions in chapter 3.6.1. at t0 (start of crash).

	Madymo AHM	SAFER HBM	THUMS v3	THUMS v6.1	THUMS TUC LS-Dyna	THUMS TUC-VW AHBM
Continuous (C) / Transition approach (T)	C	C	C	C	T	C
HBM velocity at t_0	yes	yes	yes	yes	yes	yes
Stress/Strain at t_0	n.a.	yes	yes	yes	no	yes
Tension in the belt at t_0	yes	yes	yes	yes	yes	yes
Activated muscles during in-crash (no/constant/controlled)	constant	controlled	no	no	no	controlled

Table 7: Used controller strategies / HBMs

Environment

Belt forces and pull in/out during pre-crash

Table 8 shows the belt forces for B2 to B6 during the pre-crash. The activation time of the pre-pretensioner is similar for all models at 50 ms, which is clearly visible in the diagrams.

Table 8: Belt forces

Figure 55: Shoulder belt pull in of pre-crash phase

Figure 56: Lapbelt pull in of pre-crash phase

Figure 57: Buckle pull in

Figure 58: Webbing transport through tongue
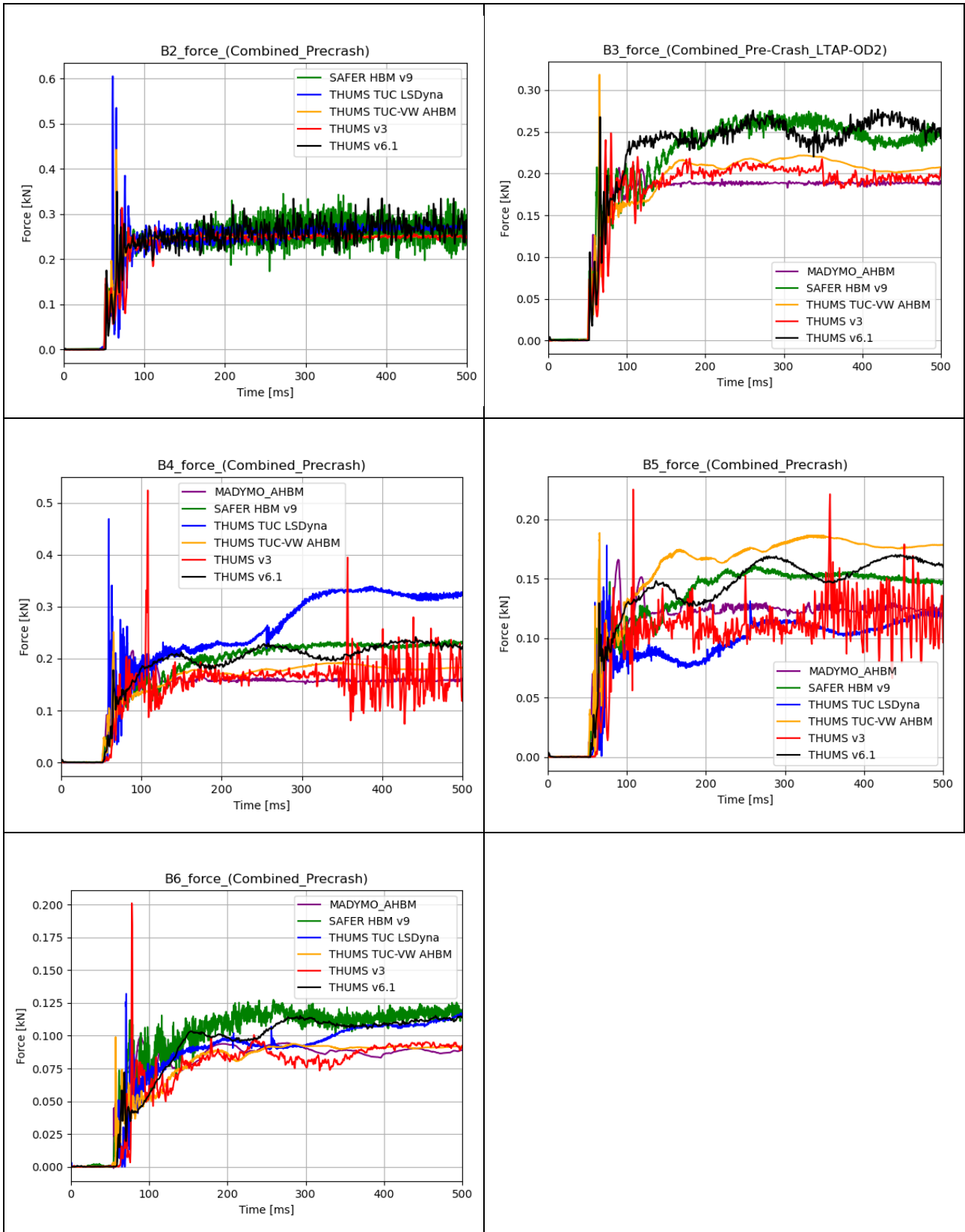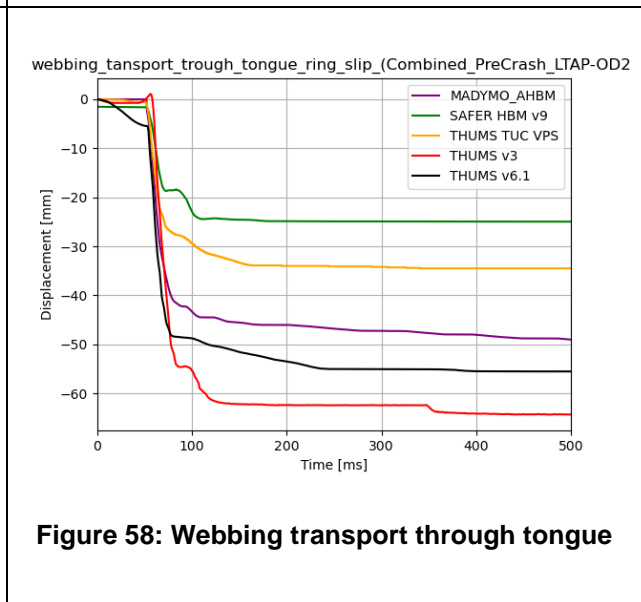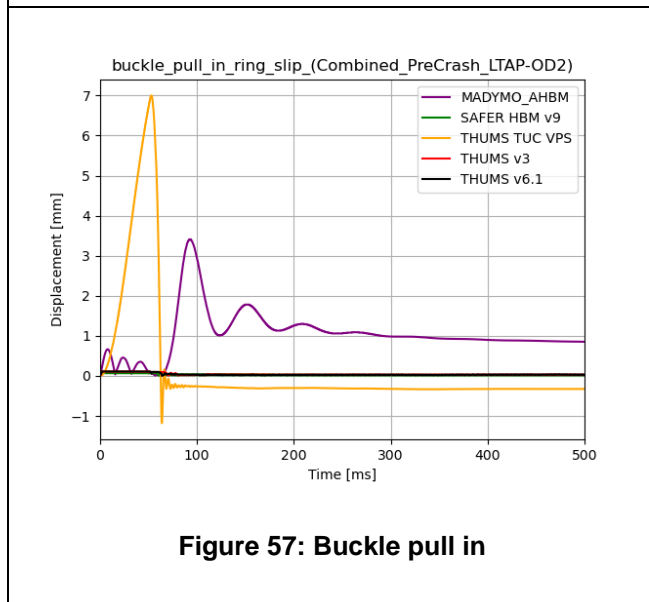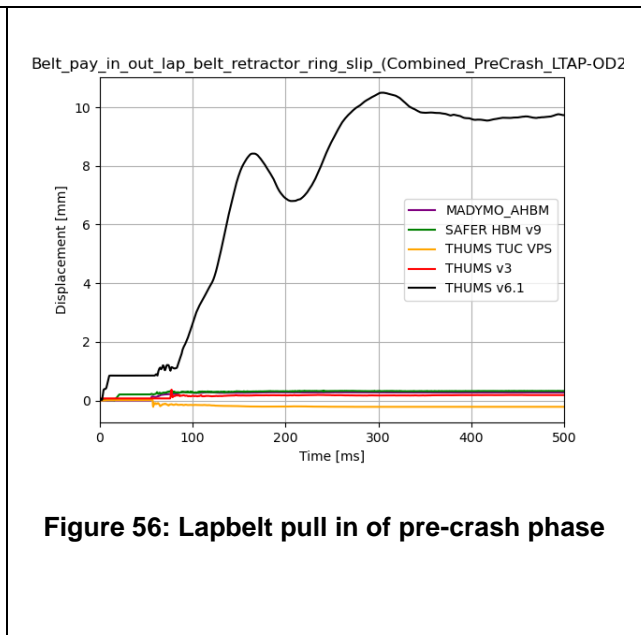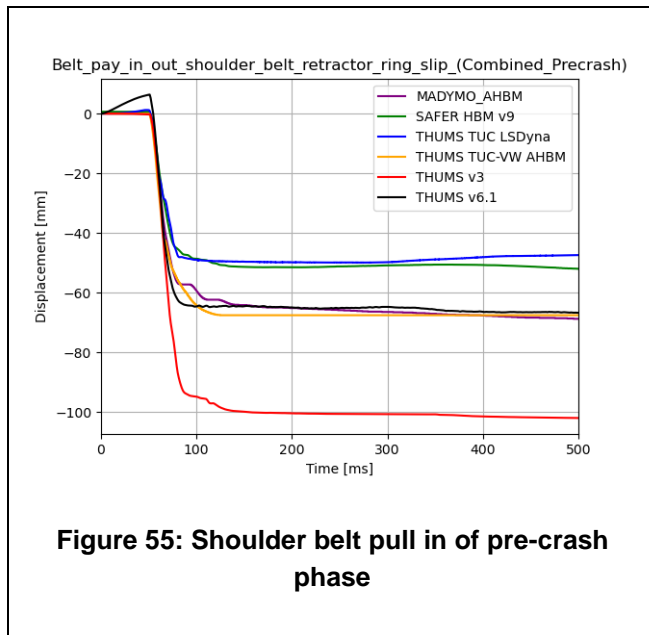
The activation time for the pre-pretensioner is clearly visible in Figure 55 and Figure 58. The activation time is equal for all models. Figure 56 and Figure 57 show, additional minor (> 10 mm) belt activities in two models. As the restraining of the HBM is caused by the belt forces, these differences were not further investigated. Moreover, a more generic (and completely accessible) belt model would help in this respect to clarify the remaining small differences.

3.7 Influence of the considered pre-crash kinematics on the in-crash evaluation for LTAP-OD2 simulations

Pre-crash and In-crash evaluation: Following diagrams demonstrate the influence of the considered pre-crash kinematics to the results of the in-crash simulation.

Environment The influence of the considered pre-crash phase to the belt forces is marginal except for B2 force (all models), B5 (both TUC models) and B6 (TUC LS-Dyna).
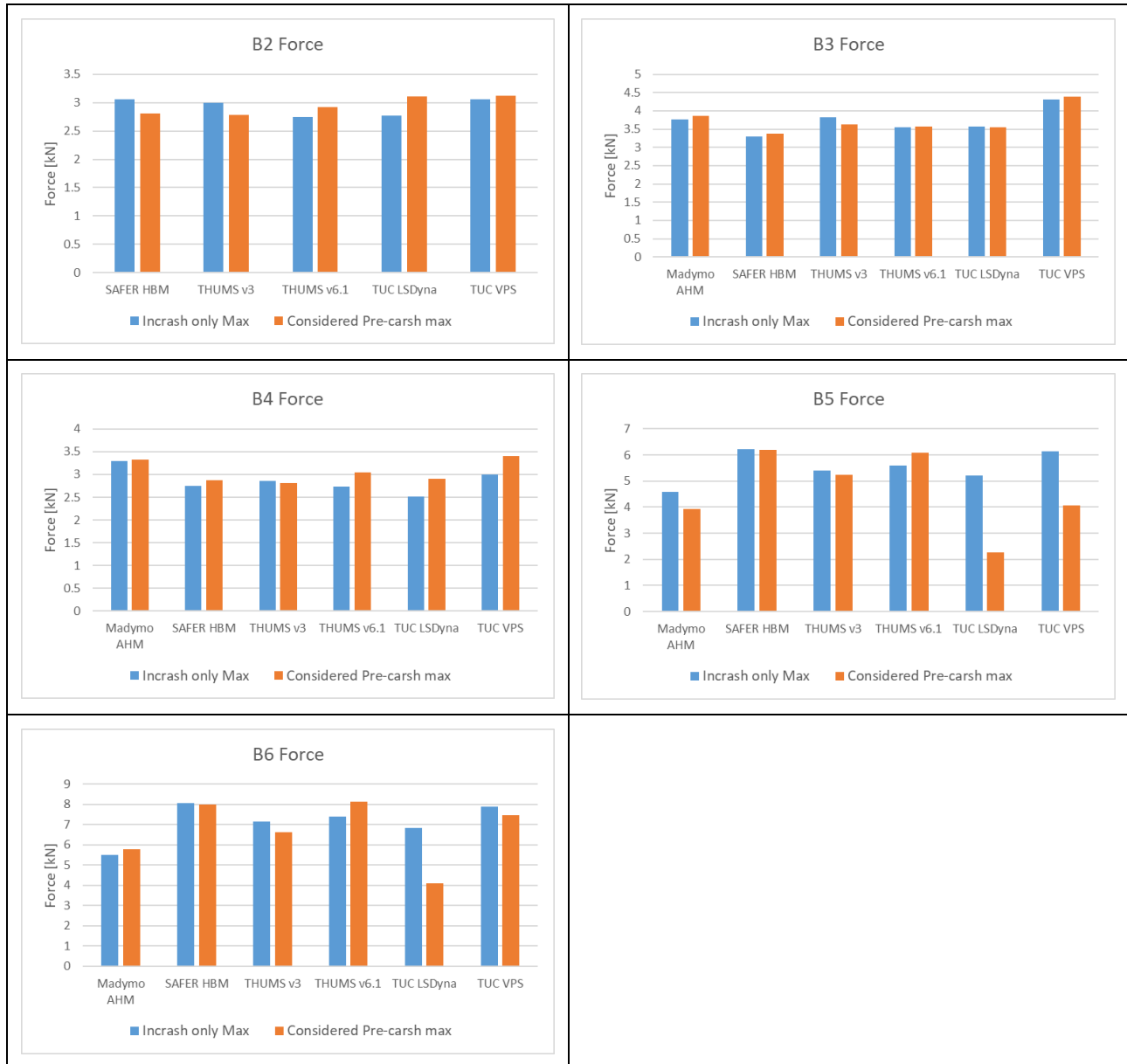
Table 9: Maximum belt forces with / without considered pre-crash phase

HBM kinematics

Figure 59 compares the initial positions for the single in-crash simulations (left) and for the in-crash simulation with considered pre-crash kinematics (right). Differences in the cervical spine and in the head positions are visible. The pre-crash forward excursion of the HBMs in this reclined sitting position is quite low compared to forward excursions in standard sitting positions [41]. This applies to all used active models in this report. It has to be mentioned, that none of the used models are

validated for a reclined sitting position in a pre-crash braking phase. In contrast to the simulation results for reclined postures, [42] published a volunteer study in reclined posture, which reports higher forward excursion.
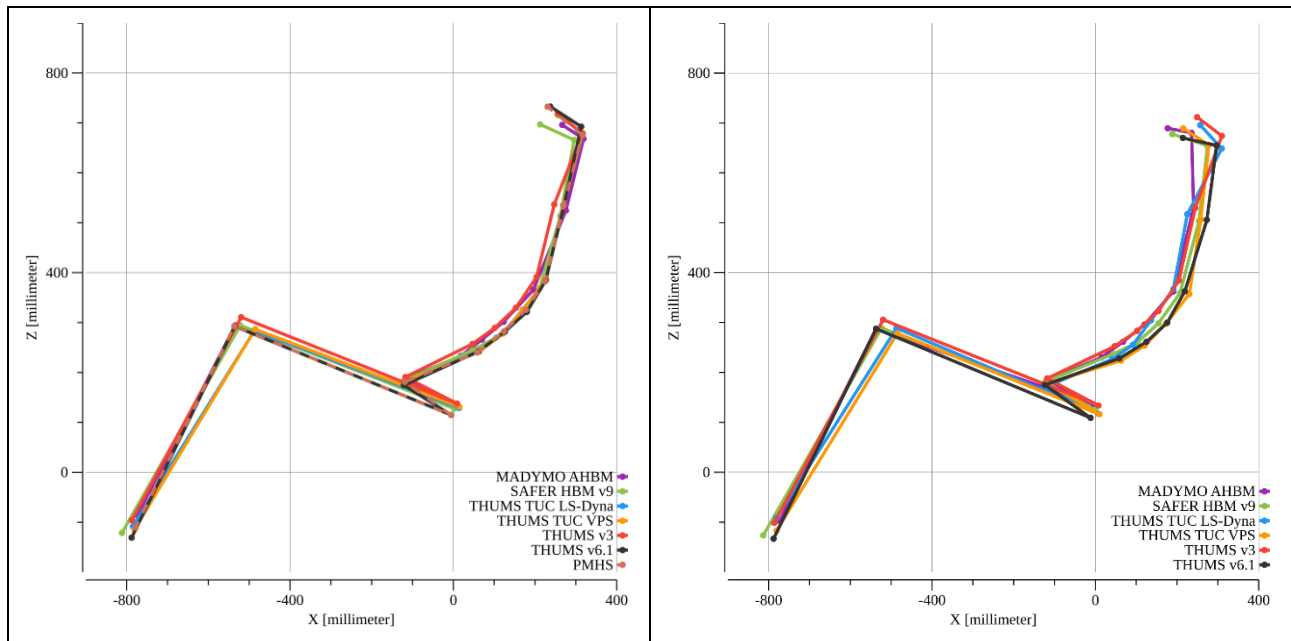
Figure 59: Left: t0 of LTAP-OD2 only; right: t500 (t0 of In-crash phase) of combined sim

Following diagrams compare the maximum forward excursion for selected landmarks and the pelvis rotation for the in-crash simulation to the in-crash simulation with considers the pre-crash kinematics.

Figure 59 shows rather low displacements in the pre-crash phase. That leads to the effect, that the considered pre-crash phase in this case has also low influence on the results of the in-crash phase. A small tendency of reduced excursion is noticed for the selected landmarks (Figure 60 - Figure 62). A clear tendency is seen for the pelvis angle (Figure 63). The interpretation is, that the pre-pretensioner in combination with the low-g pre-crash pulse and hardly forward moving HBMs leads to a tighter belt fit in the combined pre- and in-crash simulation.
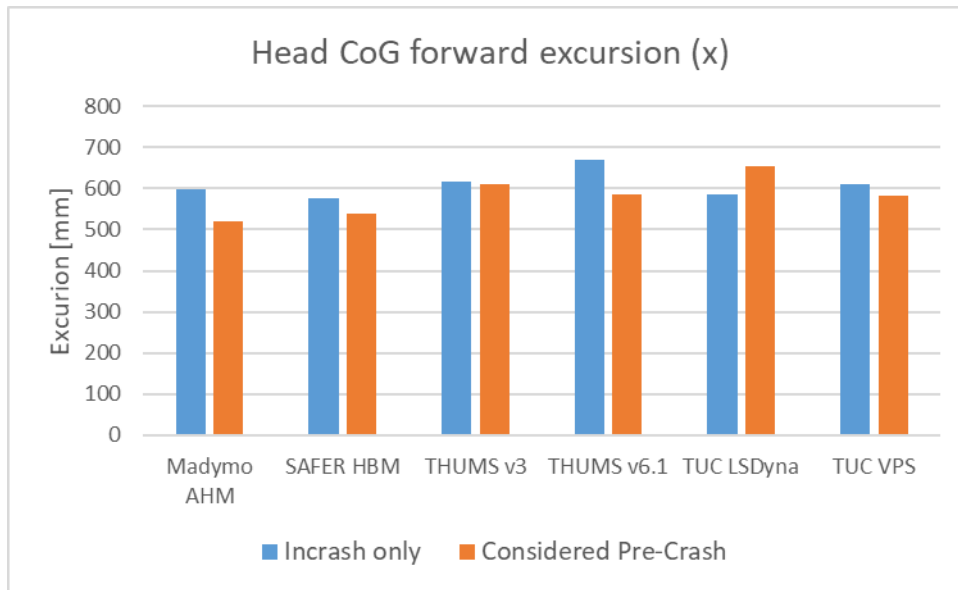
Figure 60: Maximum forward excursion of head CoG with/without considered pre-crash phase
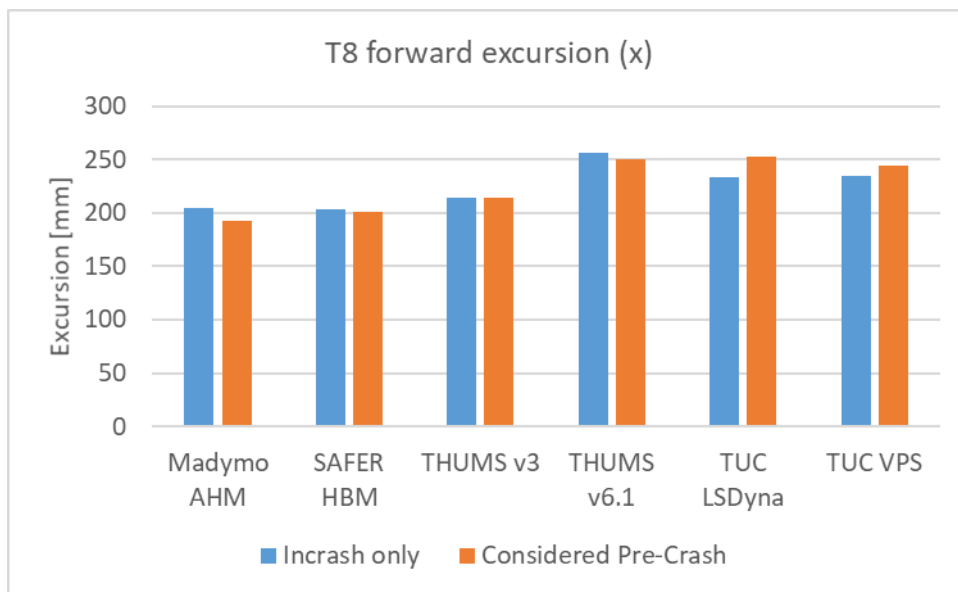
Figure 61: Maximum forward excursion of T8 with/without considered pre-crash phase
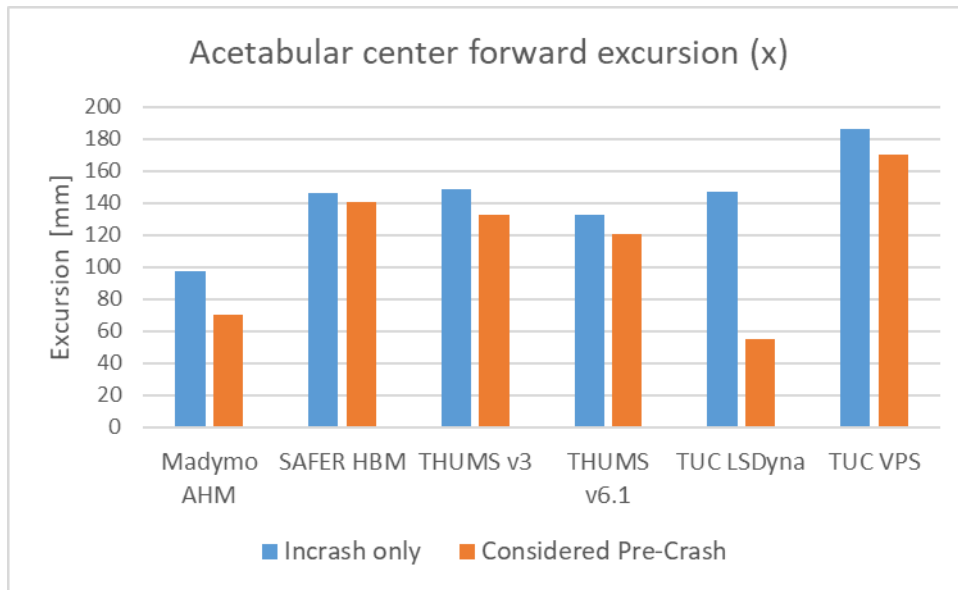
Figure 62: Maximum forward excursion of acetabular centre with/without considered pre-crash phase
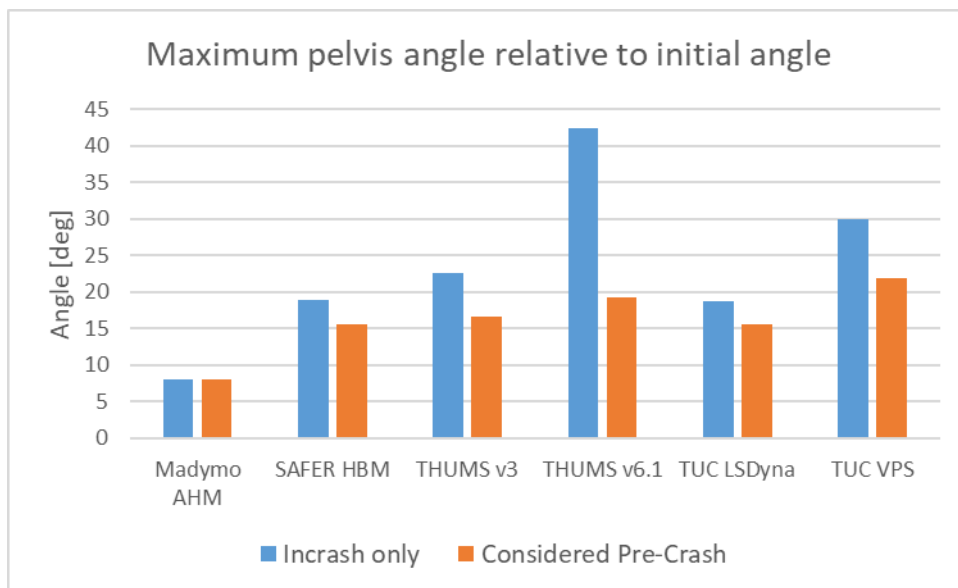
Figure 63: Maximum pelvis rotation with/without considered pre-crash phase

Injury indicators

ASIS forces R and L
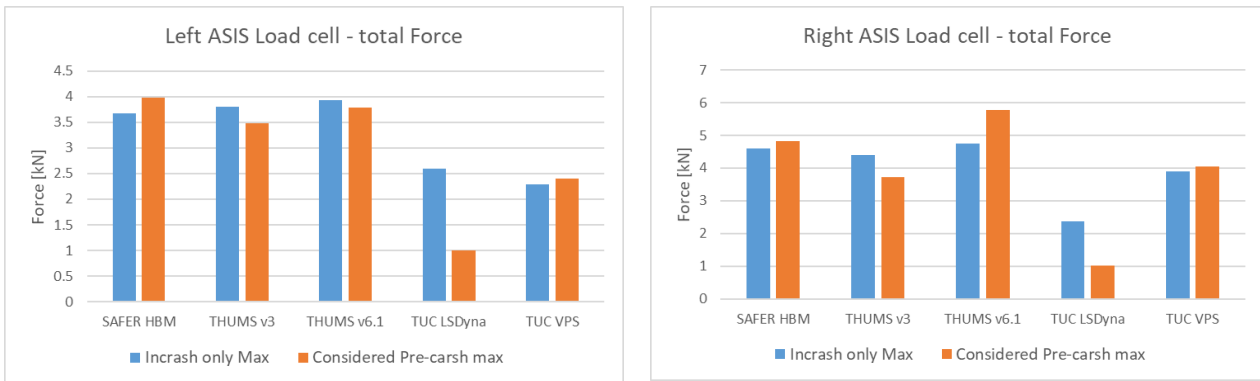
Figure 64: ASIS (left / right) forces with / without considered pre-crash phase

The influence of the considered pre-crash kinematics on the ASIS forces is found to be rather small, except for THUMS TUC LS-Dyna, which also showed decreased Lap belt forces if the pre-crash phase is considered.

Lumbar spine (L1-L5) forces(z) and moments (y)
This comparison is not possible for the Madymo AHM and THUMS v3.
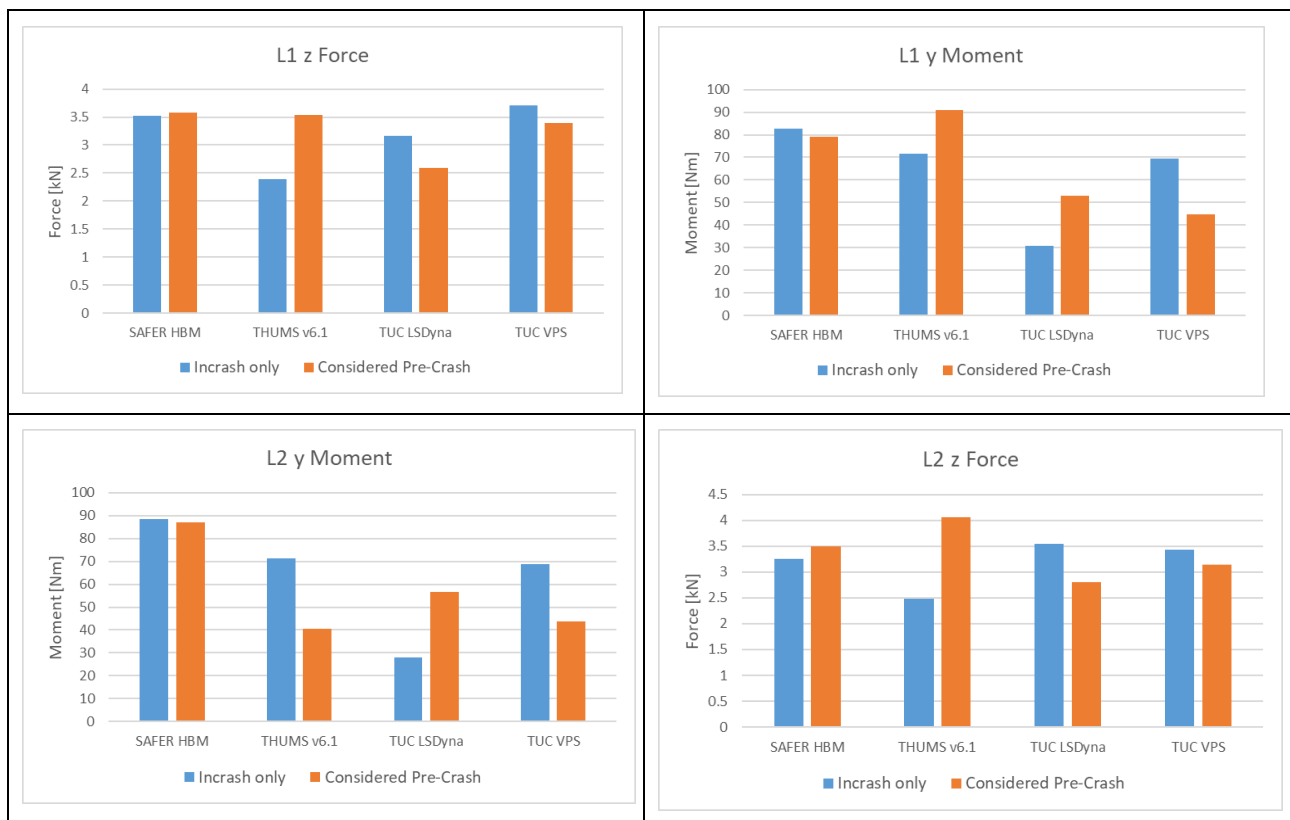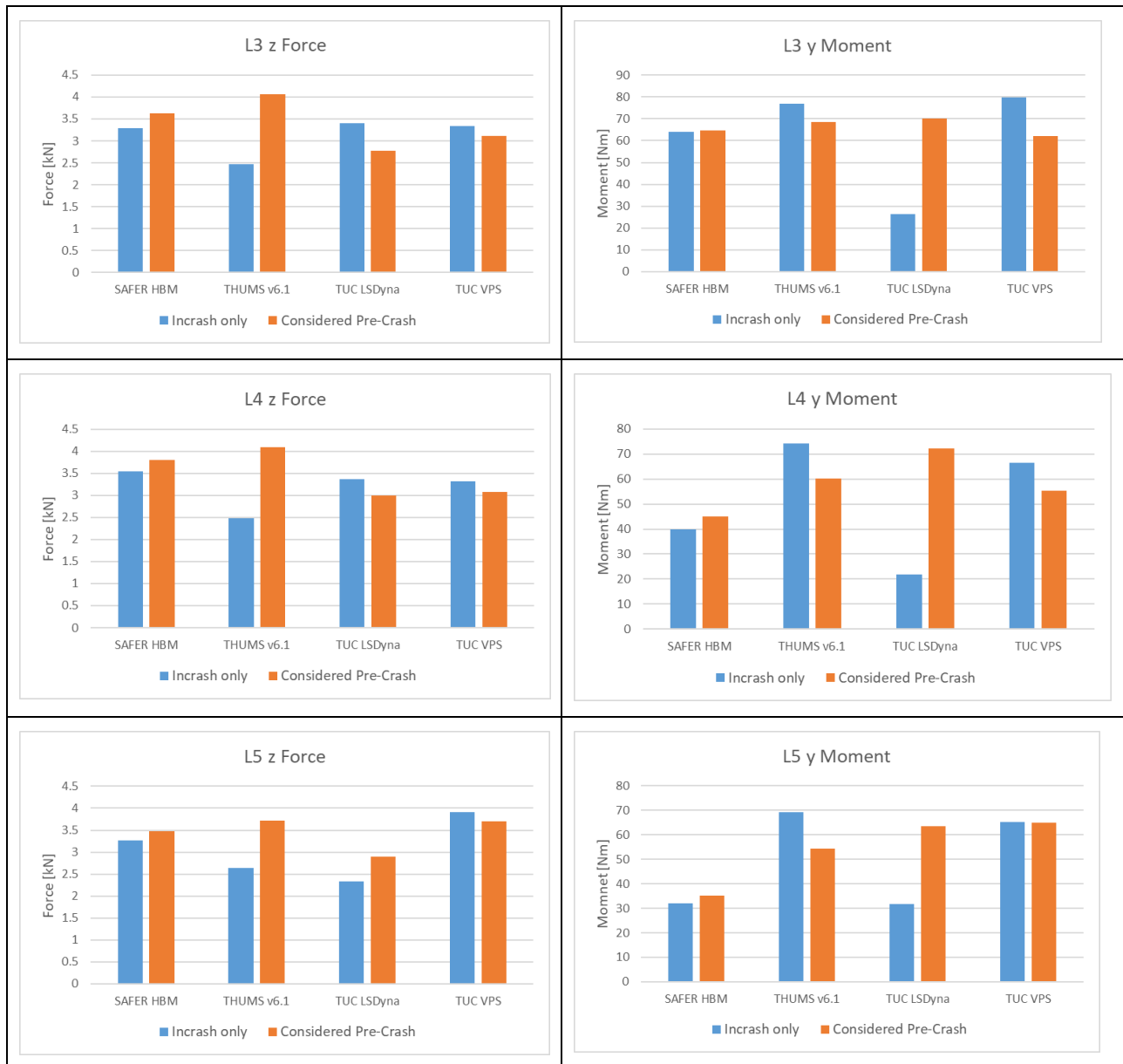
Table 10: Lumbar spine forces / moments for simulations with / without considered pre-crash phase

Different trends as far as the lumbar forces and moments are concerned can be observed when comparing pure in-crash with pre- and in-crash simulations for the different HBMs.

In the simulation with pre-crash phase

- THUMS TUC-VW AHBM always shows similar or slightly lower forces and similar or lower moments

- THUMS v6 shows always higher forces, but lower moments (except for L1)

- SAFER HBM always shows similar or slightly higher forces and moments

- For THUMS TUC-LS-Dyna a clear tendency cannot be observed

Hence, no common trend for the effect of pre-crash and muscle activation on lumbar forces and moments can be seen in this study.

Injury criteria

Following injury criteria (Table 11, Table 12 and Table 13) for the head show a minor effect on the risk, with a tendency of declining for considered pre-crash phase. With exception of the BrIC, the values for the other criteria are at a low level.

Model	HIC 15 (AIS2+)	
	In-crash only	**Considered pre-crash**
MADYMO AHBM	7 %	1 %
SAFER HBM v9	3 %	2 %
THUMS TUC LS-Dyna	5 %	4 %
THUMS TUC VPS	4 %	1 %
THUMS v3	4 %	2 %
THUMS v6.1	19 %	6 %

Table 11: HIC 15 for LTAP-OD2 with/without considered precrash

Model	BrIC (AIS2+) MPS based risk curve	
	In-crash only	**Considered pre-crash**
MADYMO AHBM	81 %	65 %
SAFER HBM v9	75 %	65 %
THUMS TUC LS-Dyna	47 %	34 %
THUMS TUC VPS	62 %	70 %
THUMS v3	74 %	63 %
THUMS v6.1	91 %	63 %

Table 12: BrIC 15 for LTAP-OD2 with/without considered precrash

Model	SUFEHM risk (AIS 2+)	
	In-crash only	**Considered pre-crash**
MADYMO AHBM	6 %	6 %
SAFER HBM v9	7 %	6 %
THUMS TUC LS-Dyna	6 %	8 %
THUMS TUC VPS	6 %	6 %
THUMS v3	6 %	6 %
THUMS v6.1	6 %	14 %

Table 13: SUFEHM 15 for LTAP-OD2 with/without considered Precrash

4 DISSEMINATION, EXPLOITATION AND STANDARDISATION

The positioning and assessment tool, input data and results, as well as parts of the used models, will be available after the OSCCAR project, to enable third parties to run the conducted simulations with their own models. Following list shows the public available data and the sources. Note, that not the entire list was created or enhanced in the OSCCAR project.

Environment

- Environment models and validation repository @ TUC (Thums User Community) https://tuc-project.org/frontal-sled-reclined/

- Validation data from sled tests (Deliverable D 2.5 [27]), Autoliv sled test data available on request: please contact schiessler@bast.de

Positioning data for HBMs in reclined seated position:
https://virginia.app.box.com/s/kpnt7v960a9fm7lsts5pa8hcfz4ojex1

Open source positioning tool: Method documented in Deliverable D 4.2 [4], Tool:
https://openvt.eu/osccar/positioning

Pulses

- FF50: [33]

- LTAP-OD-2: Method documented in Deliverable D 1.3 [32], data @ TU Graz repository (https://repository.tugraz.at/) DOI:10.3217/datacite.2400t-cxv49

Simulation results of HBM simulations (Appendix A, B and D in this report)

Assessment: Dynasaur (https://gitlab.com/VSI-TUGraz/Dynasaur)

5 SUMMARY AND CONCLUSION

For the conducted occupant simulations with HBMs in a validated environment, the output of the models and the environment were harmonized. Two in-crash simulations and one combined pre- and in-crash pulse were conducted. The used pulses are a Full Frontal pulse, which was also used for environment validation and a pulse which was developed within OSCCAR. Six 50% male HBMs either in MB (Madymo) or in FE (LS-Dyna, VPS) were used. For each of the used pulses, the results of the used HBMs were compared with the aim to demonstrate to demonstrate the necessary alignment. It was not the goal to investigate the validation levels of the HBMs themselves.

For each simulation, the environment and the interaction of the HBMs with the environment was assessed at first. That was necessary to ensure the same boundary conditions apply for all HBMs. Besides the sled acceleration, the belt forces and belt component displacements were verified to ensure identical firing times in the belt system. Further, the contact forces between HBM and seat components (seat pan, anti-submarining pan, footrest) were monitored. During the investigations for this task, several issues were identified and either solved or reported in this document.

The kinematics of the HBMs were analysed by using the trajectories of selected landmarks. The focus of the investigation was on the landmarks of the upper body. Differences in the kinematics could be observed due to different validation levels of the used HBMs. Especially pelvis and lumbar spine modelling influenced the interaction with the lap belt and further the HBM kinematics (bending over the lap belt).

As far as potential injury indicators were considered, the lumbar spine forces and moments as well as the ASIS forces are documented. That was possible for four of the six models. The section in the models for determining forces and models were defined according to Deliverable D 3.3 [22]. It was observed, that ASIS forces usually correspond with the lap belt forces in terms of the force over time characteristics. Differences in the level of the ASIS forces might indicated that the lap belt force interacted with the abdomen in a different way for the different HBMs. However, it was not conclusively investigated in this task.

The determination for head injury risk (AIS 2+) was aligned by using the SUFEHM for all models. Therefore, head acceleration and rotational velocities were determined in each model in a local coordinate system and were analysed with a SUFEHM model. The used injury risk parameters besides those obtained by using SUFEHM are HIC 15 and BrIC. As the environment (sled) did not contain an airbag, a dashboard or a steering wheel, the HIC15 based injury risk was rather low. Furthermore, as far as the brain injury risk was concerned, SUFEHM showed a rather low risk whereas BrIC showed a relatively high one.

The rib strains were compared between all models by using two different tools (Dynasaur for LS-Dyna, TUC Tool for VPS). The suggestions for rib strain assessment which were given in Deliverable D 3.3 [22] were used. Nevertheless, further harmonization was necessary to exclude possible differences between strain determination with reasonable certainty. Therefore, the conducted processes of determining the principal surface strains were documented in this report.

For the selective in-crash comparison of two identical HBMs in two different codes, namely THUMS TUC in LS-Dyna VPS, it was observed, that the models were overall well in agreement in terms of kinematics, forces and injury indicators, although a slightly different behaviour between both restraint system models needed to be taken into account. This is the major limitation of the selective study, since the boundary conditions should be ideally the same to estimate solely the differences due to the two HBMs. The rib injury risk assessment was done according to Forman et al. [24] and risks

were determined with the TUC tool. The rib fracture injury risk pointed out to be very similar between the models.

The pre-crash phase was considered by combing a generic pre-crash pulse with the LTAP-OD2 pulse. For this combined approach, it was also ensured, that the HBMs were simulated under the same boundary conditions. Therefore again, sled acceleration, belt forces and component displacement (firing times) and contact with the environment were assessed. This task included the application of active HBMs. The used active models had different controller strategies and different validation data basis. None of the used active models was validated for reclined sitting position in the pre-cash phase.

The influence of considering the pre-crash kinematics for the in-crash phase was investigated, by comparing maximum values of belt forces, forward excursion and injury parameters. As the pre-crash kinematics of the active models were low in the conducted case, the influence of considering the pre-crash phase was also mainly low.

For any further investigation which aims to assess and compare rib strains or rib fracture risk among different models, the assessment needs to be harmonized practically (tools), since a harmonized method is already provided in Deliverable D 3.3 [22]. For a more accurate comparison, especially between codes, a further simplified, even more generic environment is needed (see limitations in this study due to differences in the restraint system or belting process). Moreover, certified HBMs would be necessary, to use the demonstrated procedure in e.g. a test rating or a type approval.

The goal of the homologation testcase was to present a possible procedure for a virtual assessment, which could be used as a basis for consumer test rating or type approval. That requires, that simulations are conducted under the same boundary conditions. This report demonstrates, how that can be assured.

6 REFERENCES

[1]   Richardson R., et al., "Test methodology for evaluating the reclined seating environment with human surrogates." Proceedings of the 26th International Technical Conference on the Enhanced Safety of Vehicles (ESV). Paper Number 19-0243., 2019.

[2]   EU, „Commission Regulation No 371/2010 of 16 April 2010 replacing Annexes V, X, XV and XVI to Directive 2007/46/EC of the European Parliament and of the Council establishing a framework for the approval of motor vehicles and their trailers, and of systems," 2010.

[3]   Klug C., Ellway J. „ Pedestrian Human Model Certification" EuroNCAP Technical Bulleting 024, November 2019.

[4]   Klein C. et al..; "Demonstrator for continuous integral virtual assessment of complex crash simulation tasks including HBMs"; Deliverable D4.2; OSCCAR Project; Grant Agreement No. 768947; 2020.

[5]   Laso M., et al.; "Virtual environment check tool and documentation"; Deliverable D4.1; OSCCAR Project; Grant Agreement No. 768947; 2021.

[6]   Klein C. et al., "A Method for Reproducible Landmark-based Positioning of Multibody and Finite Element Human Models", Proceedings of the IRCOBI, IRC-21-53, 2021.

[7]   Iwamoto, M. et al. "Development of advanced human models in THUMS", Proceedings of the 6th European LS-DYNA Users' Conference, Gothenburg, Sweden, 2007.

[8]   Iwamoto, M. et al., "Development of a Finite Element Model of the Total Human Model for Safety (THUMS) and Application to Injury Reconstruction", Proceedings of IRCOBI Conference, Munich, Germany, 2002.

[9]   THUMS USER Community (accessed 30.11.2021) https://tuc-project.org/

[10]   Davidsson, J. et al; "Validated and computationally robust active HBMs"; Deliverable D3.2; OSCCAR Project; Grant Agreement No. 768947; 2021.

[11]   Kato, D. et al. „Development of Human-Body Model THUMS Version 6 containing Muscle Controllers and Application to Injury Analysis in Frontal Collision after Brake Deceleration", Proceedings of the IRCOBI, IRC-18-32, pp.207-223, Athens, Greece, 2018.

[12]   Shigeta, K., Kitagawa, Y., Yasuki, T. „Development of next generation human FE model capable of organ injury prediction", Proceedings of the 21st ESV Conference, Stuttgart, Germany, 2009.

[13]   Iwamoto, M., Nakahira, Y., Kimpara, H. „Development and validation of the Total HUman Model for Safety (THUMS) toward further understanding of occupant injury mechanisms in precrash and during crash", Traffic Injury Prevention, 16(sup1):S36-S48, 2015.

[14]   Iraeus, J., and Pipkorn, B., "Development and Validation of a Generic Finite Element Ribcage to be used for Strain based Fracture Prediction", Proceedings of the IRCOBI Conference, Florence, Italy, 2019.

[15]   Afewerki, H., "Biofidelity Evaluation of Thoracolumbar Spine Model in THUMS", Master's thesis in Biomedical Engineering, Chalmers University of Technology, Sweden, 2016.

[16]   Östh, J., Bohman, K., Jakobsson, L., "Evaluation of Kinematics and Restraint Interaction when Repositioning a Driver from a Reclined to Upright Position Prior to Frontal Impact using

Active Human Body Model Simulations", Proceedings of the IRCOBI Conference, Munich, Germany, 2020.

[17] Pipkorn, B. et al., "Multi-Scale Validation of a Rib Fracture Prediction Method for Human Body Models", Proceedings of the IRCOBI Conference, Florence, Italy, 2019.

[18] Mroz, K. et al., "Effect of Seat and Seat Belt characteristics on the Lumbar Spine and Pelvis Loading of the SAFER Human Body Model in reclined Postures", Proceedings of the IRCOBI Conference, Munich, Germany, 2020.

[19] Östh J, Brolin K, Bråse D. „A Human Body Model with Active Muscles for Simulation of Pretensioned Restraints in Autonomous Braking Interventions." Traffic Injury Prevention, 16(3): 304–313. IRC-20-50 IRCOBI conference, 368, 2015.

[20] Ólafsdóttir JM, Östh J, Brolin K., "Modelling Reflex Recruitment of Neck Muscles in a Finite Element Human Body Model for Simulating Omnidirectional Head Kinematics." Proceedings of the IRCOBI Conference, Florence, Italy, 2019

[21] Siemens Digital Industries Software (2021) Simcenter Madymo Model Manual

[22] Mayer C. et al.; "Criteria and risk functions for prediction of injury risks in new sitting positions and new crash scenarios"; Deliverable D3.3; OSCCAR Project; Grant Agreement No. 768947; 2021

[23] C. Deck et R. Willinger, "Improved head injury criteria based on head FE model", Int. J. Crashworthiness, vol. 13, no 6, p. 667678, 2008.

[24] Forman, J. L., et al. "Predicting rib fracture risk with whole-body finite element models: development and preliminary evaluation of a probabilistic analytical framework." Paper presented at the the 56th annual AAAM Scientific Conference, Seattle, Washington, 2012, Oct 14-17

[25] Becker J., Sprenger M., Schaub S.; "Interior Models for Occupant Protection Simulations in OSCCAR; Deliverable D2.2"; OSCCAR Project; Grant Agreement No. 768947; 2018

[26] Hamacher M., et al., "Final virtual design of advanced passenger protection principles"; Deliverable D2.4; OSCCAR Project; Grant Agreement No. 768947; 2021

[27] Schiessler M., et al.; "Validation and Demonstration of Advanced Passenger Protection Principles"; Deliverable D2.5; OSCCAR Project; Grant Agreement No. 768947; 2021

[28] THUMS User Community, "Frontal Sled Reclined" (accessed 30.11.2021) https://tuc-project.org/frontal-sled-reclined/

[29] Peldschus S. et al; "Standardised validation procedure for qualitfying the HBM to be used for assessing effectiveness of pilot protection principles"; Deliverable D5.2; OSCCAR project; OSCCAR Project; Grant Agreement No. 768947; 2021

[30] Östling, M. et al.,"Potential future seating positions and the impact on injury risks in a Learning Intelligent Vehicle (LIV). How to avoid submarining in a reclined seating position in a frontal crash", Conference: 11. VDI-Tagung Fahrzeugsicherheit, Berlin, Germany, 2017

[31] Richardson R. et al. "Kinematic and Injury Response of Reclined PMHS in Frontal Impacts", Stapp Car Crash Journal Vol. 64, 2020.

[32] Dobberstein J. et al. "Final results on detailed crash configurations from collisions expected to remain for automated vehicles"; Deliverable D1.3; OSCCAR Project; Grant Agreement No. 768947; 2021

[33] Uriot J., et al. "Reference PMHS sled tests to assess submarining" (No. 2015-22-0008). SAE Technical Paper, 2015

[34] Wu et al. „ISB recommendation on definitions of joint coordinate systems of various joints for the reporting of human joint motion—part I: ankle, hip, and spine" Journal of Biomechanics (35), p. 543 – 548, 2002

[35] Robins, D. H. "Anthropometric specifications for mid-sized male dummy", Volume 2, UMTRI-83-53-2, 1983

[36] Meyer, F. et al. „Cervical Spine Segmental Loads from Frontal Impact using a Validated Finite Element Model." Proceedings of IRCOBI, IRC-A-18-29, 2018, Lonavala, India, 2018

[37] D. Sahoo, C. Deck, et R. Willinger, "Finite element head model simulation and head injury prediction", Comput. Methods Biomech. Biomed. Engin., vol. 16, no sup1, p. 198199, juill. 2013, doi: 10.1080/10255842.2013.815908.

[38] Richolt, J. A., Effenberger, H., Rittmeister, M. E. "How does soft tissue distribution affect anteversion accuracy of the palpation procedure in image-free acetabular cup navigation?"An ultrasonographic assessment", Computer Aided Surgery, 10:2, 87-92, DOI: 10.3109/10929080500229447, 2005

[39] M. Gonzalez-Garcia, J. Weber, and S. Peldschus, "Numerical Study to Quantify the Potential Influence of Pre-Activated Muscles during the In-Crash Phase", in International Symposium: Human Modeling and Simulation in Automotive Engineering, 2020.

[40] Kroell, C. K., Schneider, D. C., & Nahum, A. M. „Impact tolerance and response of the human thorax II." SAE Transactions, 3724-3762, 1974

[41] Philipp Huber et al, "Passenger kinematics in braking, lane change and oblique driving maneuvers", Proceedings of the IRCOBI conference 2015, p783 - 802

[42] Reed, M. P. et al. "Occupant dynamics during crash avoidance maneuvers" (Report No. DOT HS 812 997). National Highway Traffic Safety Administration, 2021

[43] Wu, G. et al.; "ISB recommendation on definitions of joint coordinate system of various joints for the reporting of human joint motion—part I: ankle, hip, and spine", Journal of biomechanics, 2002, Vol. 35 No. 4, pp. 543–548. doi: 10.1016/S0021-9290(01)00222-6.

[44] Wu, G.et al.; "ISB recommendation on definitions of joint coordinate systems of various joints for the reporting of human joint motion—Part II. Shoulder, elbow, wrist and hand", 2005 Journal of biomechanics, Vol. 38 No. 5, pp. 981–992. doi: 10.1016/j.jbiomech.2004.05.042.

A. LTAP-OD2 IN-CRASH SIMULATION

This chapter presents the data according to the definitions in chapter 3.2 and 3.3 for the incrash simulation with the LTAP-OD2 pulse.

Porion (left/right)   x(t), y(t), z(t)
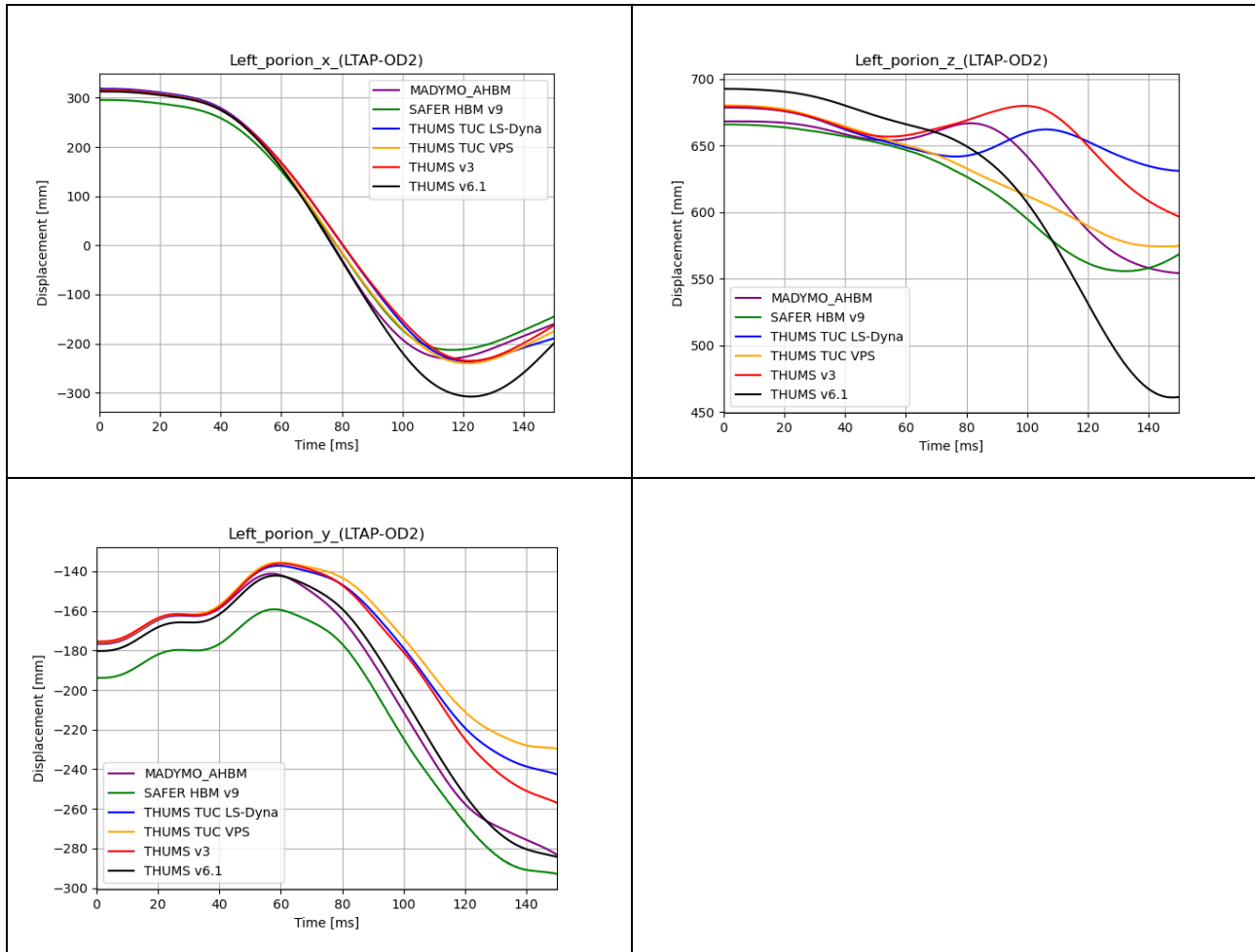
Head rotation
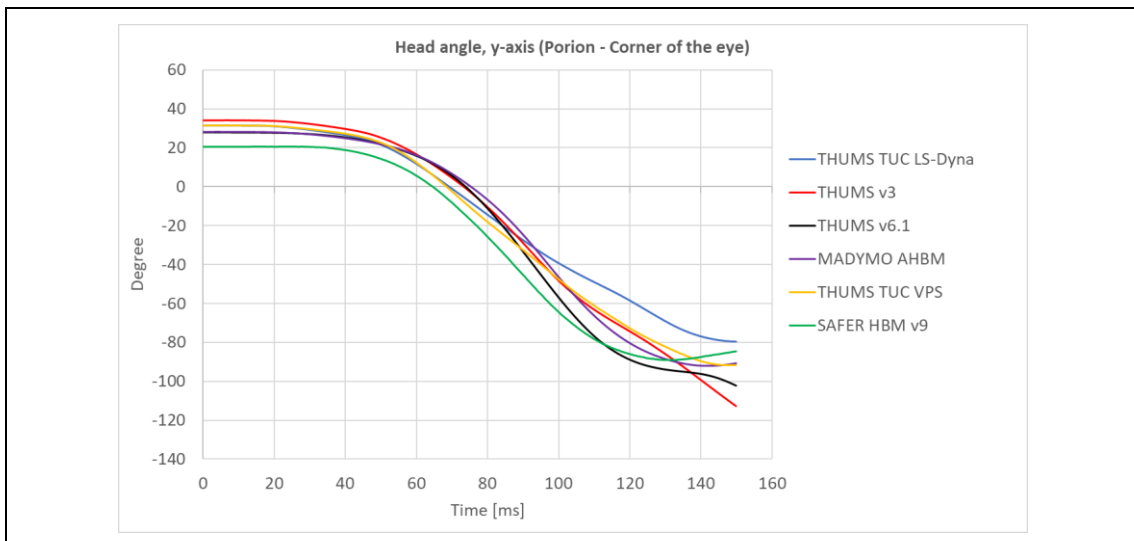
T1 (Left/right midpoint)   x(t), y(t), z(t)
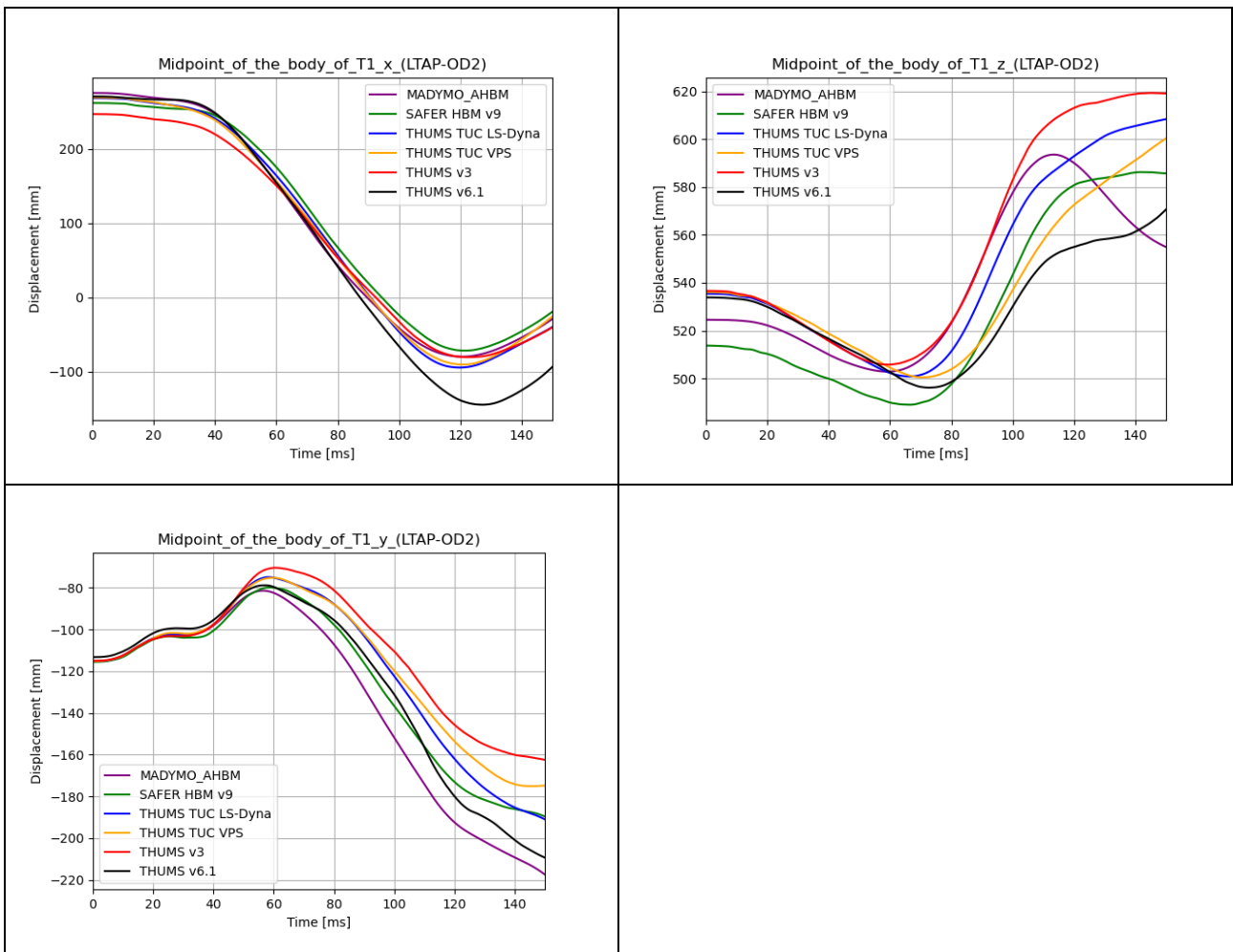
T8 (Left/right midpoint)   x(t), y(t), z(t)
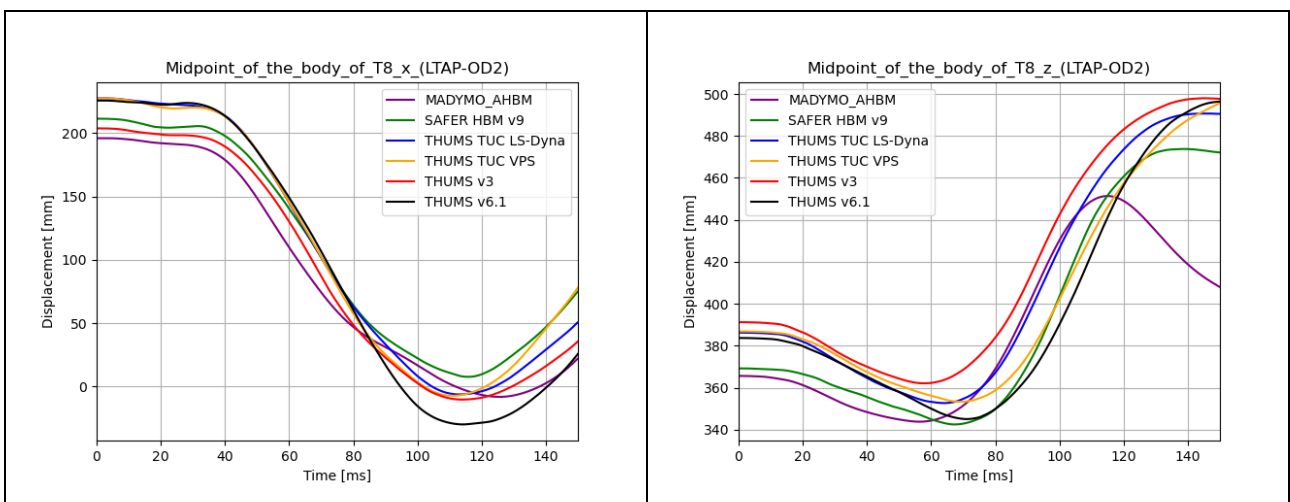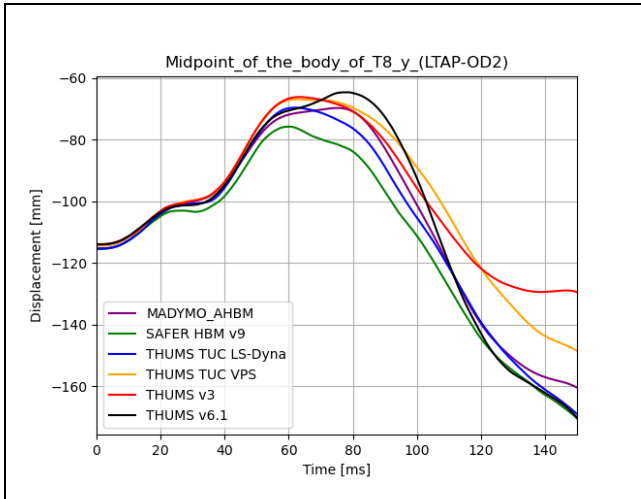
T11 (Left/right midpoint)
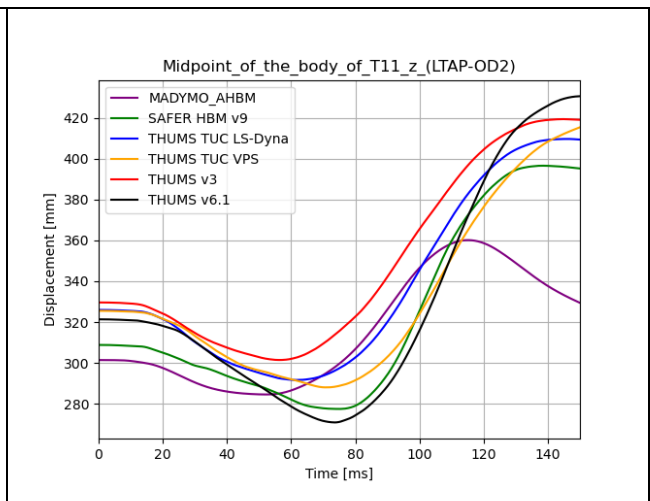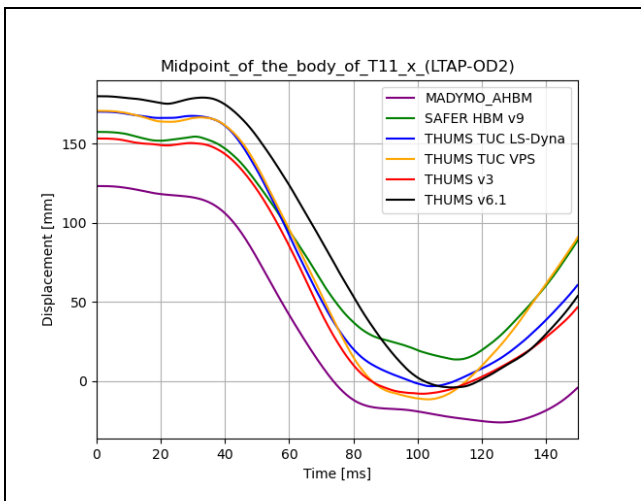
L1 (Left/right midpoint)
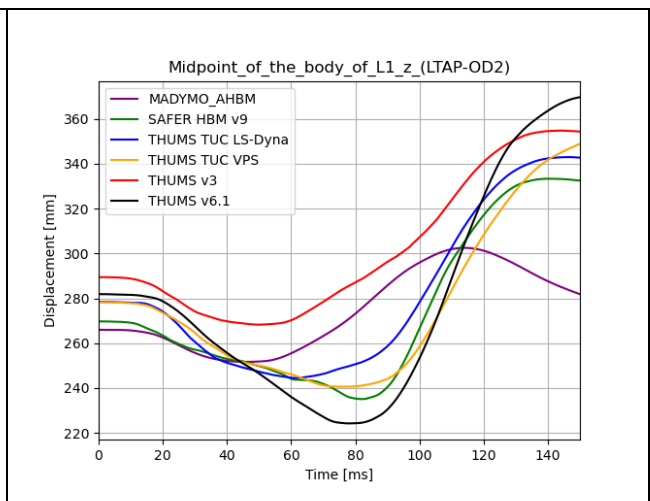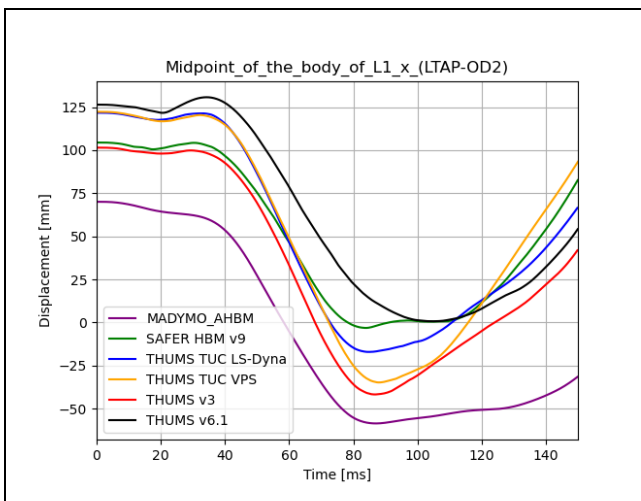
L3 (Left/right midpoint)
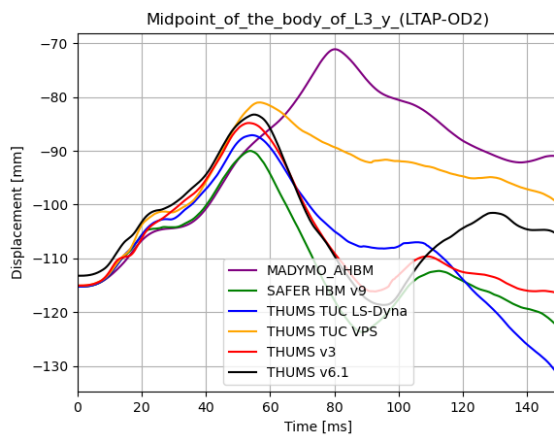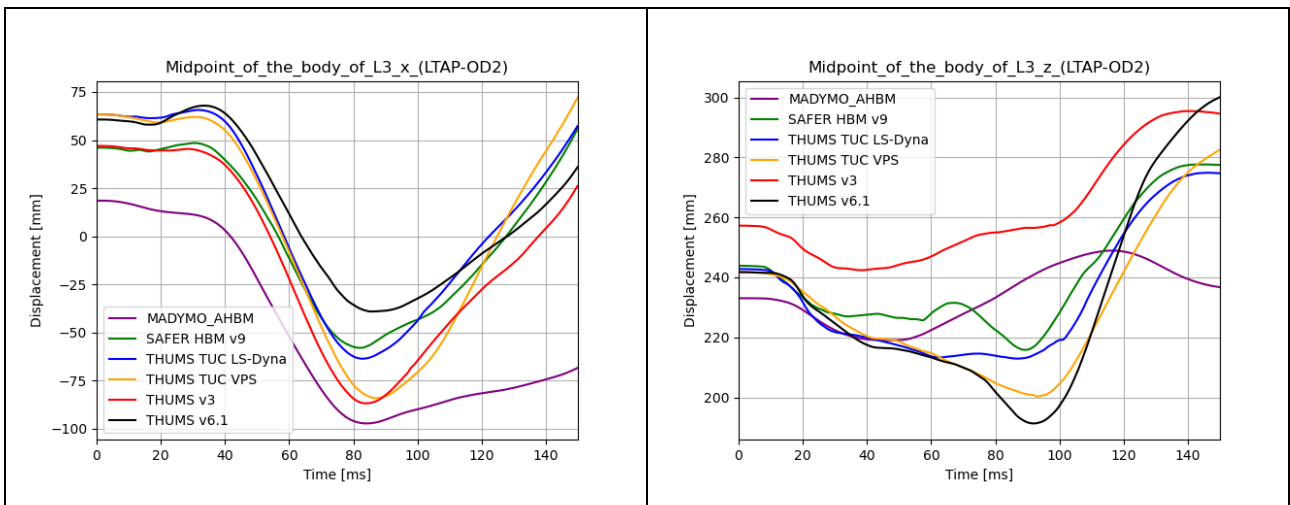
Acetabular centre (left/right)
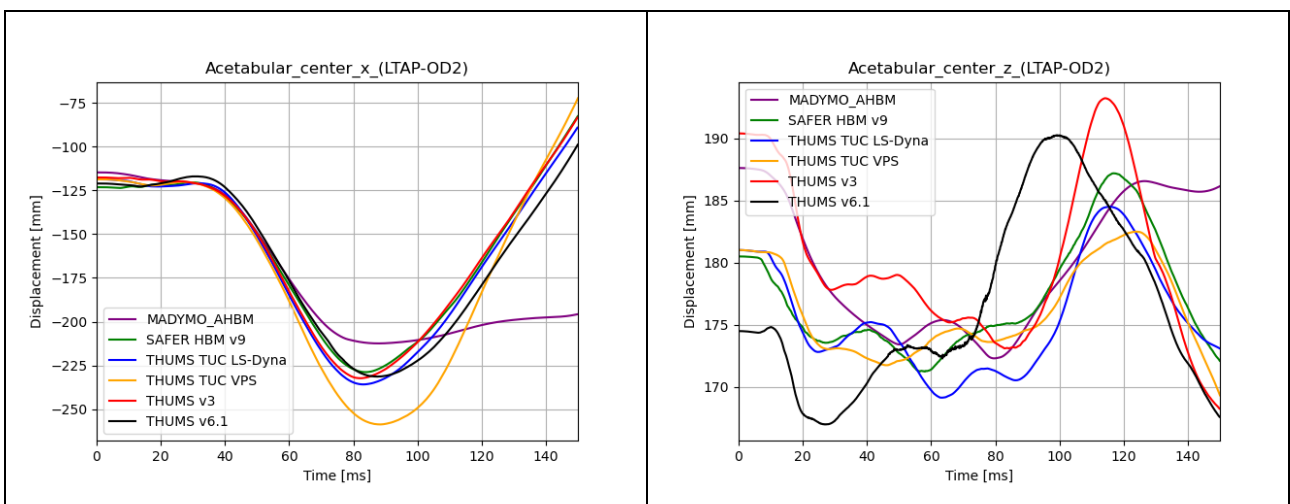
Pelvis angle (t)
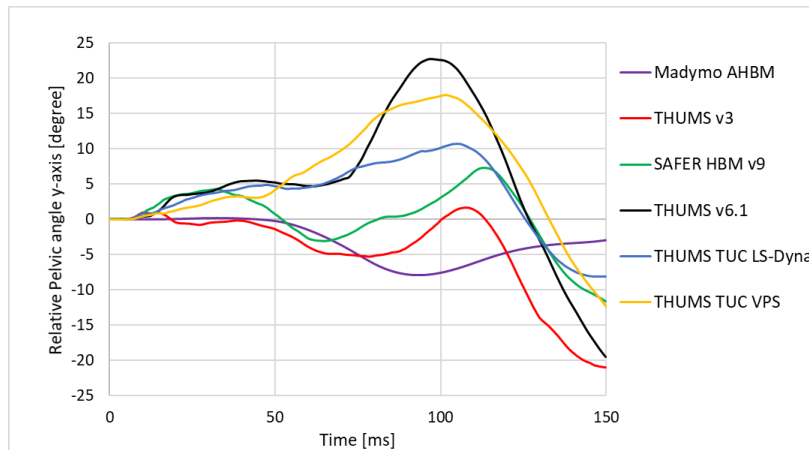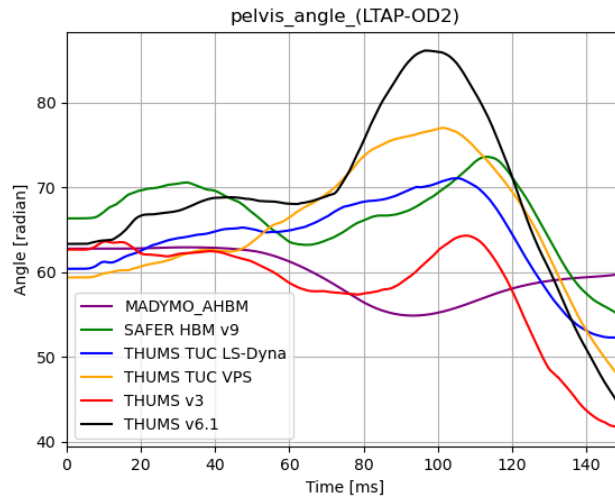
Lumbar spine
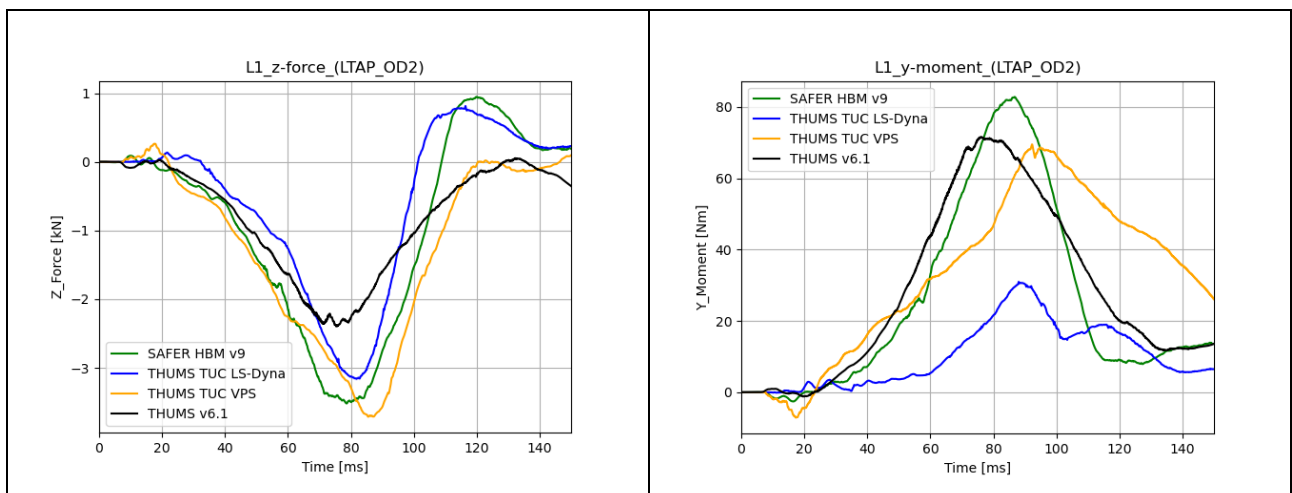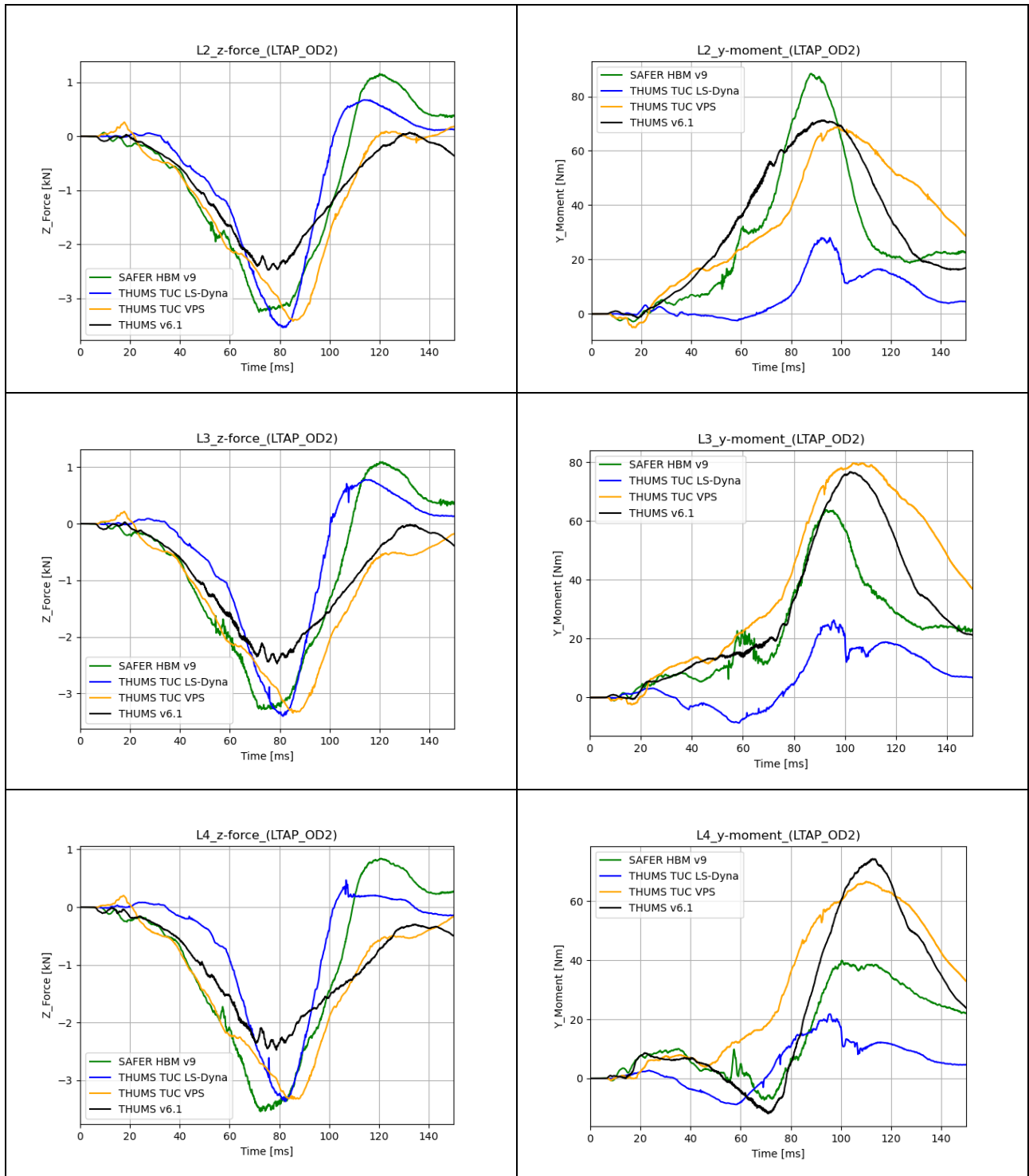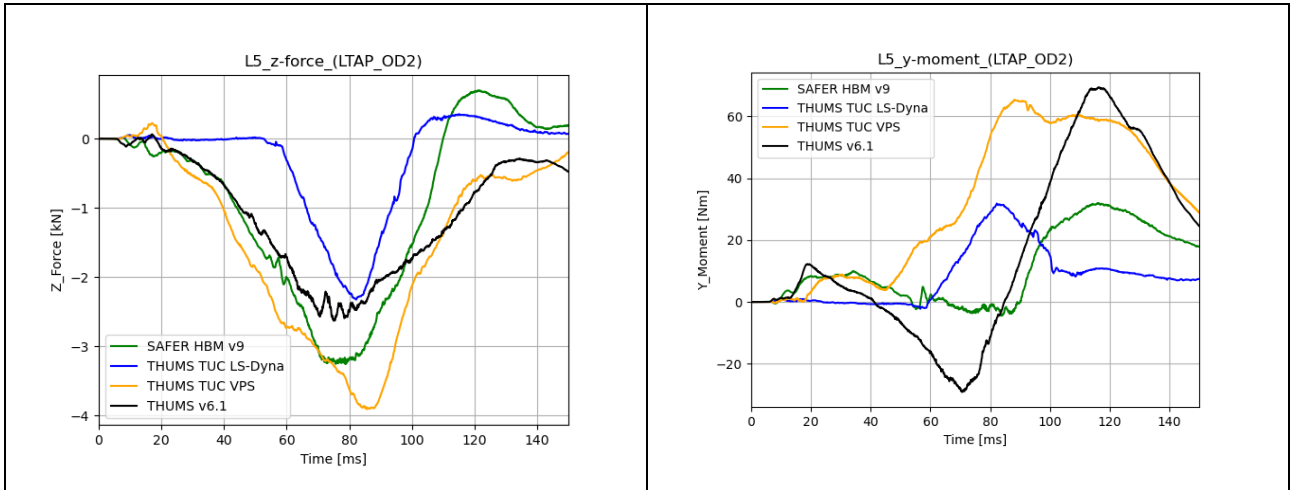
B. RESULTS FOR IN-CRASH SIMULATION FF50

This chapter presents the data according to the definitions in chapter 3.2 and 3.3 for the incrash simulation with the FF50 pulse.

Acceleration pulse

Figure 65: In-crash acceleration

Figure 66: sled x-acceleration of simulations

Kinematic overview:

t=0ms

t=10ms

t=20ms

t=30ms

t=40ms

t=50ms

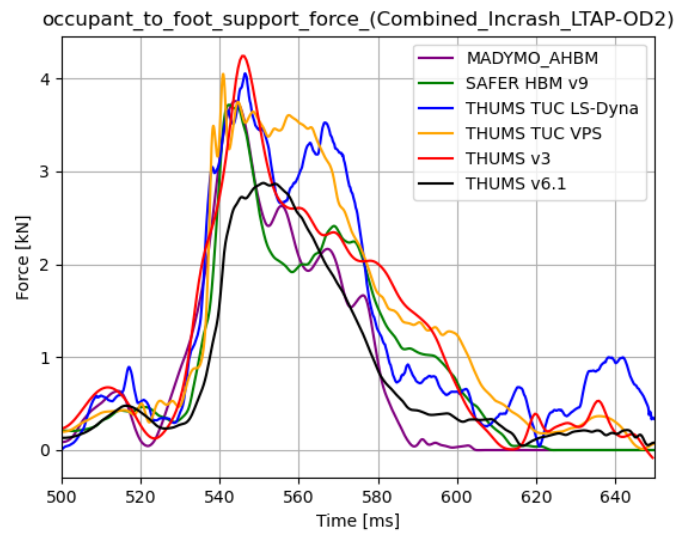t=60ms

t=70ms

t=80ms

t=90ms

t=100ms
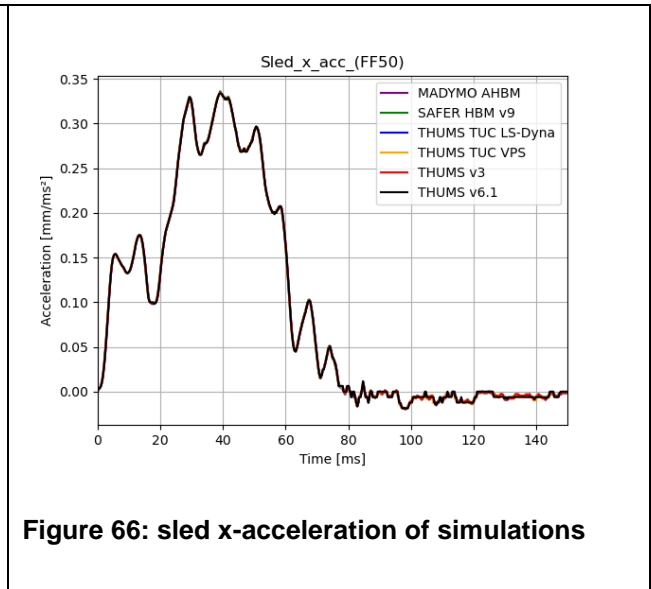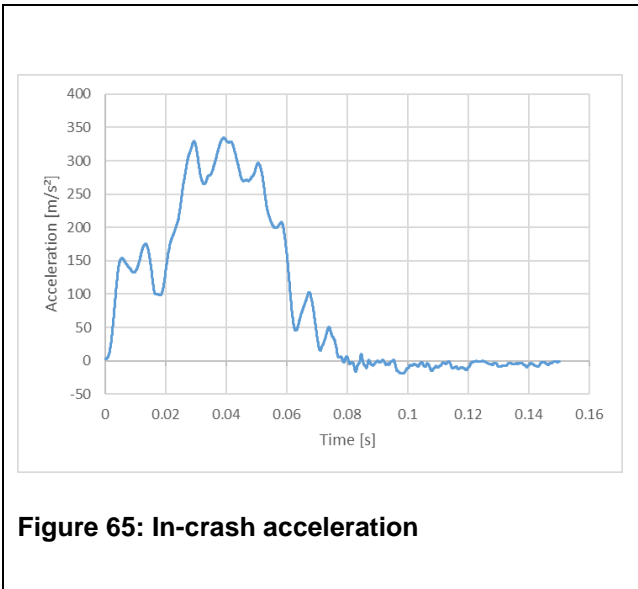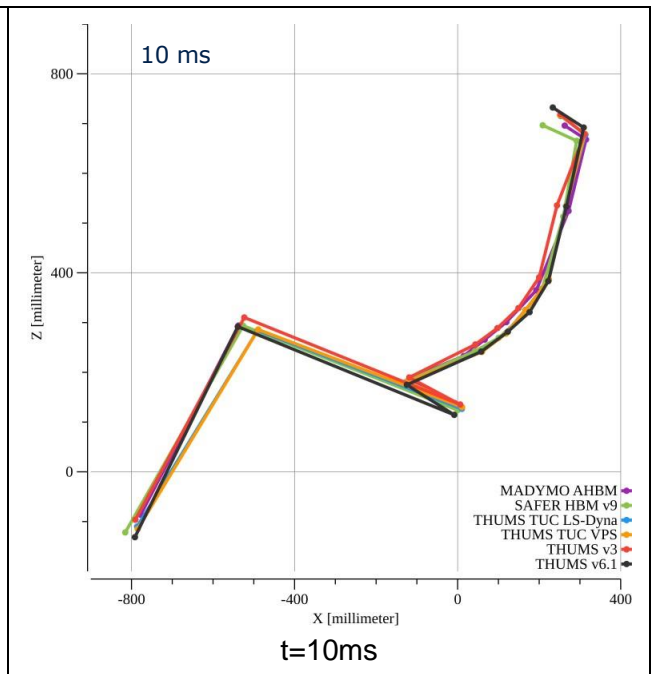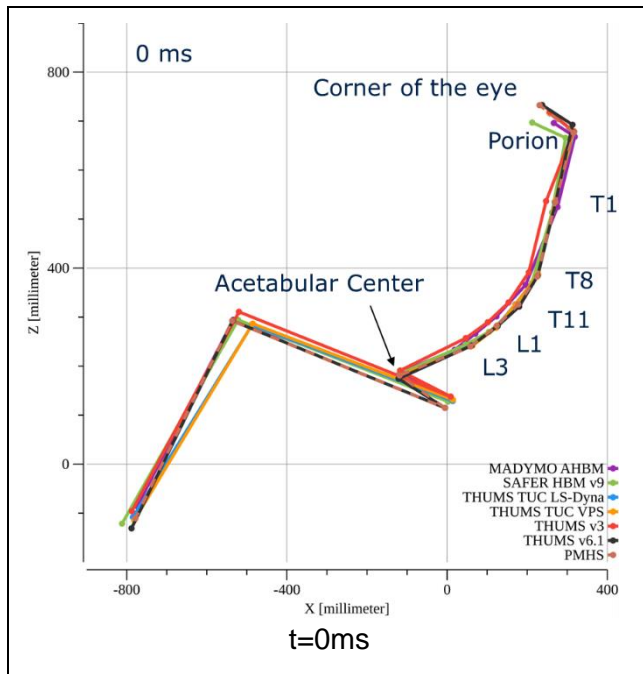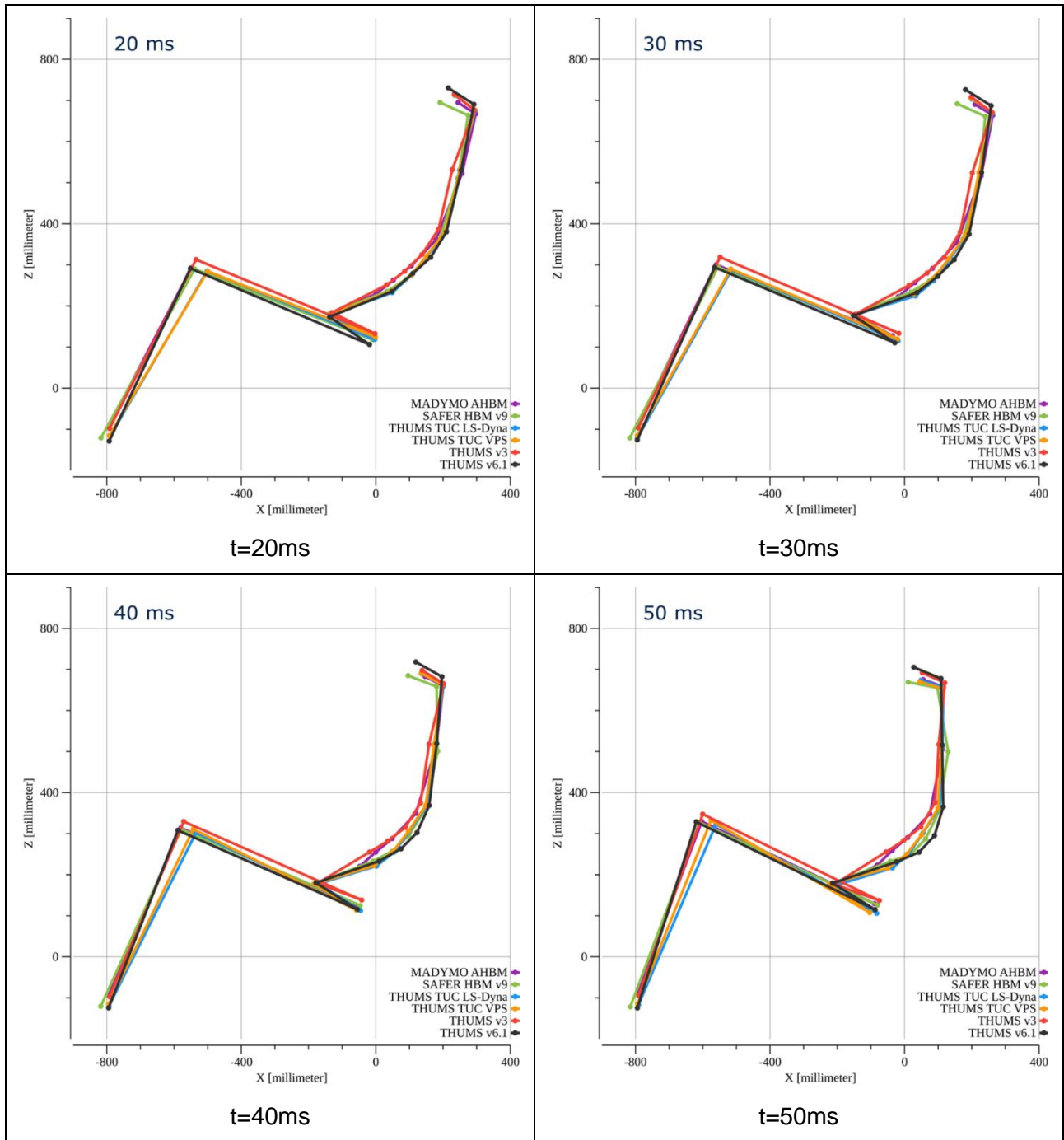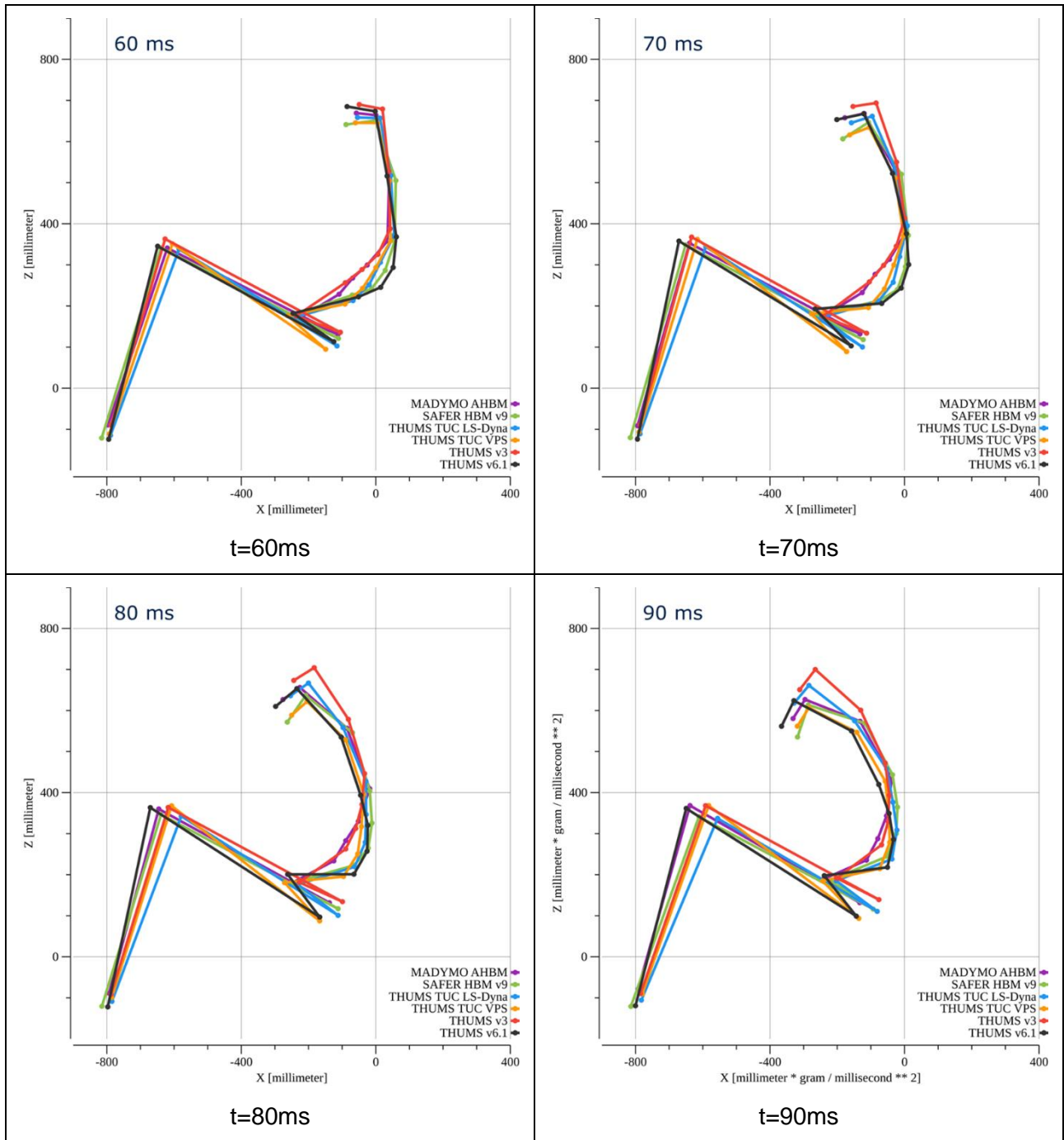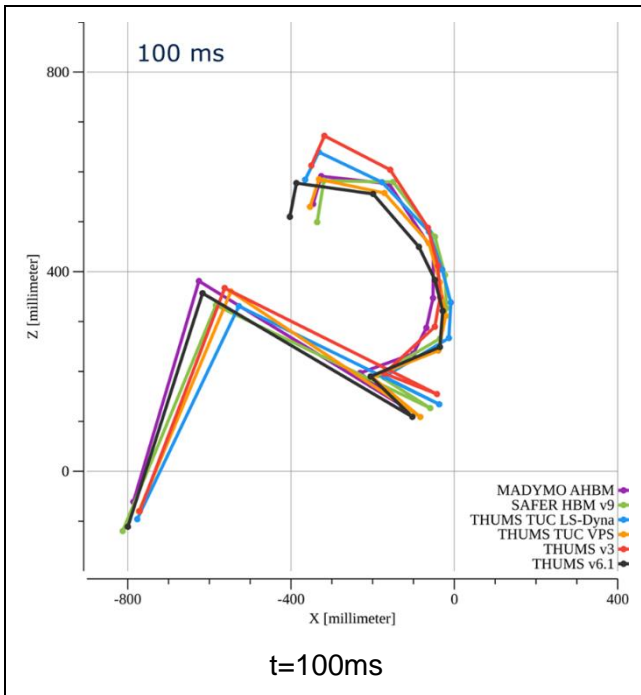
Seat

Seat Pan

Sub Pan

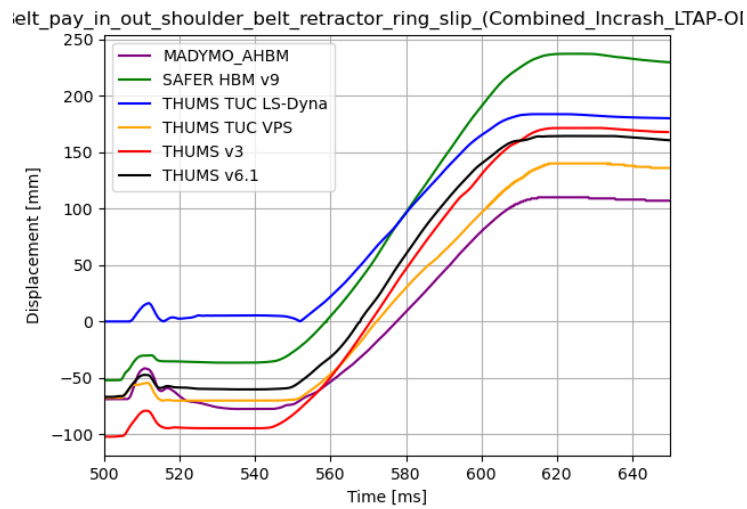
Toe pan resultant force
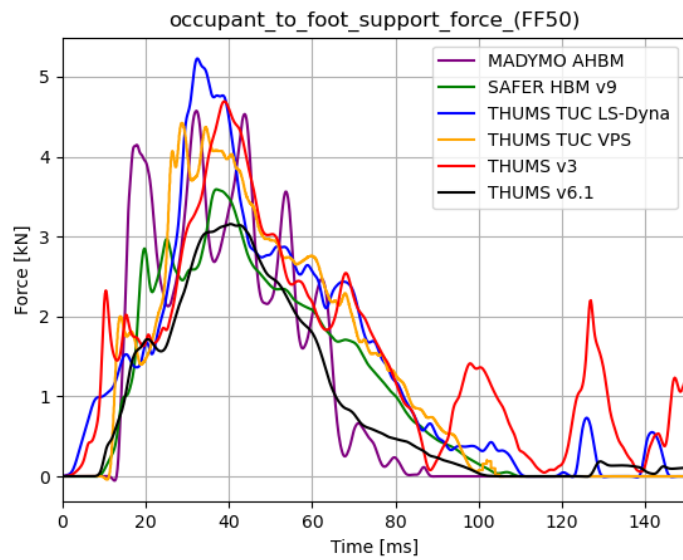
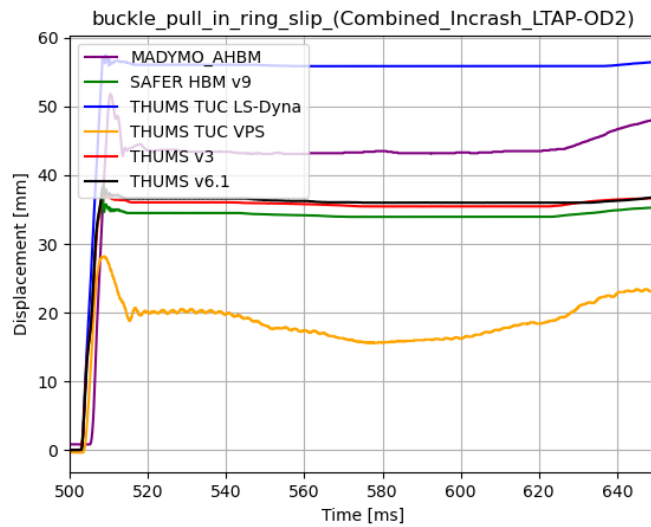# Seatbelt system

Belt pay in/out shoulder belt retractor
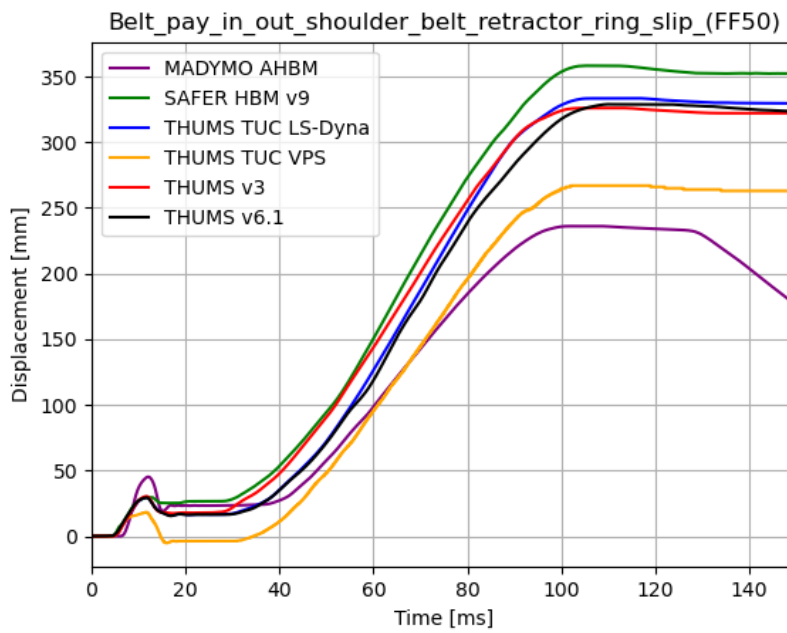
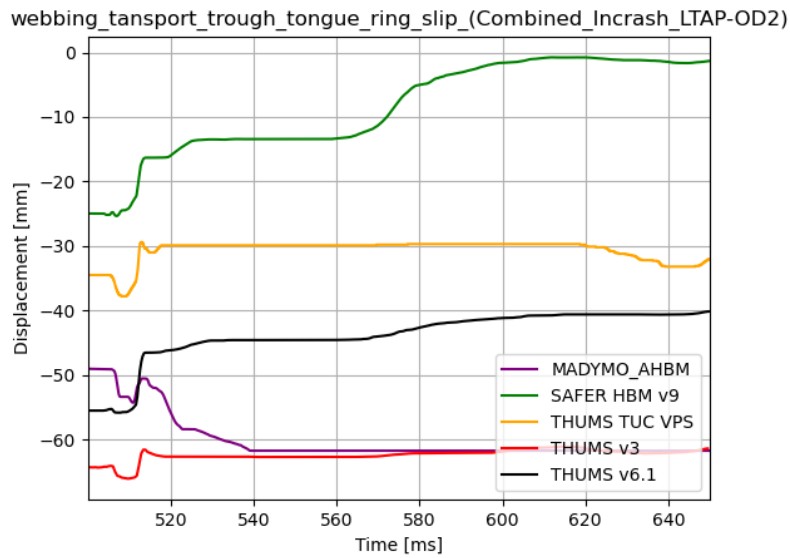Retractor pretensioner: 9 ms

Belt pay in/out lap belt retractor
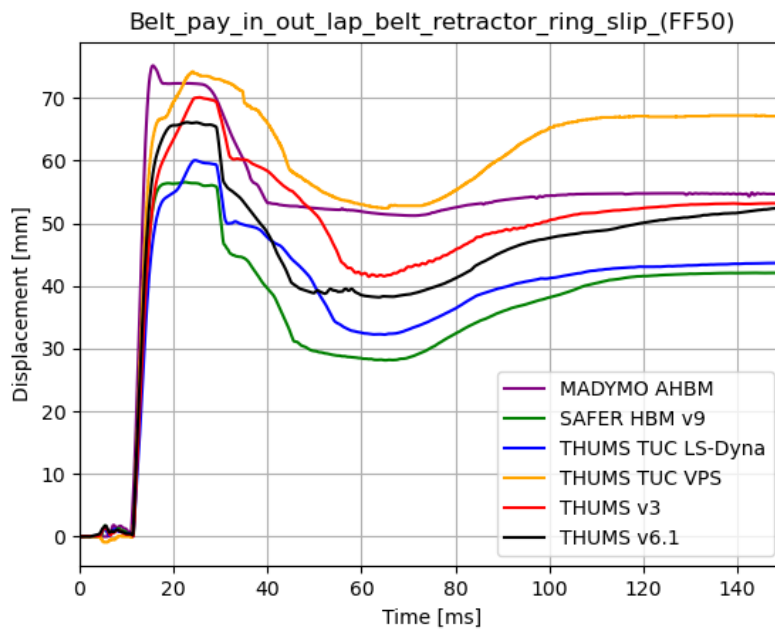
Lap belt pretensioner: 9 ms

Buckle pull in
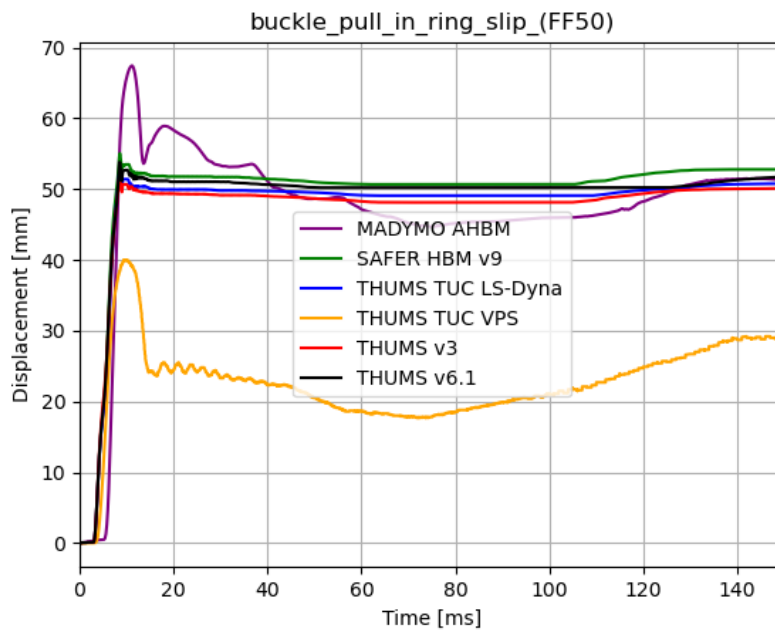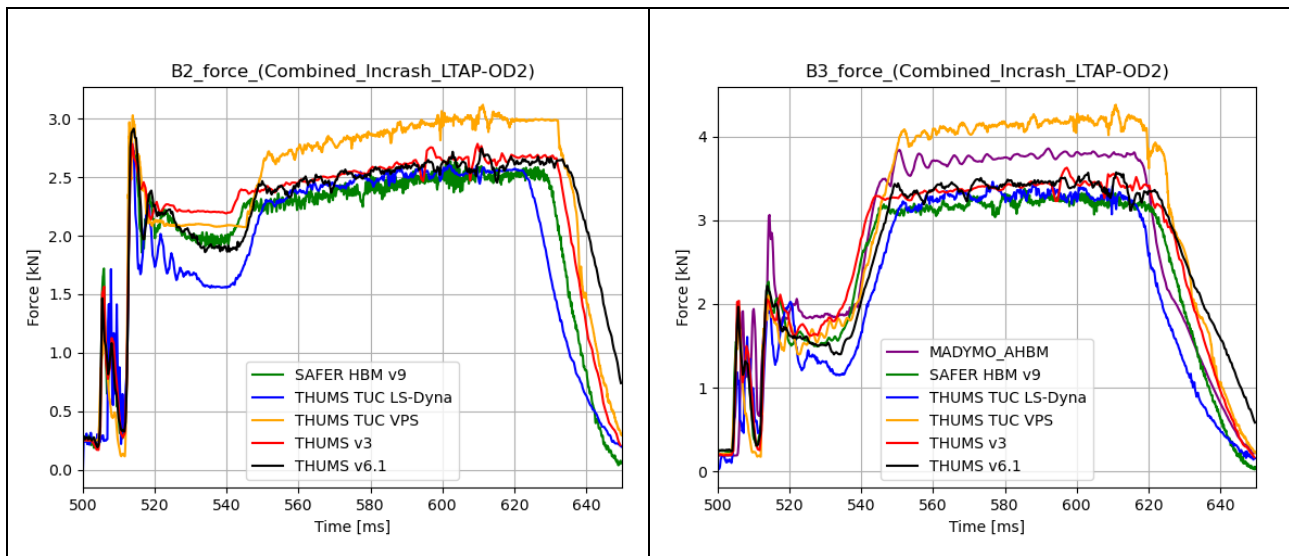

Buckle pull in: 3ms

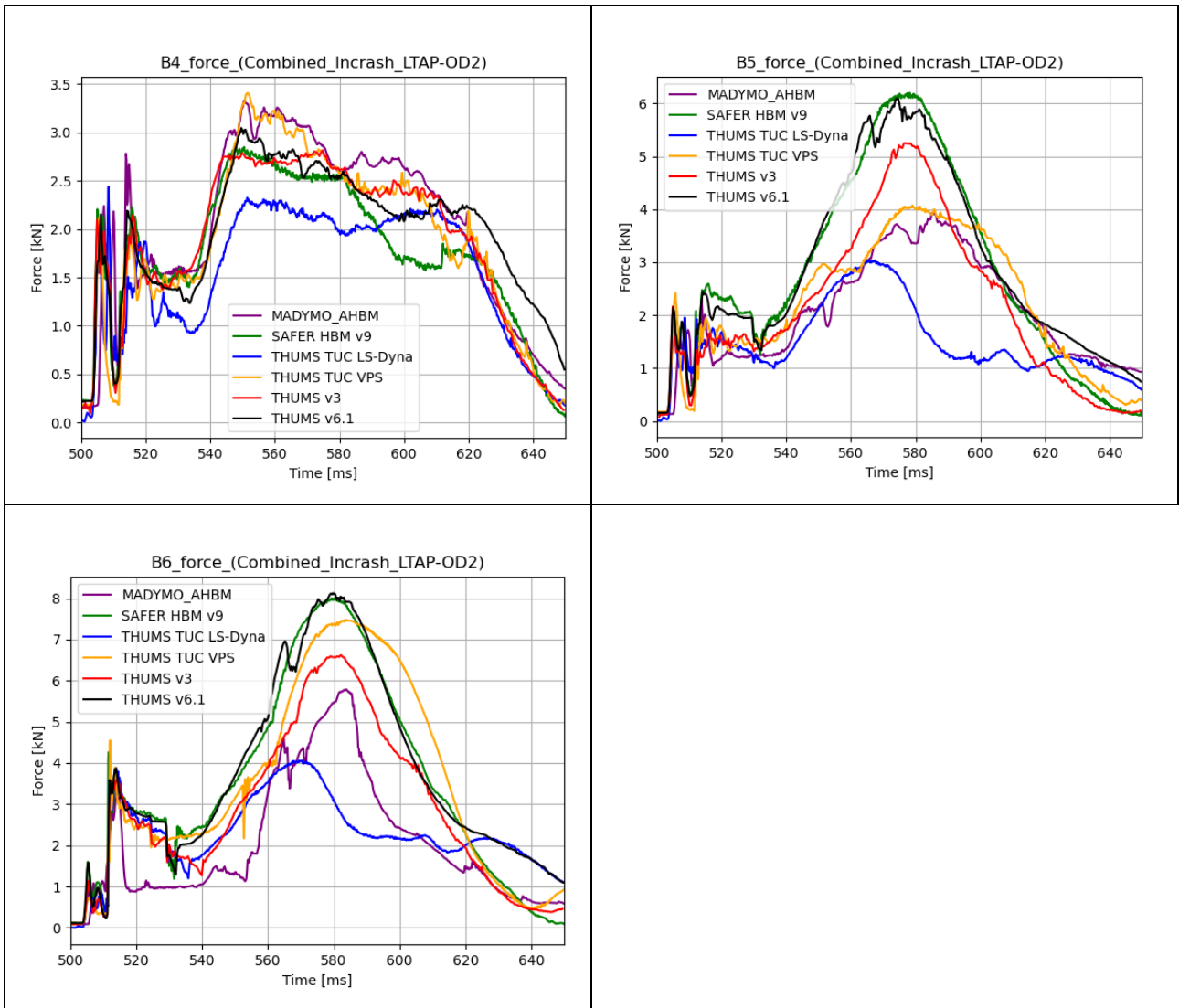## Webbing transport through tongue
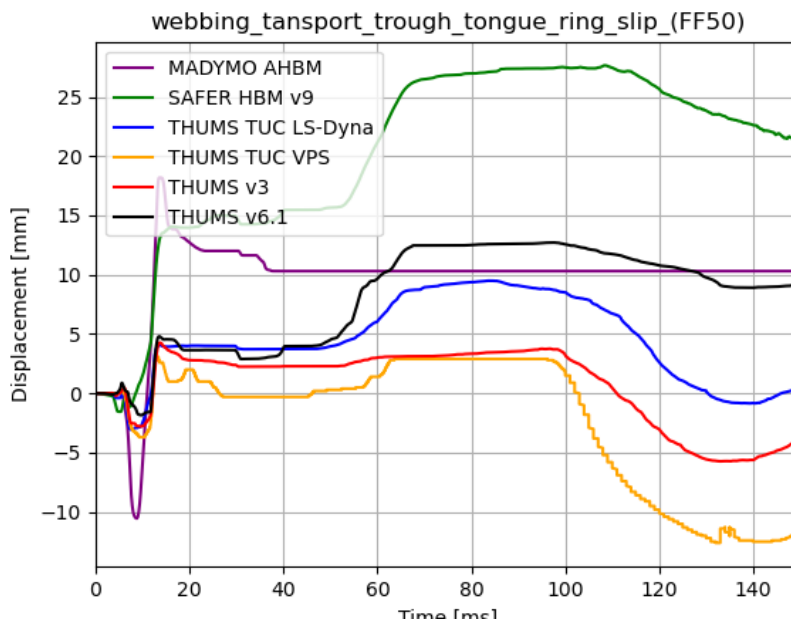
Crash locking tongue: 40 ms

Shoulder belt force (B2, B3)

Retractor pretensioner trigger time: 9ms
Lap belt trigger time: 9ms

Buckle Pretensioner: 3ms

Retractor pretensioner trigger time: 9ms
Lap belt trigger time: 9ms

Buckle Pretensioner: 3ms

Lap belt force (B5, B6)

Retractor pretensioner trigger time: 9ms
Lap belt trigger time: 9ms

Buckle Pretensioner: 3ms
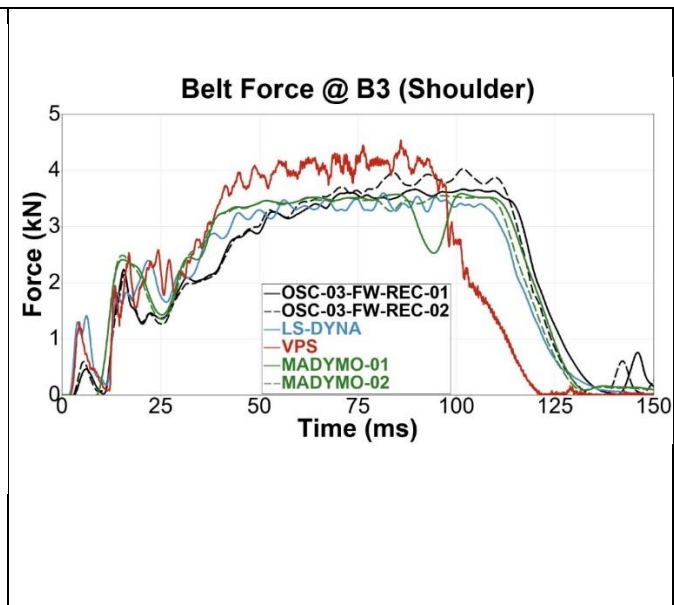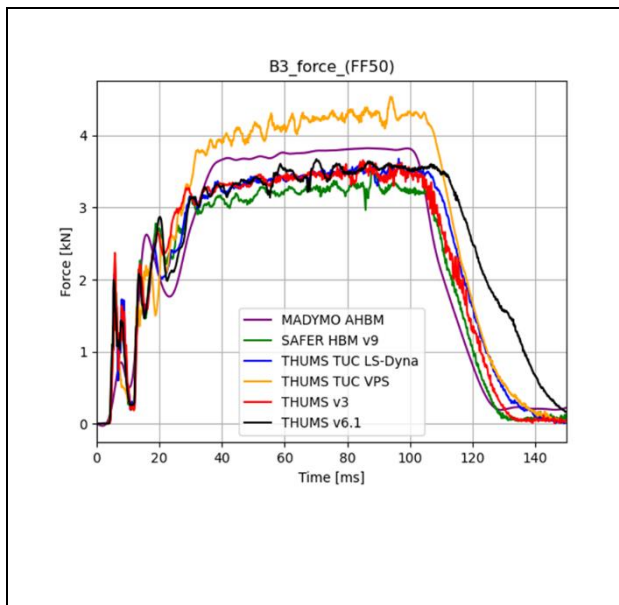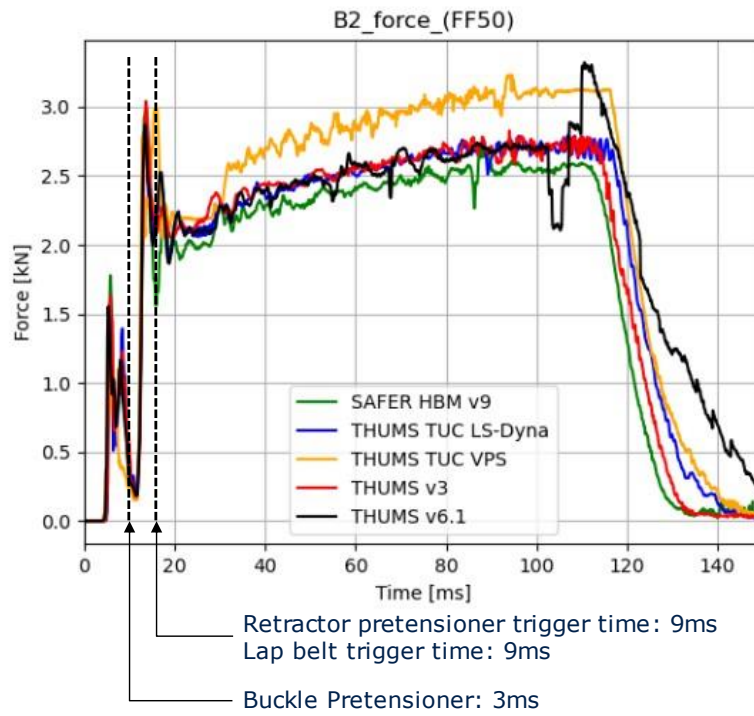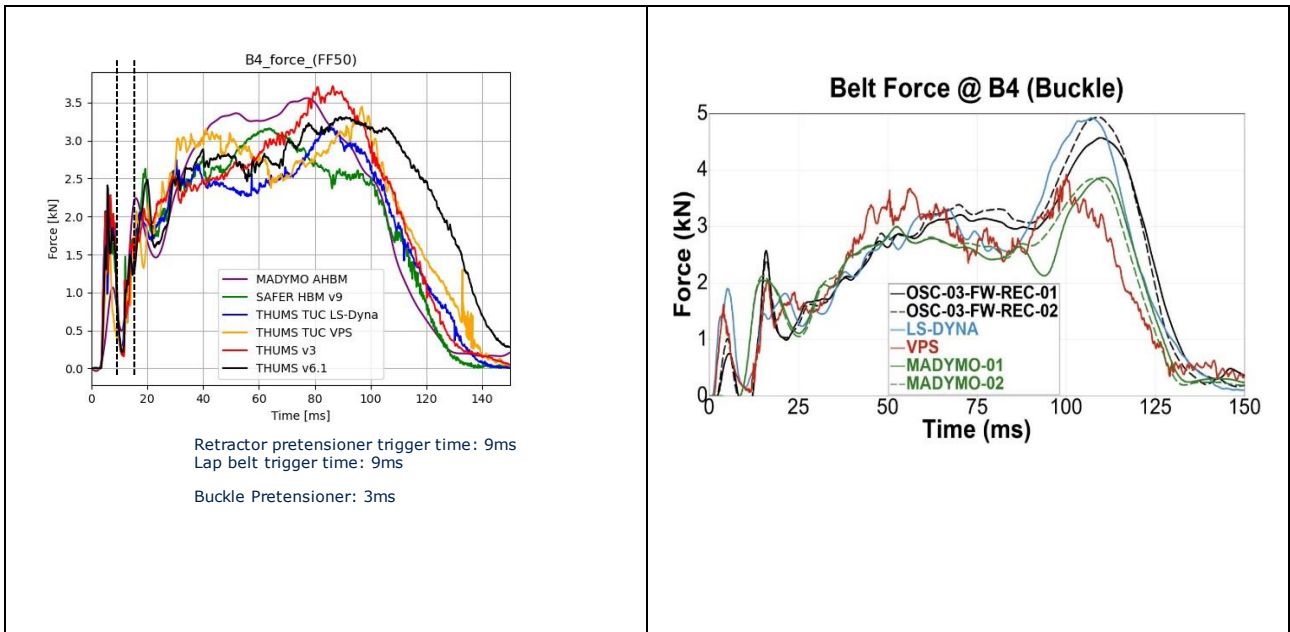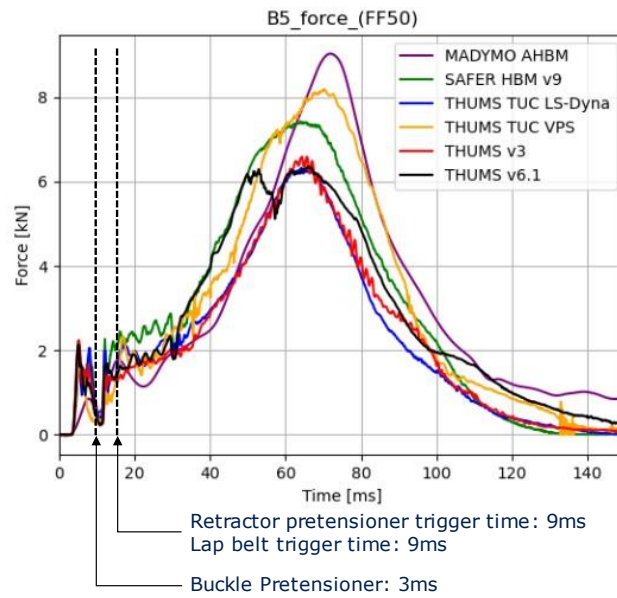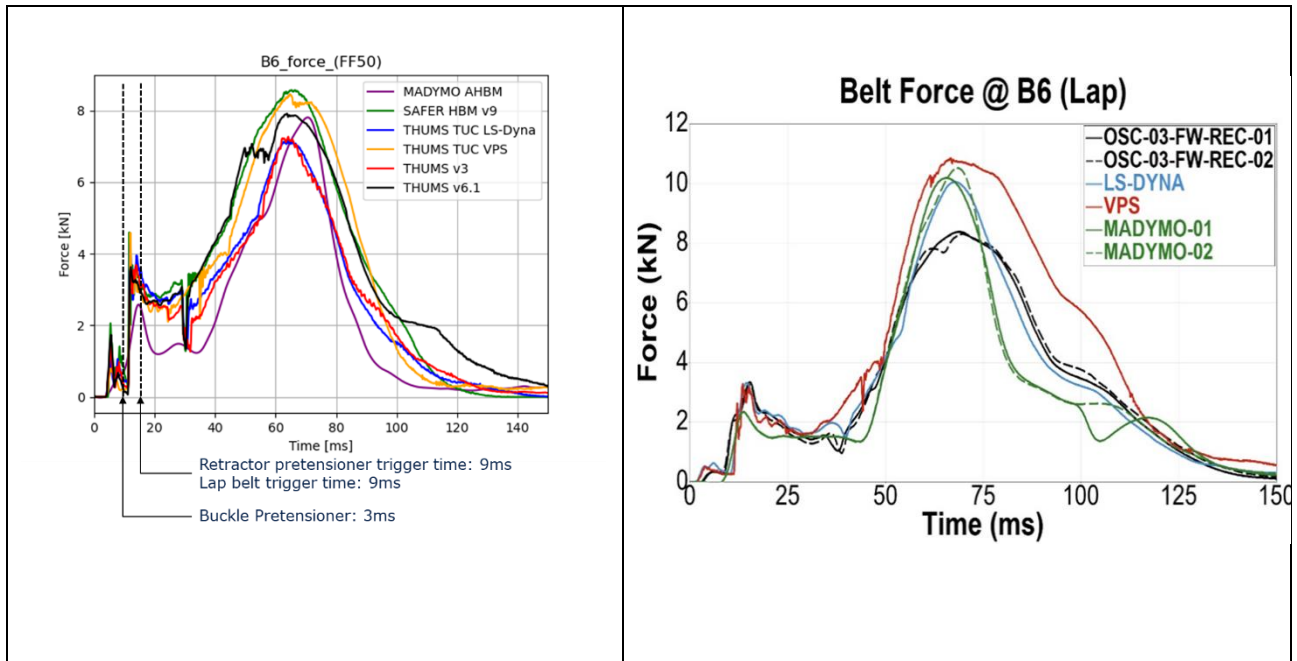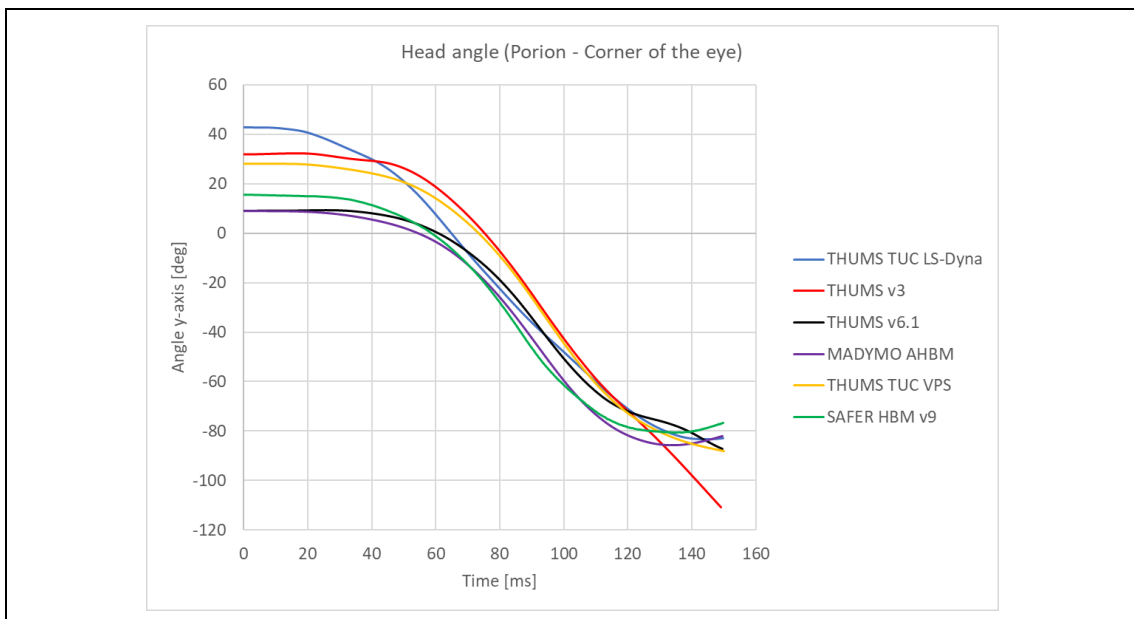
Proposed landmarks for HBM kinematic assessment

Porion (left/right)
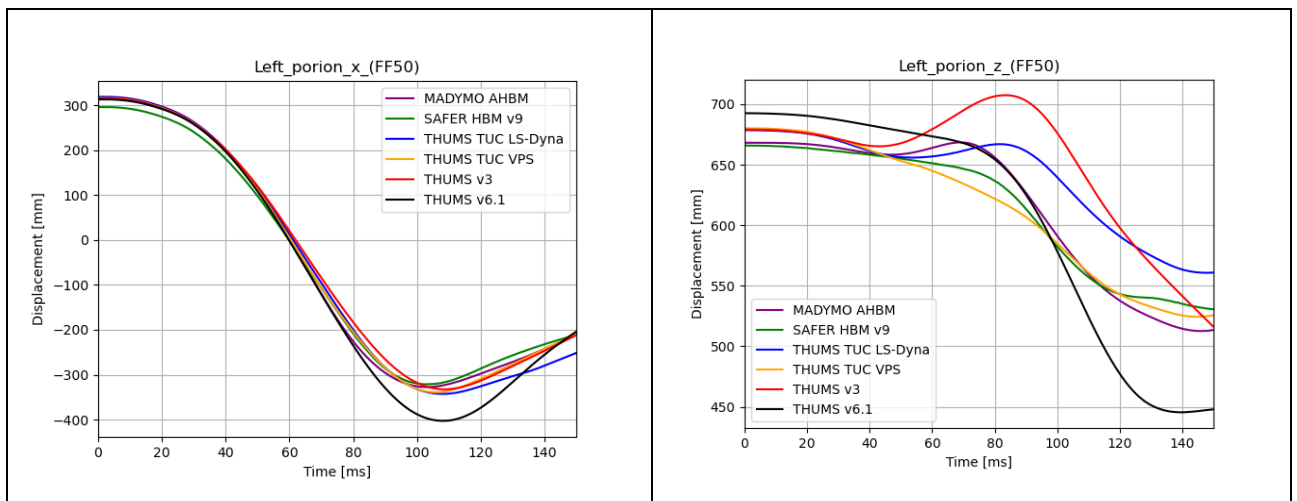
Head rotation
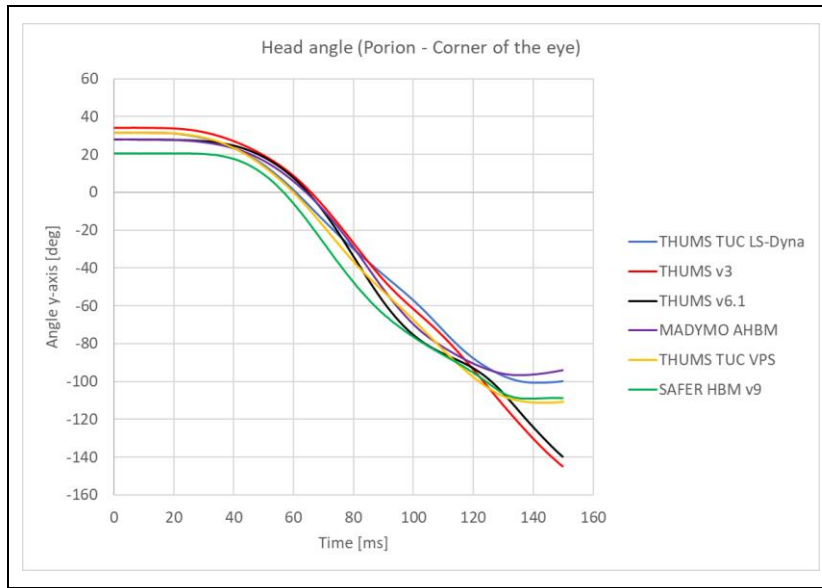
T1
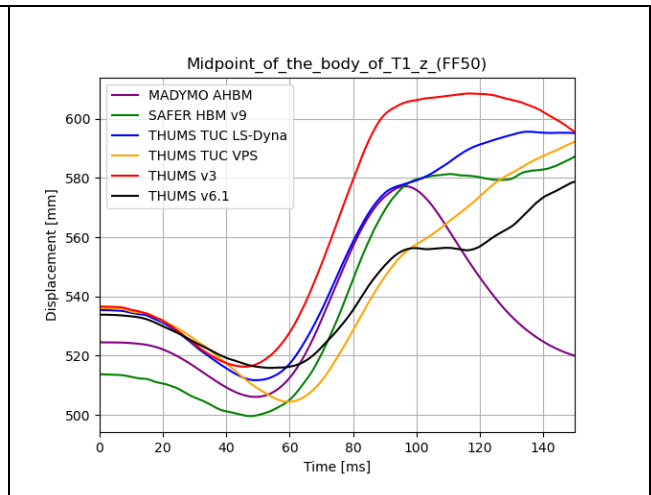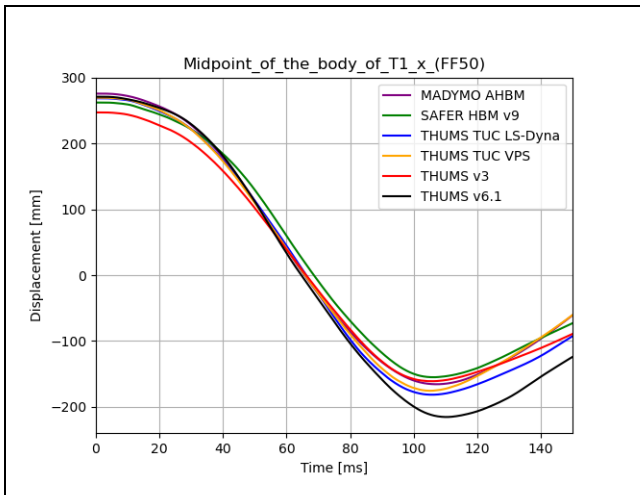
T8
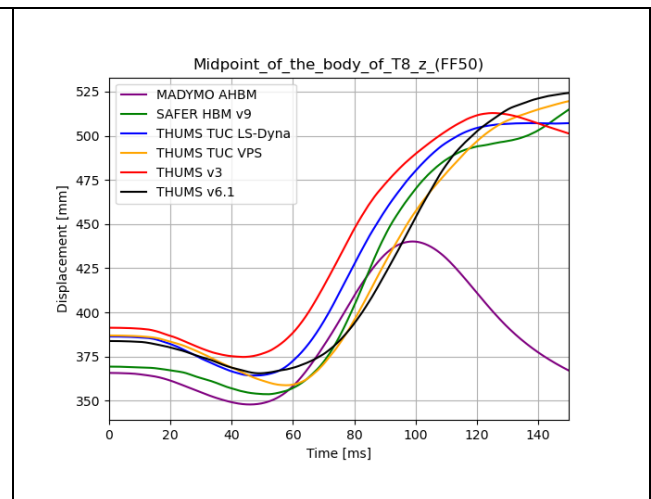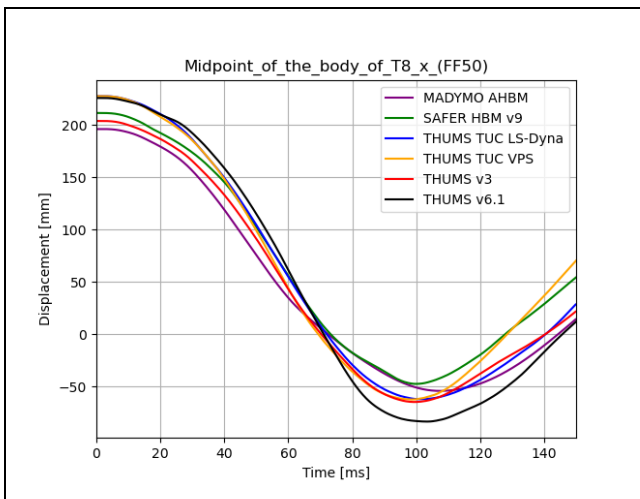
T11
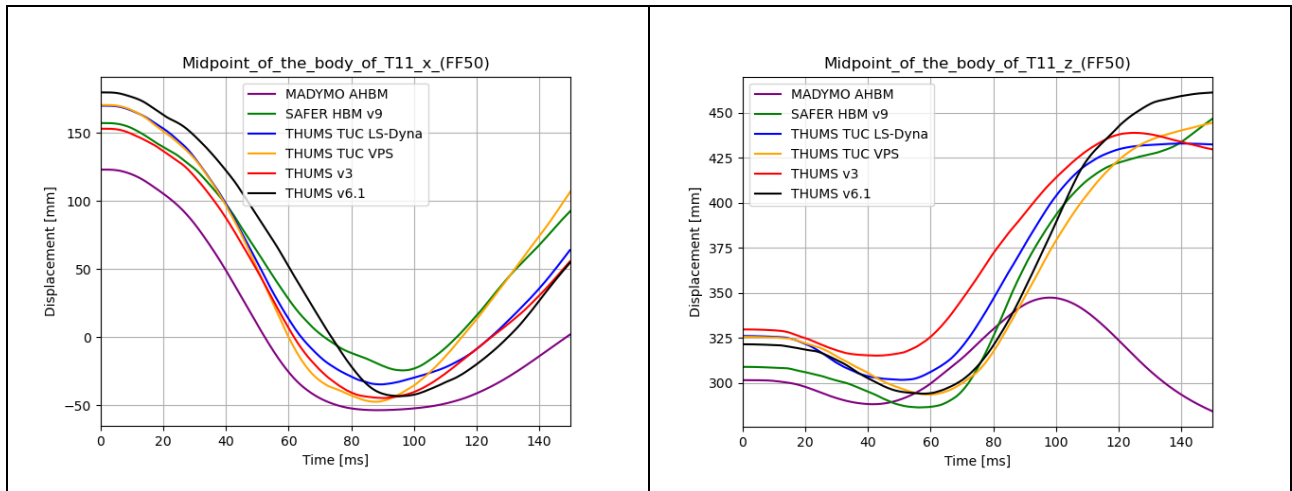
L1

L3
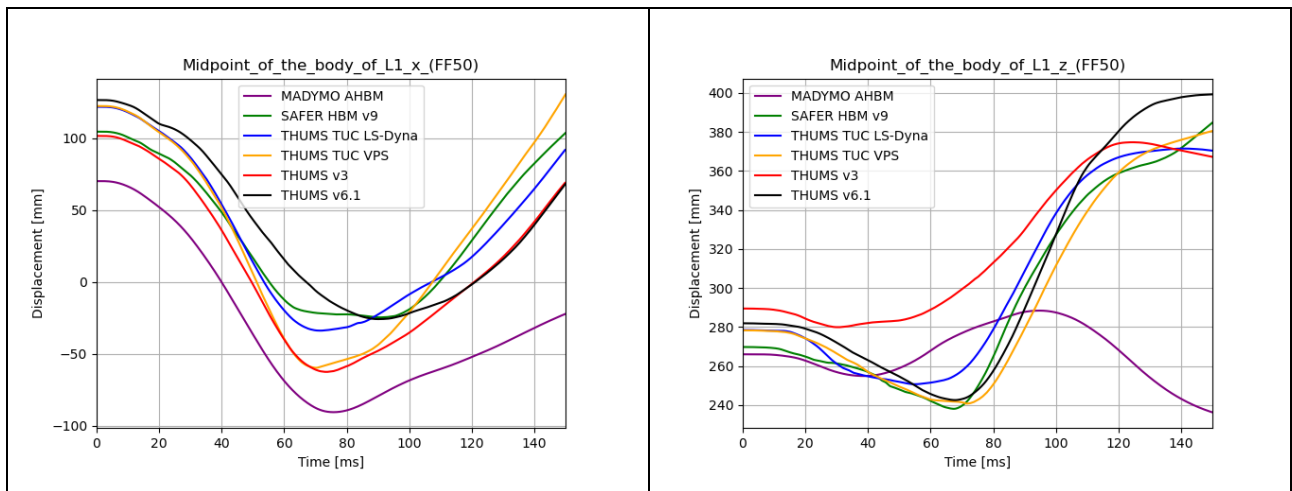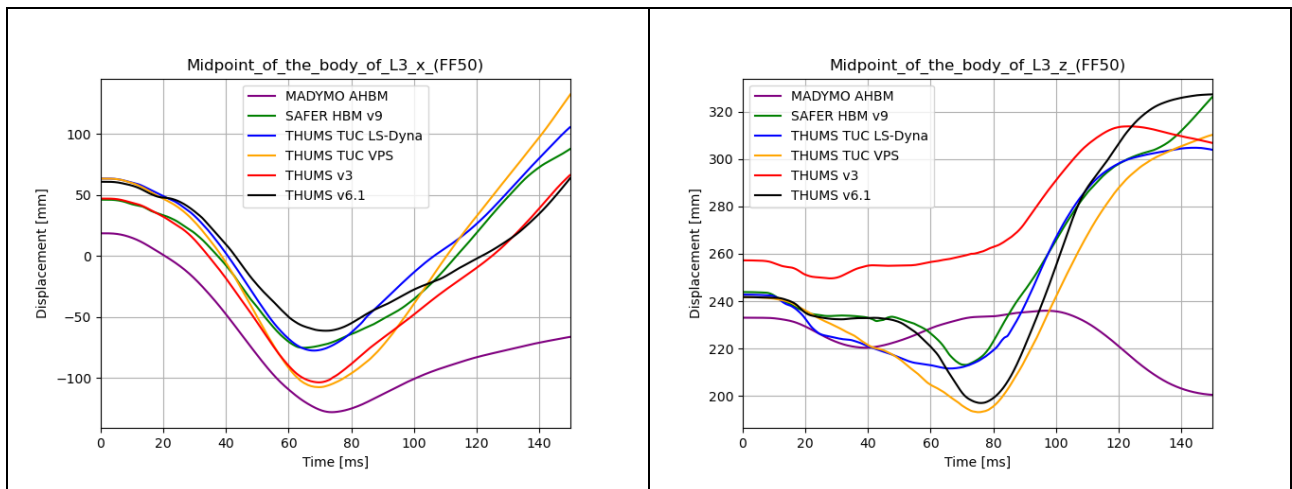
Acetabular centre
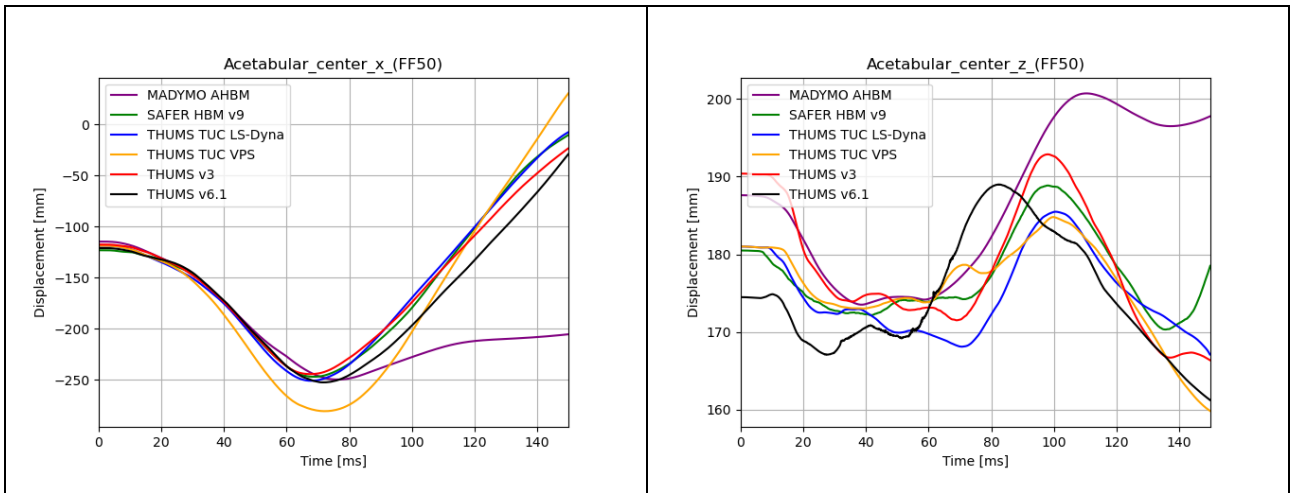
Pelvis angle (t)
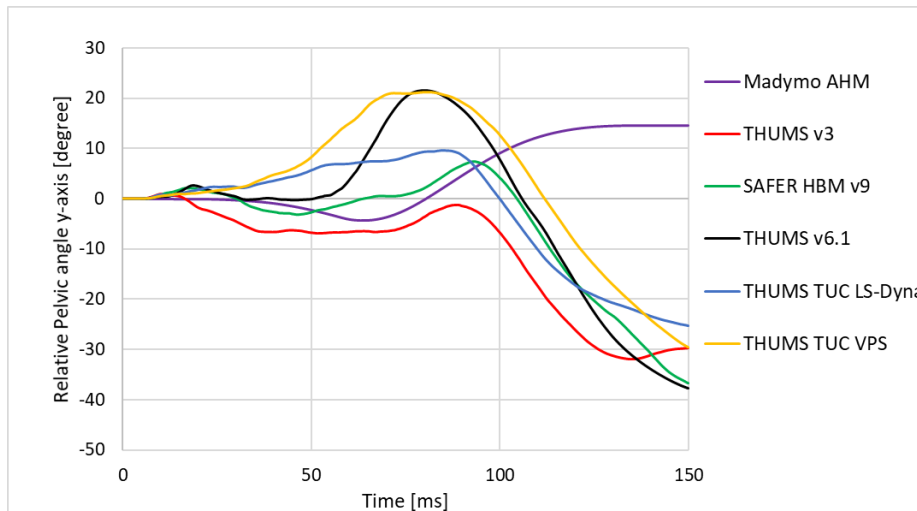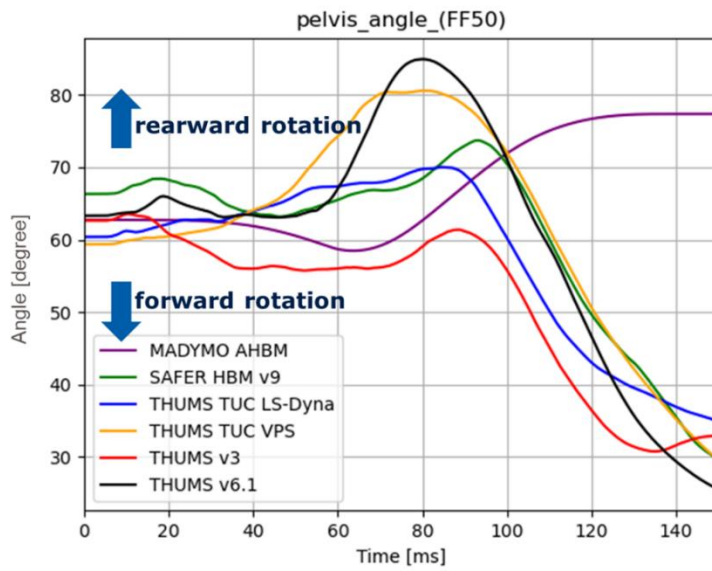
Injury indicators and risk assessment parameters

Lumbar Spine

Forces (z) and Moments (y)
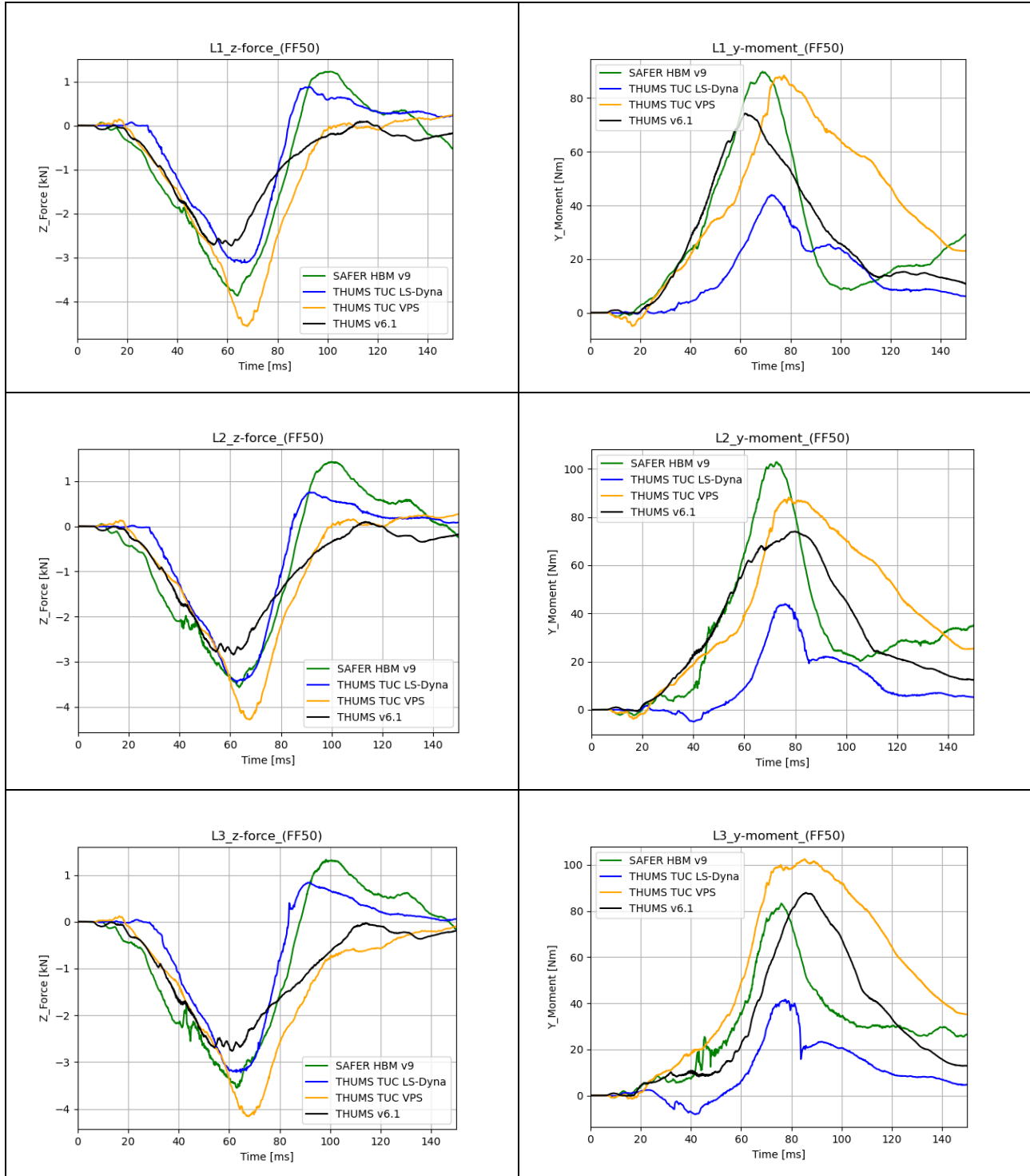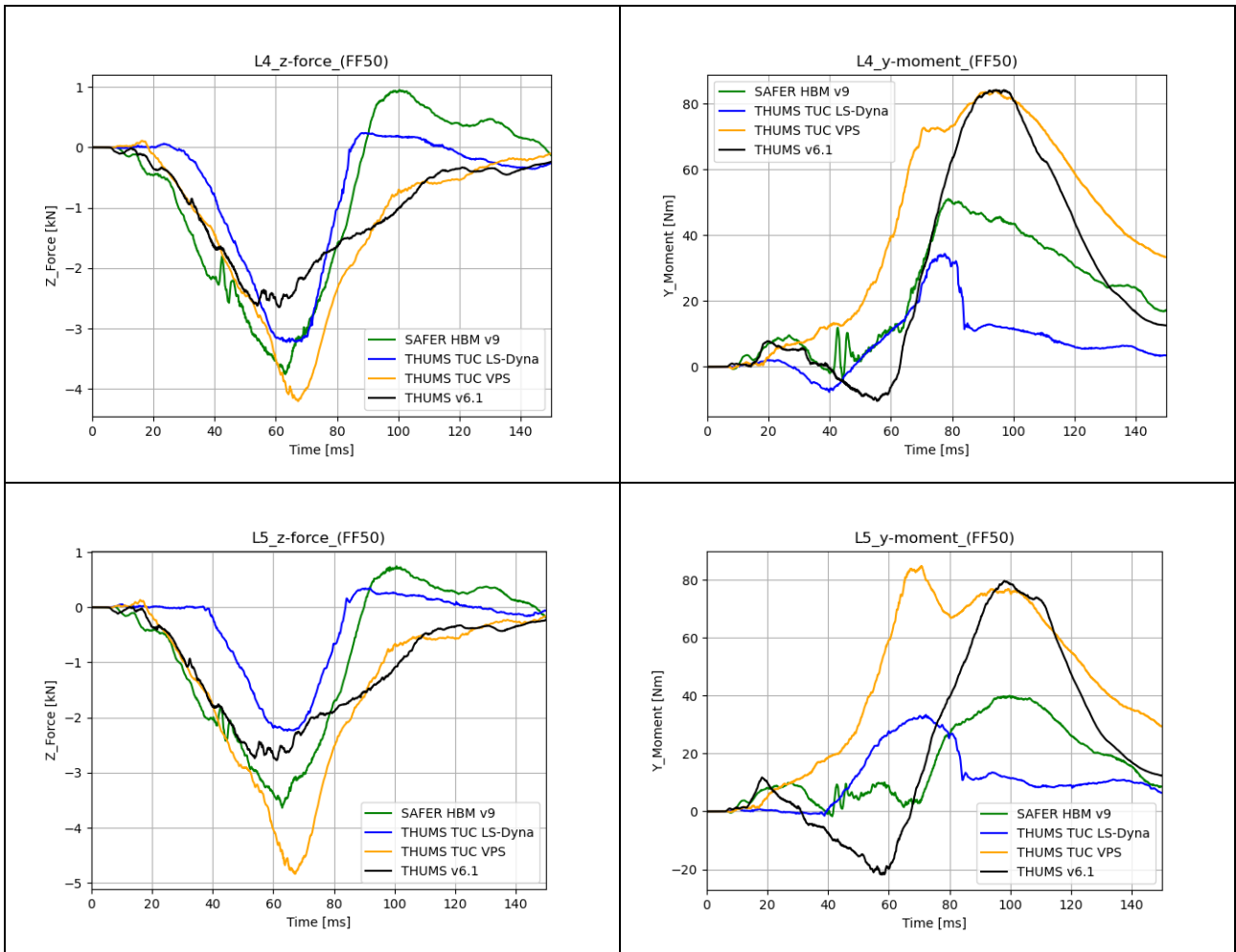
ASIS Loadcells
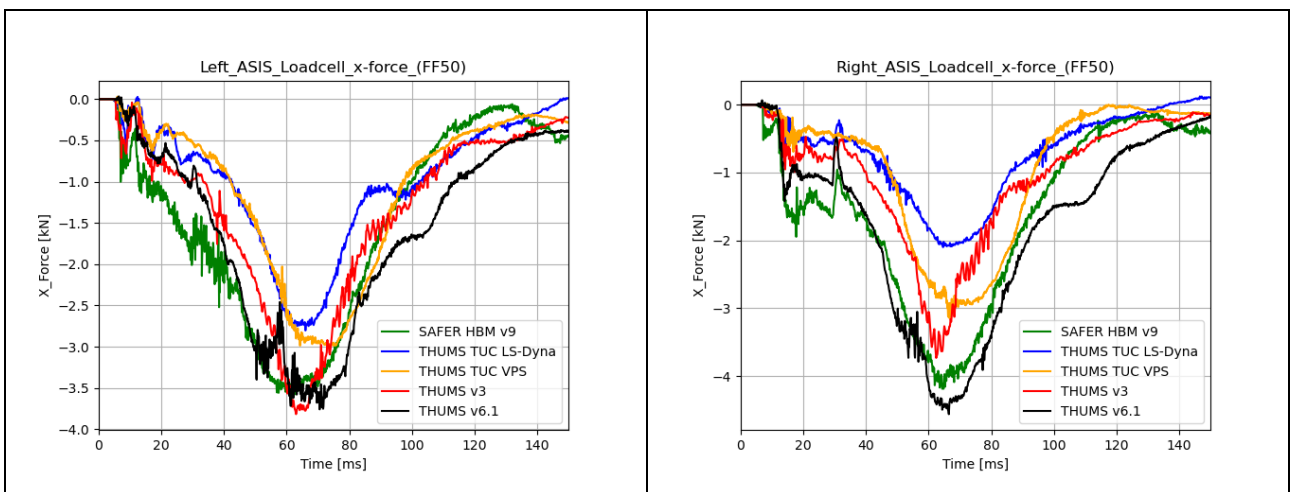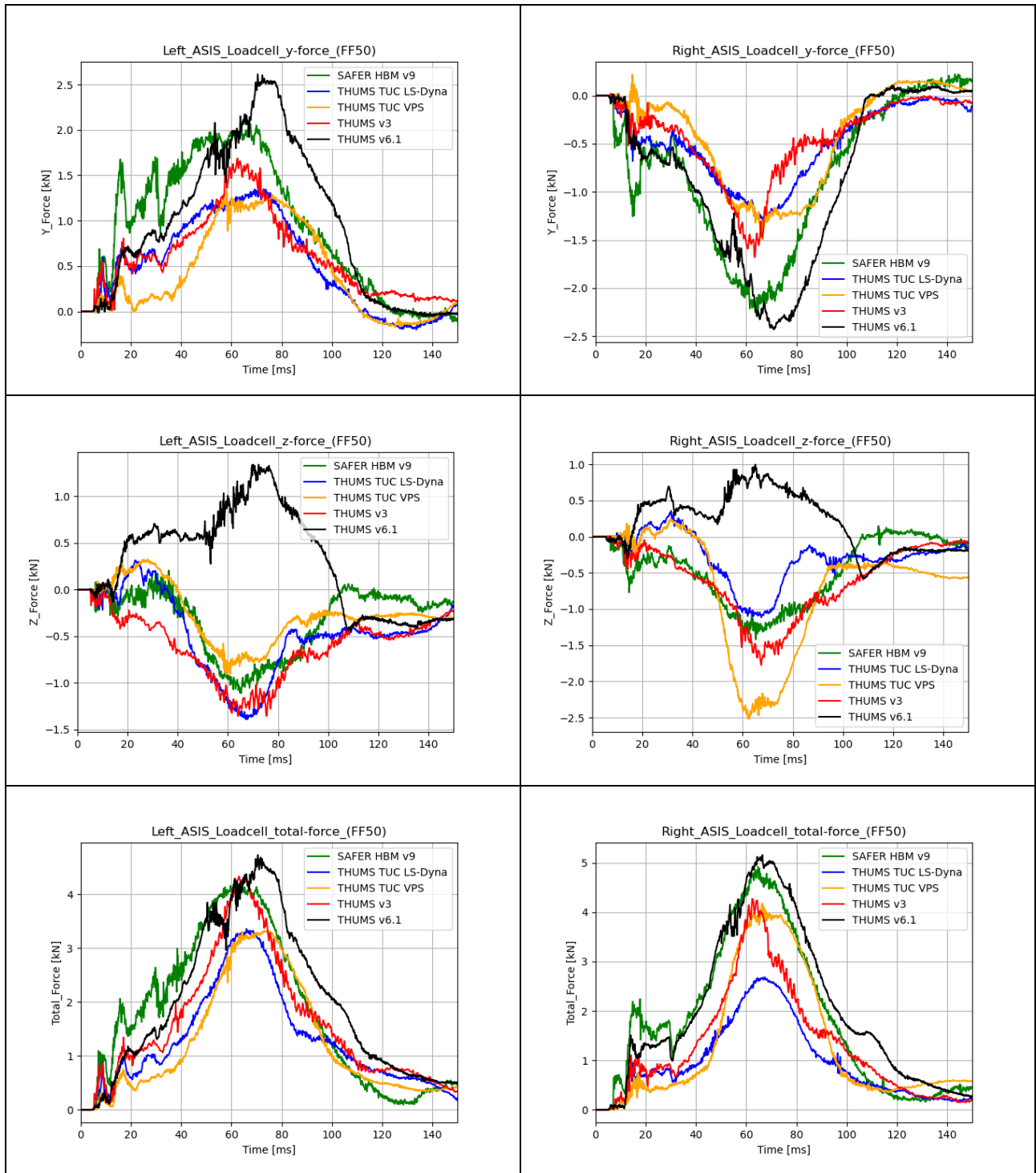
Head injury risks

Model	HIC15	HIC 15 AIS 2+	BRIC	BriC MPS AIS2+	SUFEHM	UFEHM_RIS	HIC36	A3MS
SAFER HBM v9	169	13%	0.70	78%	7.0	7%	298	43
Madymo AHM	178	15%	0.77	86%	5.9	7%	345	44
THUMS v6.1	193	17%	0.84	93%	6.1	7%	392	44
THUMS v3	182	15%	0.65	70%	5.8	6%	300	44
THUMS TUC VPS	229	24%	0.66	73%	7.3	7%	307	49
THUMS TUC LS-Dyna	196	18%	0.61	65%	9.7	9%	313	46

C. FF50 IN-CRASH SIMULATION (LS-DYNA AND VPS)

Kinematics comparison of the THUMS-TUC model in VPS (orange) and LS-Dyna (blue)
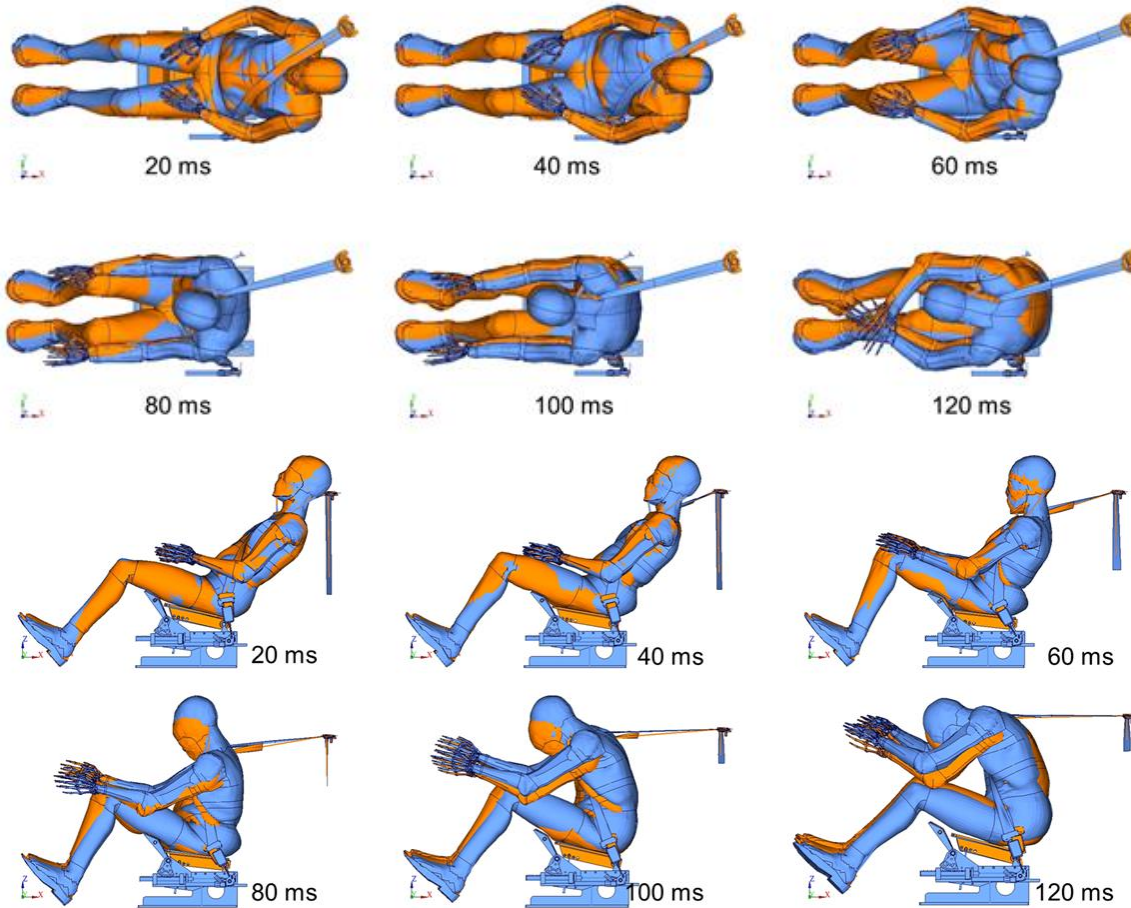
D. COMBINED SIMULATION – IN-CRASH PHASE (LTAP-OD2)

This chapter presents the data according to the definitions in chapter 3.2, 3.3 and 3.6.1 for the incrash phase of a combined pre- and incrash simulation with the LTAP-OD2 pulse.

Seat
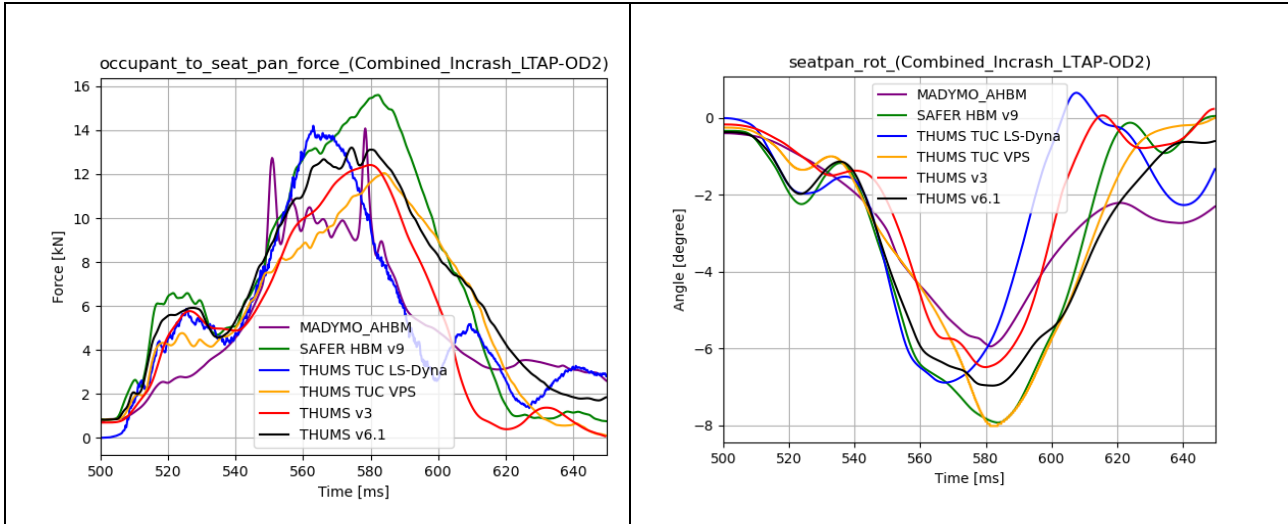
Sub Pan
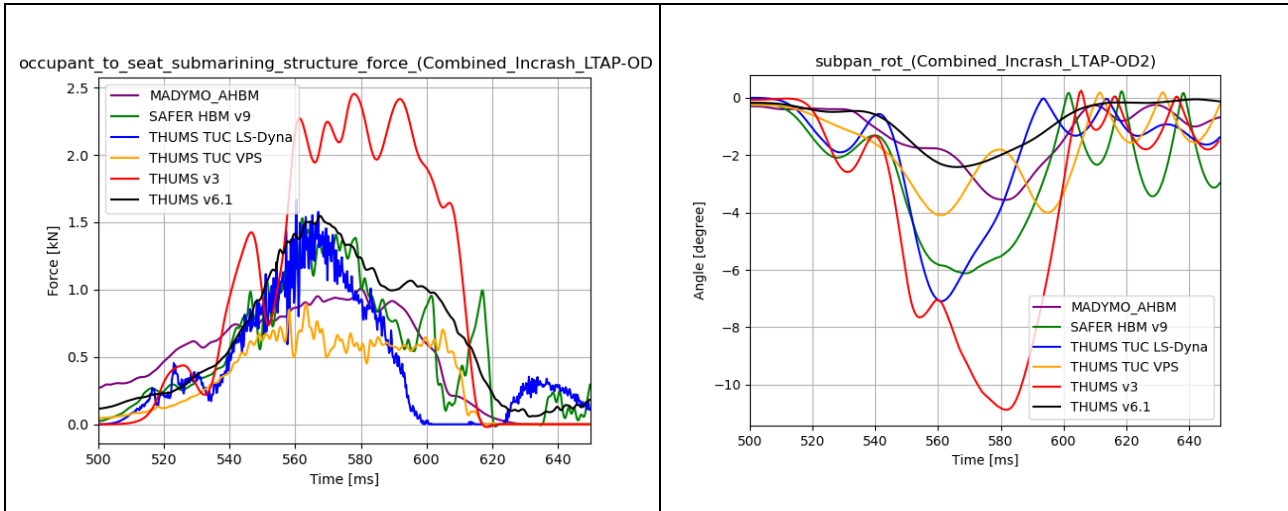
Toe pan resultant force

Seatbelt system

Belt pay in/out shoulder belt retractor

Retractor pretensioner: 509 ms

Belt pay in/out lap belt retractor
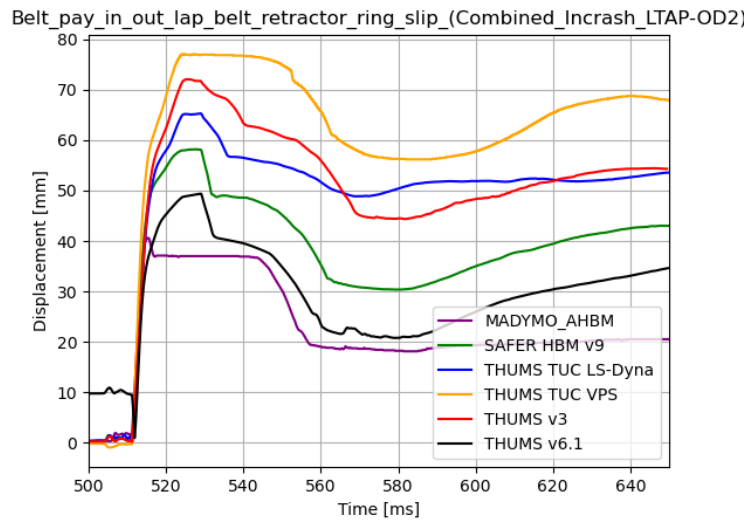
Lap belt pretensioner: 509 ms

Buckle pull in

Buckle pull in: 503ms

Webbing transport through tongue

webbing_tansport_trough_tongue_ring_slip_(Combined_Incrash_LTAP-OD2)

Crash locking tongue: 540 ms

Belt forces

B4_force_(Combined_Incrash_LTAP-OD2)

B5_force_(Combined_Incrash_LTAP-OD2)

B6_force_(Combined_Incrash_LTAP-OD2)

Proposed landmarks for HBM kinematic assessment

Porionx(t), y(t), z(t)
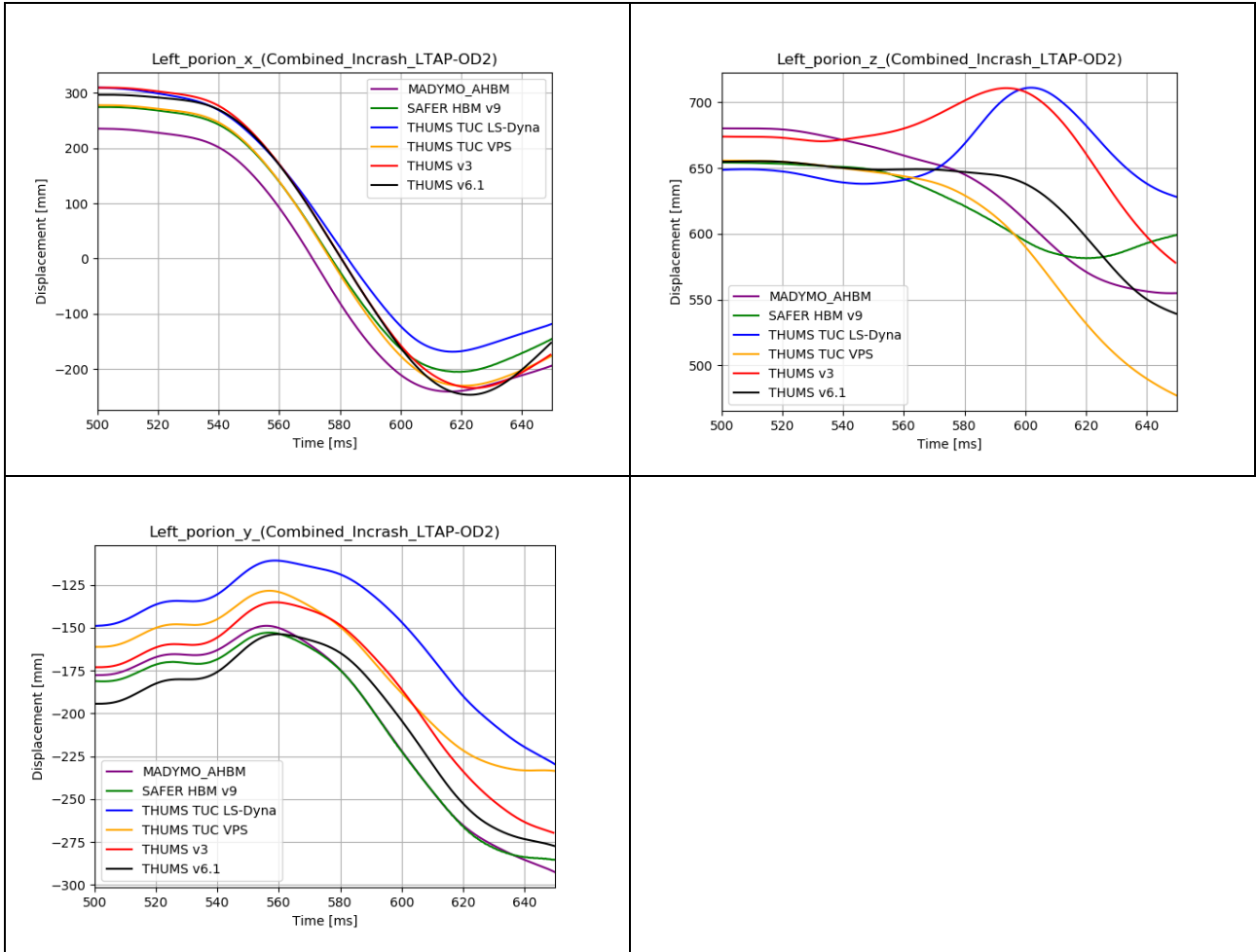
Head rotation

T1   x(t), y(t), z(t)

T8   x(t), y(t), z(t)

Left_midpoint_of_the_body_of_T8_y_(Combined_Incrash_LTAP-OD2)

T11

Midpoint_of_the_body_of_T11_x_(Combined_Incrash_LTAP-OD2)

Midpoint_of_the_body_of_T11_z_(Combined_Incrash_LTAP-OD2)

L1

Midpoint_of_the_body_of_L1_x_(Combined_Incrash_LTAP-OD2)
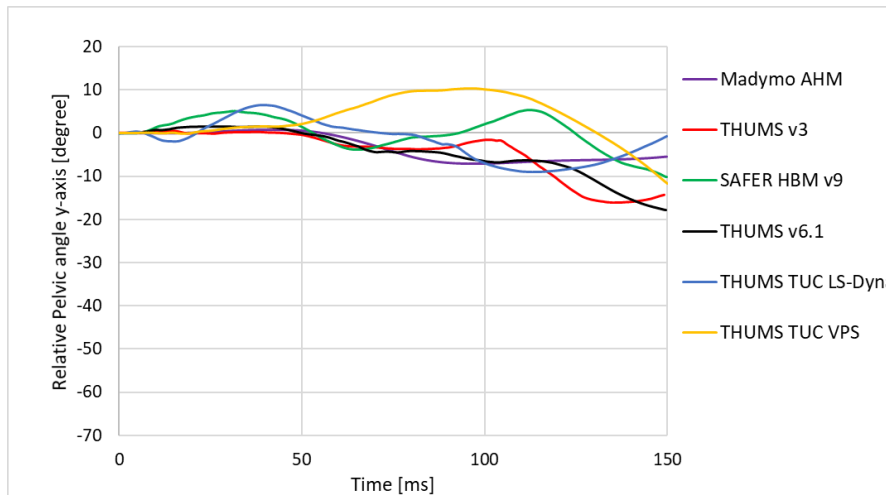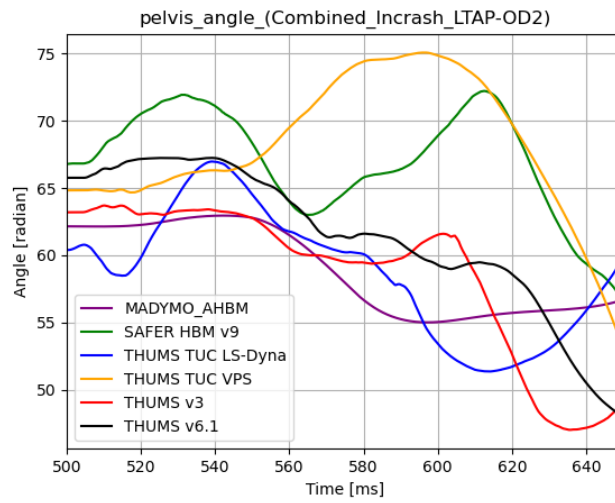

Midpoint_of_the_body_of_L1_z_(Combined_Incrash_LTAP-OD2)
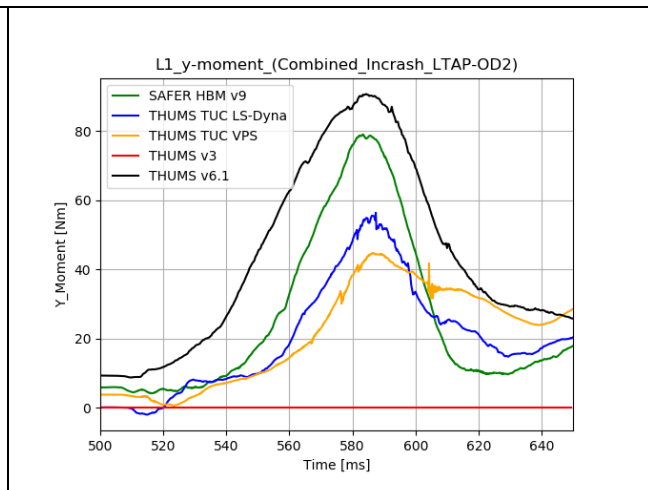
L3
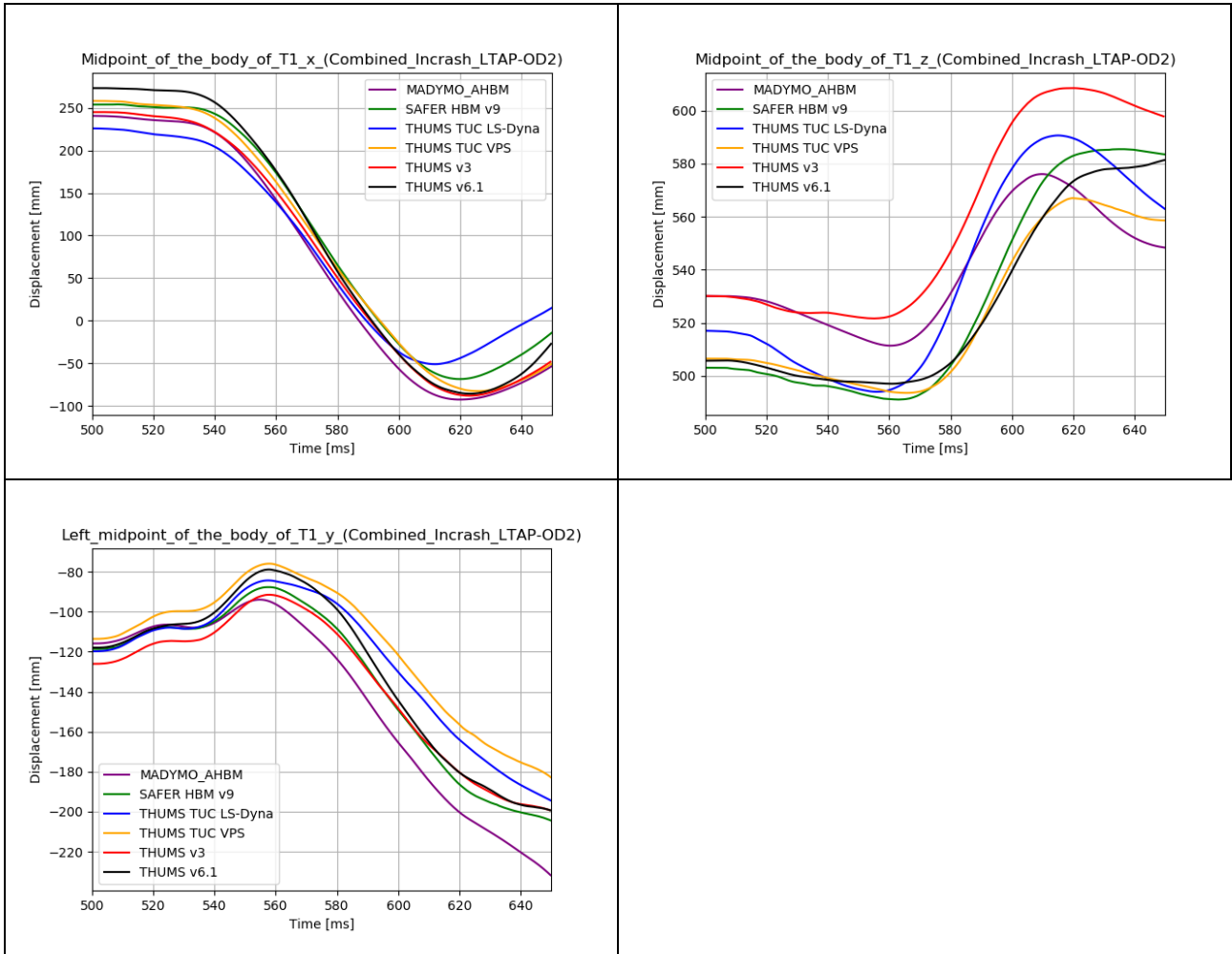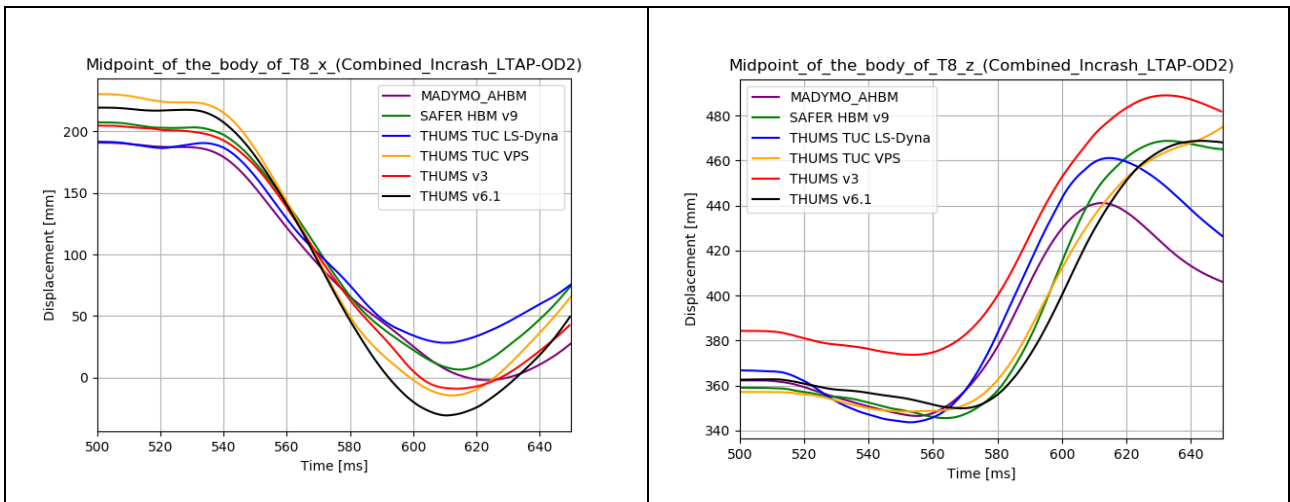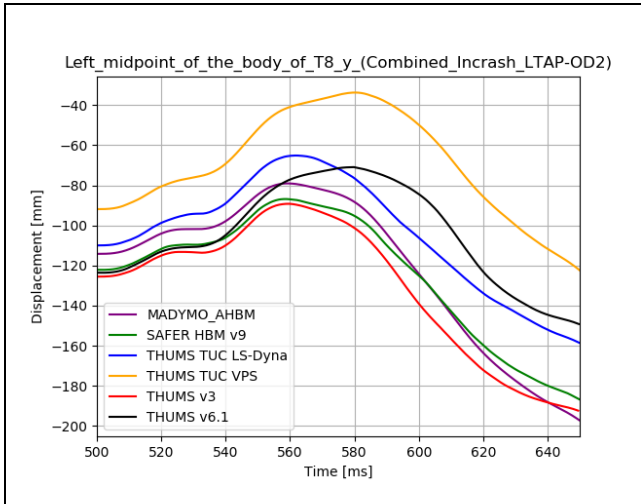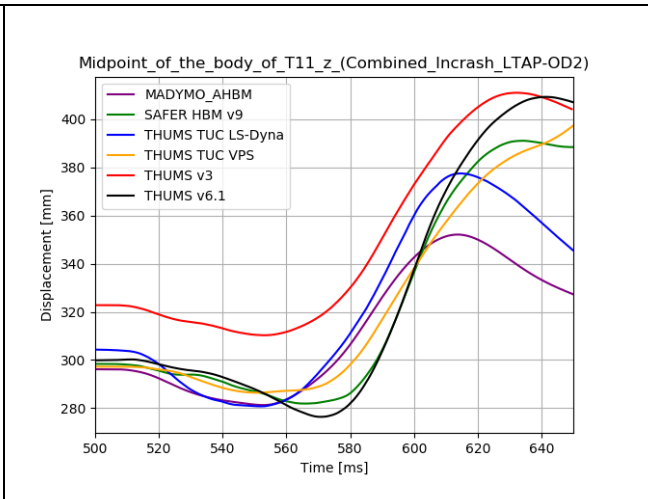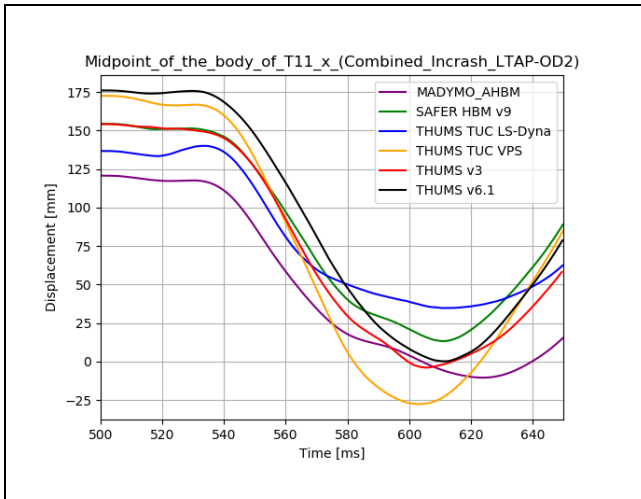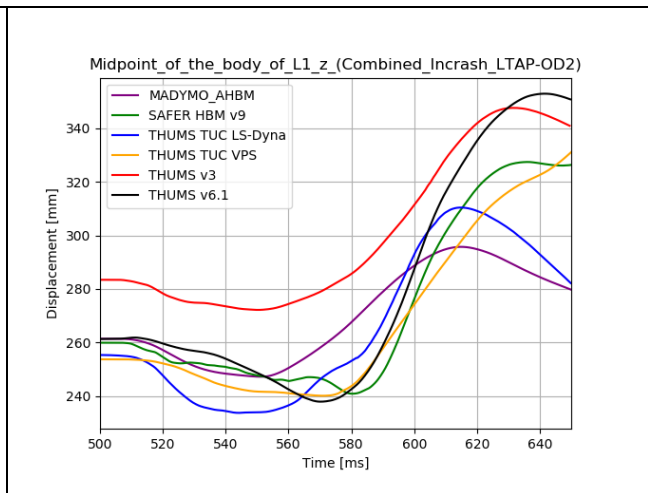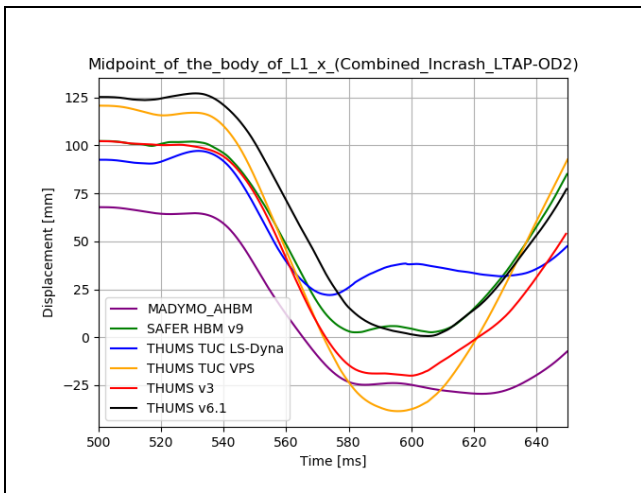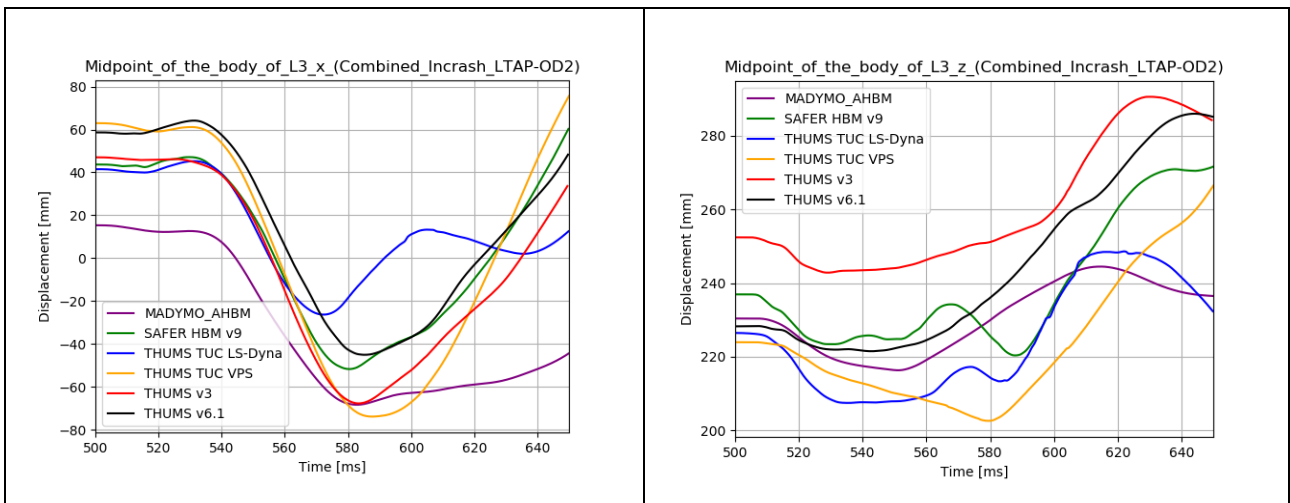
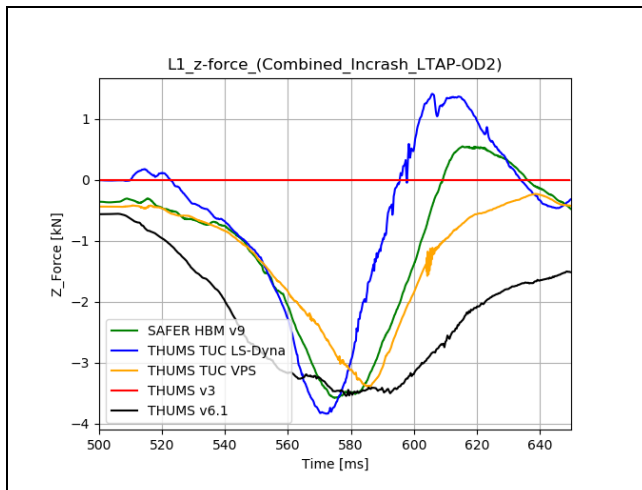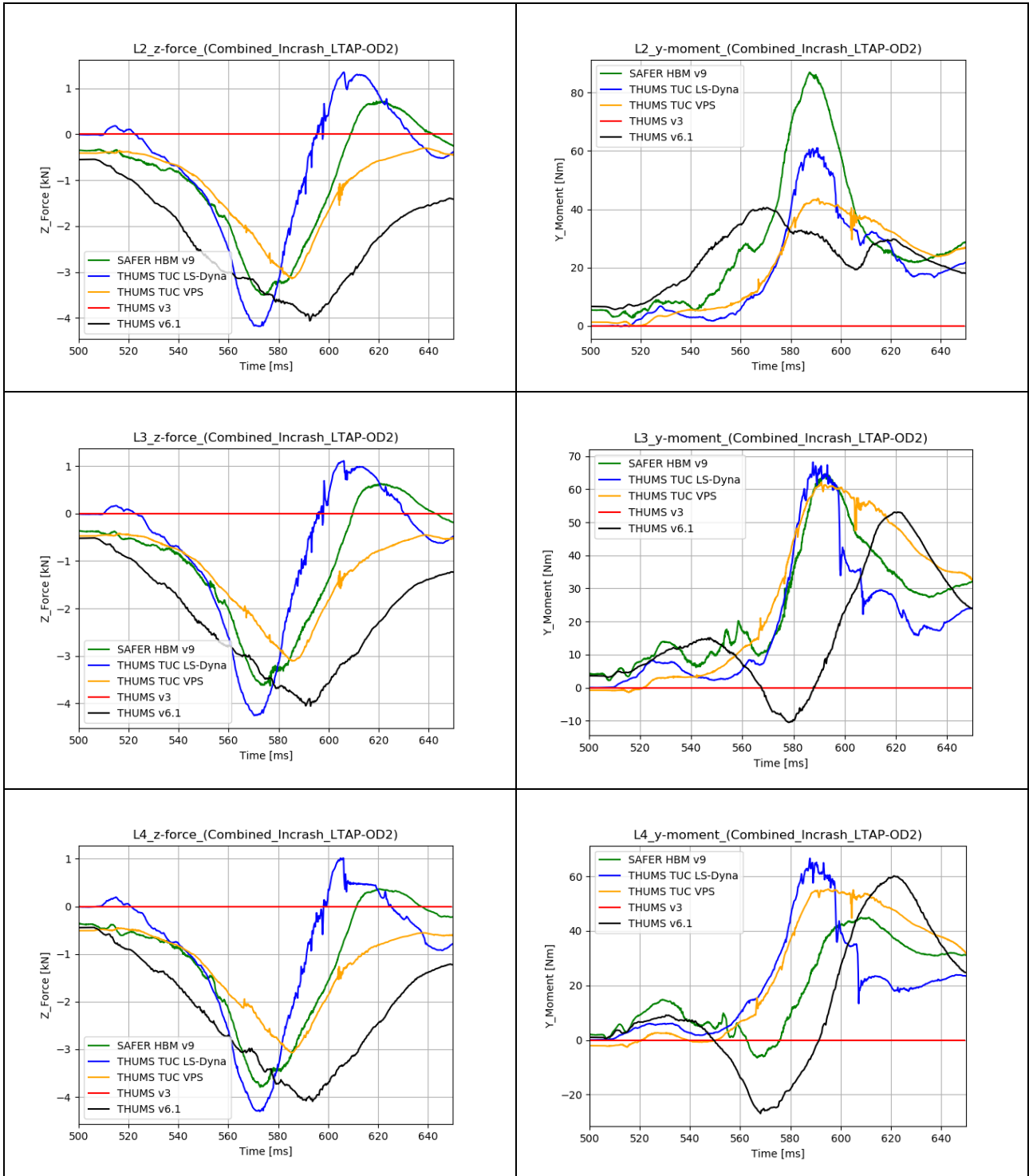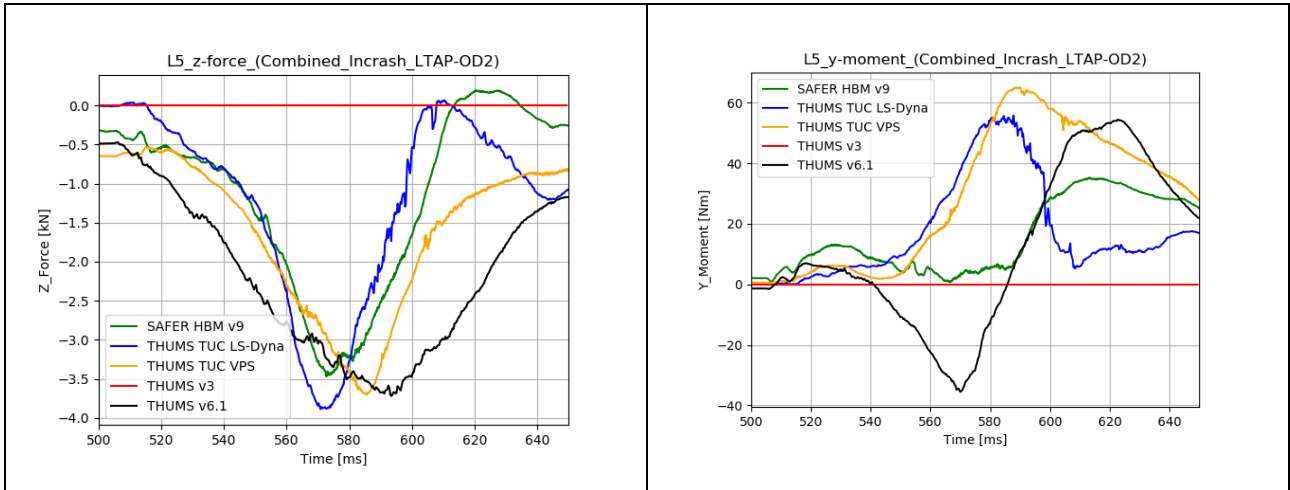## Acetabular centre (left/right)   x(t), z(t) y rotation
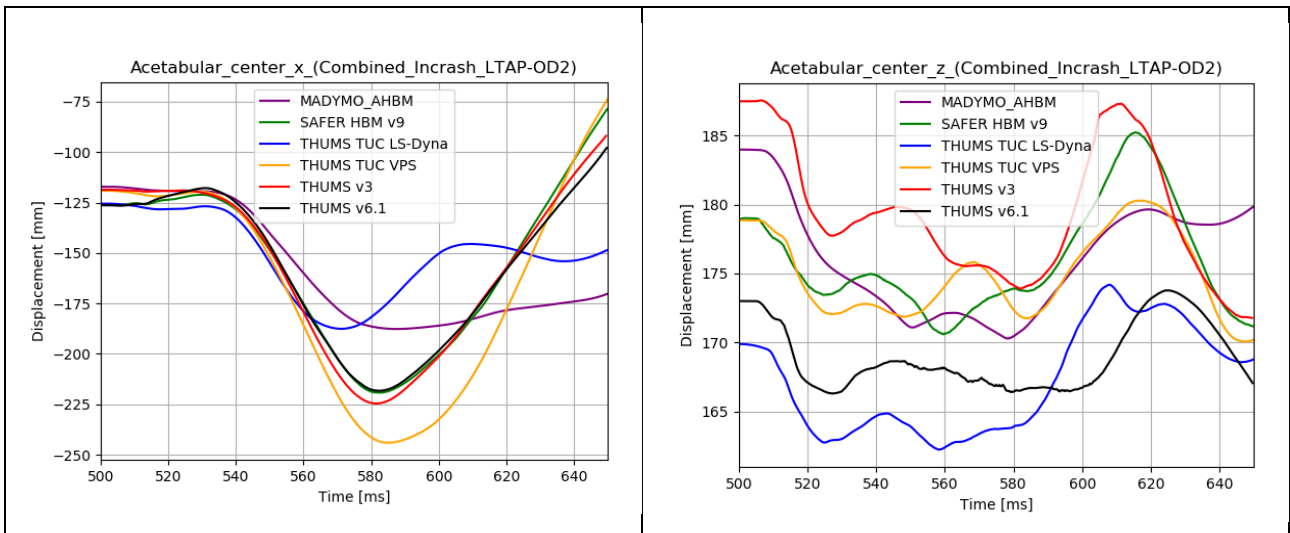
Pelvis angle (t)

Lumbar spine diagrams

E. ABBREVIATIONS AND DEFINITIONS

- Anatomical landmark definition

  Definitions for anatomical landmarks follow the recommendations in literature (see references [3][28][43][44]) and are documented in Deliverable D 4.2. [4]

Abbreviation	Definition
ATD	Anthropomorphic Test Device
D	Deliverable
DYNASAUR	Dynamic simulation analysis of numerical results
FE	Finite Elemente
FF	Full Frontal
HBM	Human Body Model
LTAP-OD	Left Turn Across Path – Opposite Direction
MB	Multi Body
SUFEHM	Strasbourg University Finite Element Head Model
THOR	Test device for Human Occupant Restraint
THUMS	Total Human Model for Safety
TUC	Thums User Community
VPS	Virtual Performance Solution
VT	Virtual Testing
WorldSID	Worldwide Harmonized Side Impact Dummy
WP	Work Package